

ADA 084464

NAVAL POSTGRADUATE SCHOOL
Monterey, California



DTIC
SELECTED
MAY 22 1980
S D

A

THESIS

COMPARISON OF AN α - β AND KALMAN FILTER
IN TRACK WHILE SCAN RADARS

by

Dimitrios Emmanuel Mayiatis

December 1979

Thesis Co-Advisors:

J. Bouldry
S.R. Parker

Approved for public release; distribution unlimited.

FILE COPY

80 5 20 009

UNCLASSIFIED

SECURITY CLASSIFICATION OF THIS PAGE (When Data Entered)

REPORT DOCUMENTATION PAGE		READ INSTRUCTIONS BEFORE COMPLETING FORM
1. REPORT NUMBER	2. GOVT ACCESSION NO.	3. RECIPIENT'S CATALOG NUMBER
4. TITLE (and Subtitle) Alpha-Beta Comparison of an old and Kalman Filter In Track While Scan Radars.		9
6. TYPE OF REPORT & PERIOD COVERED Master's Thesis, December 1979		7. PERFORMING ORG. REPORT NUMBER
7. AUTHOR(s) Dimitrios Emmanuel Mayiatis	8. CONTRACT OR GRANT NUMBER(s)	
9. PERFORMING ORGANIZATION NAME AND ADDRESS Naval Postgraduate School Monterey, California 93940	10. PROGRAM ELEMENT, PROJECT, TASK AREA & WORK UNIT NUMBERS	
11. CONTROLLING OFFICE NAME AND ADDRESS Naval Postgraduate School Monterey, California 93940	12. REPORT DATE Dec 1979	
14. MONITORING AGENCY NAME & ADDRESS (if different from Controlling Office)	13. NUMBER OF PAGES 152 (12) 153	
15. SECURITY CLASS. (of this report) Unclassified		
16. DISTRIBUTION STATEMENT (of this Report) Approved for public release; distribution unlimited.		
17. DISTRIBUTION STATEMENT (of the abstract entered in Block 20, if different from Report)		
18. SUPPLEMENTARY NOTES		
19. KEY WORDS (Continue on reverse side if necessary and identify by block number) α-β Filter Kalman Filter Track While Scan Radar		
20. ABSTRACT (Continue on reverse side if necessary and identify by block number) The efficient use of a search-surface radar or sonar, in which one or more targets appear on the screen intermittently usually demands a device for tracking the targets automatically. Such a device, called a "track while scan system", must make an estimate of each target's instantaneous position from the sampled-data information provided by the radar.		

UNCLASSIFIED

SECURITY CLASSIFICATION OF THIS PAGE/When Data Entered

#20 - ABSTRACT - CONTINUED

For this purpose, an ~~α-β~~ filter and an optimal Kalman filter, that must track maneuvering targets, are analyzed here and compared in terms of tracking accuracy for tactical applications.

c¹⁷¹⁹-beta

Accessories for

None
DD FORM
12-1967
Z
A

A

Approved for public release; distribution unlimited.

Comparison of an α - β and Kalman Filter
In Track While Scan Radars

by

Dimitrios Emmanuel Mayiatis
Lieutenant Commander, Hellenic Navy
B.S., Naval Postgraduate School, 1978

Submitted in partial fulfillment of the
requirements for the degree of

MASTER OF SCIENCE IN ELECTRICAL ENGINEERING

from the

NAVAL POSTGRADUATE SCHOOL
December 1979

Author

D. Mayiatis

Approved by:

John M. Sorey

Co-Advisor

J. R. Parker

Co-Advisor

H. T. Kirk

Chairman, Department of Electrical Engineering

William M. Tolles

Dean of Science and Engineering

ABSTRACT

The efficient use of a search-surface radar or sonar, in which one or more targets appear on the screen intermittently usually demands a device for tracking the targets automatically. Such a device, called a "track while scan system", must make an estimate of each target's instantaneous position from the sampled-data information provided by the radar.

For this purpose, an α - β filter and an optimal Kalman filter, that must track maneuvering targets, are analyzed here and compared in terms of tracking accuracy for tactical applications.

TABLE OF CONTENTS

I.	INTRODUCTION -----	12
II.	FUNDAMENTALS OF TRACK WHILE SCAN -----	15
A.	A TRACK WHILE SCAN METHOD -----	17
1.	Target Detection -----	18
2.	Generation of Target Acquisition and Tracking "Window" -----	18
3.	Track Initiation -----	20
4.	Resolution of Track Ambiguity -----	21
5.	Track Window Prediction, Smoothing, and Positioning -----	22
B.	DEFINITION OF TRACKING EQUATIONS FOR α - β FILTER -	22
1.	Stability Analysis -----	27
2.	Frequency Response Characteristics -----	32
III.	NOISE CHARACTERISTICS OF α - β FILTER -----	56
A.	NORMALIZED NOISE POWER OF PREDICTED POSITION ---	56
B.	PREDICTION ERROR DUE TO MEASUREMENT ADDITIVE NOISE ERROR -----	59
C.	PREDICTION ERROR DUE TO CONSTANT ACCELERATION ---	61
D.	TRANSIENT ERROR -----	64
E.	OPTIMAL STEADY STATE RELATIONS FOR THE - TRACKER -----	65
F.	DISCOUNTED LEAST-SQUARES (CRITICALLY DAMPED) CRITERION -----	71
1.	Numerical Example -----	75
IV.	ESTIMATING OPTIMAL TRACKING FILTER FOR MANEUVERING TARGETS -----	78
A.	SENSOR AND VEHICLE MODELING-DYNAMIC EQUATIONS ---	79

B.	STATISTICAL DESCRIPTION OF TARGET MANEUVER -----	83
C.	DISCRETE EQUATIONS Of MOTION -----	84
D.	FILTER DESCRIPTION -----	88
1.	The Kalman Filter -----	89
2.	The Simplified Kalman Filter -----	92
3.	Recursive Algorithm -----	93
V.	IMPLEMENTATION AND SIMULATION RESULTS -----	95
A.	EXAMPLE 1 - AIR SEARCH RADAR -----	103
1.	The Kalman Filter Evaluation -----	103
2.	The Simplified Kalman Filter Evaluation -----	104
B.	EXAMPLE 2 - SURFACE AND AIR SEARCH RADAR -----	105
1.	The Kalman Filter Evaluation -----	105
2.	The Simplified Kalman Filter Evaluation -----	106
C.	THE α - β FILTER EVALUATION -----	107
D.	COMPARISON OF FILTER ACCURACIES -----	108
VI.	SUMMARY AND CONCLUSIONS -----	110
APPENDIX A:	SIMULATION RESULTS - PROGRAM OUTPUTS -----	112
LIST OF REFERENCES -----	149	
INITIAL DISTRIBUTION LIST -----	151	

LIST OF TABLES

Table	Page
I. Accuracy between smoothed and predicted, position and velocity of α - β filter -----	55
II. Synopsis of the accuracy comparison of the three tracking filters -----	109

LIST OF FIGURES

Figure	Page
1. Track while scan volumetric windows -----	19
2. TWS principle and position tracking -----	23
3. TWS general processing -----	24
4. Block diagram of an α - β tracker -----	27
5. The stability triangle -----	31
6. Allowable values of α and β in α - β tracker -----	32
7. Amplitude and phase of smoothed position G_{xs} for $\alpha = 0.1$ -----	34
8. Amplitude and phase of predicted position G_{xp} for $\alpha = 0.1$ -----	35
9. Amplitude and phase of smoothed position G_{xs} for $\alpha = 0.5$ -----	36
10. Amplitude and phase of predicted position G_{xp} for $\alpha = 0.5$ -----	37
11. Amplitude and phase of smoothed position G_{xs} for $\alpha = 0.75$ -----	38
12. Amplitude and phase of predicted position G_{xp} for $\alpha = 0.75$ -----	39
13. Amplitude and phase of smoothed position G_{xs} for $\alpha = 0.9$ -----	40
14. Amplitude and phase of predicted position G_{xp} for $\alpha = 0.9$ -----	41
15. Amplitude and phase of smoothed position G_{xs} for $\alpha = 1.5$ -----	42
16. Amplitude and phase of predicted position G_{xp} for $\alpha = 1.5$ -----	43
17. Amplitude and phase of smoothed velocity G_{vs} for $\alpha = 0.1$ -----	44

18.	Amplitude and phase of predicted velocity G_{vp} for $\alpha = 0.1$	45
19.	Amplitude and phase of smoothed velocity G_{vs} for $\alpha = 0.5$	46
20.	Amplitude and phase of predicted velocity G_{vp} for $\alpha = 0.5$	47
21.	Amplitude and phase of smoothed velocity G_{vs} for $\alpha = 0.75$	48
22.	Amplitude and phase of predicted velocity G_{vp} for $\alpha = 0.75$	49
23.	Ampliutde and phase of smoothed velocity G_{vs} for $\alpha = 0.9$	50
24.	Amplitude and phase of smoothed velocity G_{vp} for $\alpha = 0.9$	51
25.	Amplitude and phase of smoothed velocity G_{vs} for $\alpha = 1.5$	52
26.	Amplitude and phase of predicted velocity G_{vp} for $\alpha = 1.5$	53
27.	Predicted position noise power as a function of α and β	60
28.	Prediction error due to additive noise as a function of α and β	62
29.	Predicted position noise and prediction error due to additive noise	63
30.	Transient error for $T = 0.1$ as a function of α and β	66
31.	Transient error for $T = 0.3848$ as a function of α and β	67
32.	Transient error for $T = 0.5$ as a function of α and β	68
33.	Steady state filter gain relations	70
34.	α - β gain for least-square criterion as a function of theta	73
35.	α - β gain for continually compute the least-squares line as a function of observations (N)	74

36.	Schematic of a digital filter structure in relation to signal process -----	78
37.	Typical probability density of target maneuver -----	84
38.	Block diagram and equations of the discrete Kalman filter -----	91
39.	Vehicle trajectory -----	96
40.	Range in X-axis vs time -----	97
41.	Velocity in X-axis vs time -----	98
42.	Acceleration in X-axis vs time -----	99
43.	Bearing in X-axis vs time -----	100
44.	Bearing rate in X-axis vs time -----	101
45.	Bearing acceleration in X-axis vs time -----	102
46-51.	Range, velocity, means and covariances vs time for α - β filter -----	111-118
52-63.	Range, velocity, bearing, bearing rate, means, covariances vs time for simplified Kalman filter -----	119-130
64-81.	Range, velocity, acceleration, bearing, bearing rate, bearing acceleration, means and covariances vs time for Kalman filter -----	131-148

ACKNOWLEDGMENT

This thesis is dedicated to my wife Katherine, for her great help, forbearance, devotion and understanding.

I. INTRODUCTION

Systems such as search-surface radar and sonar, in which the input data arrives intermittently, frequently require a device for continuously estimating the "present" value of the input. In radar terminology, this device is called a "track while scan system".

In a more general sense, the term "track while scan" system, may denote any system which estimates the "present" value of a signal from the "past" sampled values of the signal, the sampling taking place at regular intervals.

Vehicles, without maneuvering, of the class under consideration (such as aircraft, ships, and submarines) generally follow straight line constant velocity trajectories. If the vehicles were not able to deviate from these trajectories, i.e., could not maneuver, then the tracking problem could be solved quickly and simply using standard filtering such as an α - β filter.

Historically, α - β filters were designed to minimize the mean square error in filtered position and velocity under the assumption of small velocity changes between data samples. Thus, most α - β filters have little capacity to track targets that either accelerate or maneuver (changing direction). An important early paper [1] defines β in terms of α with α a design parameter. This greatly simplified the use of maneuver detectors by reducing the design problem to a single variable.

A later advance in α - β filter design was achieved by minimizing the mean square error in predicted position [2].

A system that developed using the above technique is the VEGA LN I (Thomson-CSF, France).

The final choice of parameters for the α - β tracker will always end in a compromise between smoothing the input noise (measurement errors) and retaining some ability to follow a maneuvering target. Various performance measures have been used for this compromise. For example, steady state noise variance reduction and the ability to follow a target capable of responding to impulse accelerations are used as performance measures in [1] to derive good steady state filter parameters. Time varying noise variance reduction and the ability to follow a randomly maneuvering target are performance criteria which follow from [3]. In this paper, such a filter is analyzed, the frequency response, stability, noise characteristics and transient error are derived and plotted, and a scheme for optimizing the two dynamic parameters (α - β) is suggested.

A criterion for α - β filter design with a numerical and graphical example is also given.

Since the majority of tactical weapons systems requires that manned maneuverable vehicles, such as aircraft, ships, and submarines, be tracked accurately, an optimal Kalman filter has been derived for this purpose, based on the early work of [4,5]. The target model for tracking applications must be sufficiently simple to permit ready implementation in weapons

systems for which computation time is at a premium yet sufficiently sophisticated to provide satisfactory tracking accuracy.

The target acceleration selected for the Kalman filter, and hence the target maneuver is correlated in time; namely, if a target is accelerating at time t , it is likely to be accelerating at time $t+\tau$ for sufficiently small τ . By simplifying the maneuvering model used in the Kalman filter above, the state vector can be reduced from six to four elements. The model simplification - simplified Kalman filter - is achieved by assuming (incorrectly) that the vehicle's change in velocity is uncorrelated between samples; i.e., the maneuver is white. In the comparison which follows, the Kalman filter and Simplified Kalman filter are compared with the $\alpha-\beta$ filter in a variety of tactical environments with tracking sensors, utilizing Monte Carlo simulation techniques on realistic target trajectories to verify their theoretical performance.

II. FUNDAMENTALS OF TRACK-WHILE-SCAN

Any system which performs a tracking function must obtain and utilize the basic target parameters of position and rates of motion. In the earlier system both position data and velocity data were used to maintain the tracking antenna on the target at all times, thus limiting the system to the classical one target-at-a-time tracking function.

In a track-while-scan system, target position must be extracted and velocities calculated for many targets without holding the radar antenna fixed on one target. Obviously in a system of this type, target data is not continuously available for each target track at a rate dependent upon the scan rate of the system.

In a typical TWS system the data rate is one unit of data per second or a scan rate for the search radar antenna.

Since the antenna is continuing to scan, some means of storing and analyzing target data from one update to the next and beyond is necessary. The digital computer with its memory and computational capability is employed to perform this function and also:

- (i) To provide a tactical picture

A display of the tracks of all vehicles observed by sensors showing present positions, courses and speeds etc., is essential for the deployment of a ship and its weapons. The computer enables rapid use to be made of sensor information thereby ensuring that the picture is accurate and up-to-date.

(ii) For use in processes such as threat evaluation and weapon assignment

The computer can forecast future likely positions of tracked vehicles and rapidly perform necessary calculations to assist operators in the assessment of threats and in the optimum weapon deployment to deal with them.

(iii) To provide target information for weapon deployment

The computer can be used to generate smooth tracks from noisy information thereby being able to pass information to a weapon sensor more accurately than information derived from a single plot on display. Hence, the central concept underlying any TWS system is that the sensor itself continues to perform its primary function of search (scanning) and data input while the remainder of the system performs the target tracking function. The sensor function simply provides target position data to the computer subsystem where target velocities and position prediction are calculated. In a military application the major advantage of a TWS system is the elimination of the process of target designation from a search radar to a fire control radar.

The tracking information, developed in the TWS system, is used as a direct data input to the computation of a fire control solution.

Therefore, as soon as a target is detected a fire control solution is available without the inherent delay caused by the designation process. The time required from first detection

to fire control solution is on the order of milli-seconds for a TWS system as opposed to seconds or even minutes for a manually designated system employing separate search and fire control sensors.

The focus of the following chapter has been to answer the question: "What functions should the TWS system perform in order to combine the search and tracking tasks into one integrated unit?"

A. A TRACK WHILE SCAN METHOD

The method of solving the track while scan problem is based upon the assumption that the radar furnishes target position information once each scan. The scheme can be implemented by a combination of special radar circuits (hardware) and software. Existing systems also provide for operator modification of system tracking.

Any track-while-scan system must provide for each of the following functions:

- (i) Target detection
- (ii) Generation of target acquisition and tracking "windows" or "gates"
- (iii) Target track initiation (assignment of targets to track files)
- (iv) Target data input and track correlation
- (v) Track "window" prediction, smoothing and positioning

1. Target Detection

Target detection, localization and designation are accomplished by the radar sub-system in the usual sense. Hence, the TWS receives the following data from the outside, via wire links:

- (i) The surveillance antenna azimuth
- (ii) The radar synchronization (presyne)
- (iii) The surveillance radar video

2. Generation of Target Acquisition and Tracking "Windows"

A "window" can be defined as a small volume of space initially centered on a target, which will be monitored on each scan for the presence of target information. Each initial target detection will cause a relatively large acquisition "window" to be generated, centered on the position of the detection. When a target is initially detected the algorithm receives only the position data for that initial, instantaneous target position. The acquisition window is then generated, for example:

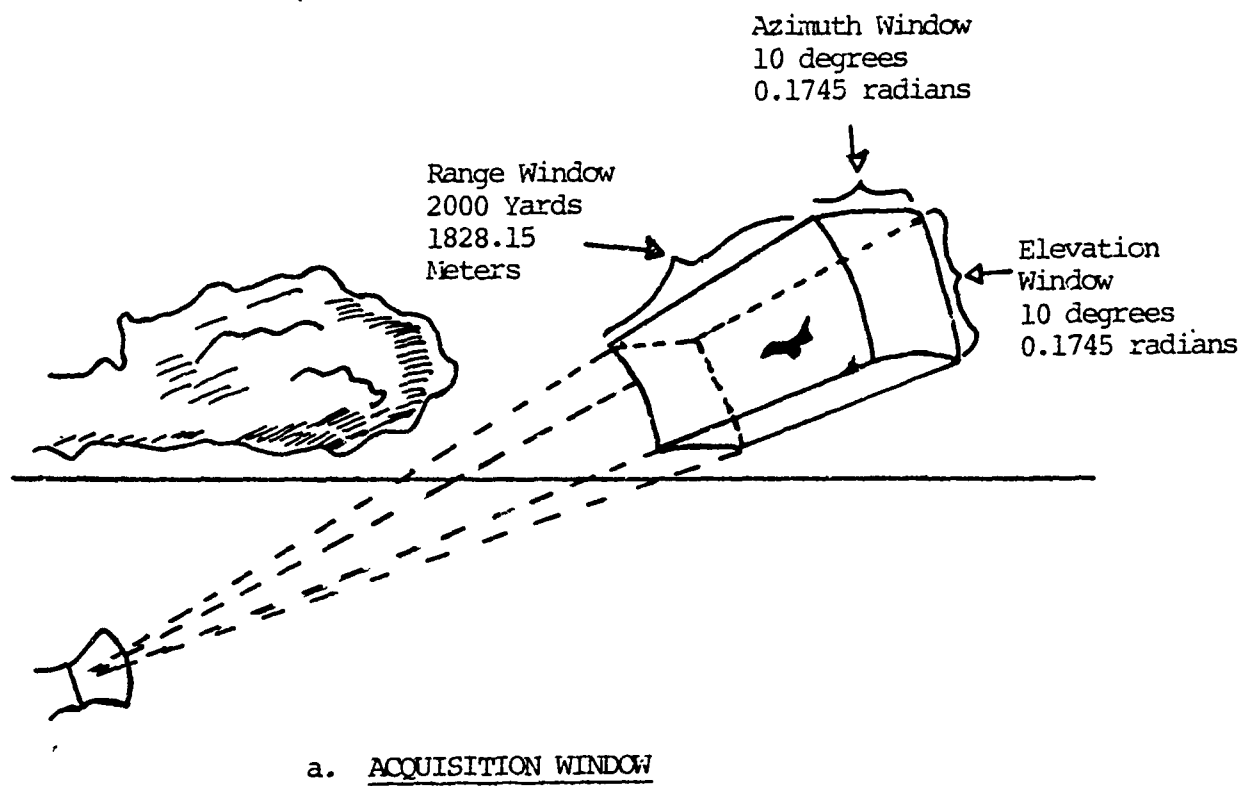
Initial position = (Range, Bearing, Elevation)

Range window = $R \pm 1000$ yards (914.1 meters)

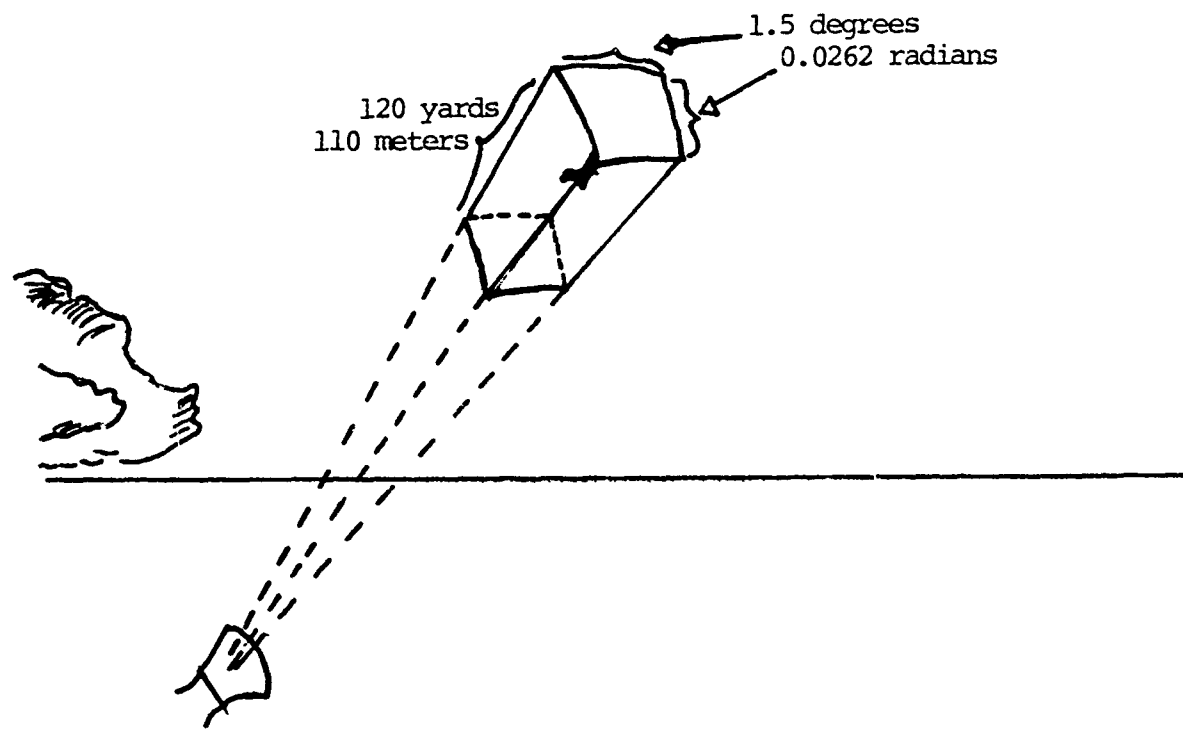
Bearing window = $B \pm 5^\circ$ (0.0873 radians)

Elevation window = $E \pm 5^\circ$ (0.0873 radians)

The acquisition window, Fig. 1a, is large in order to allow for target displacement during the following scans of the radar. If on the next radar scan the target is within the acquisition window, a tracking window is generated in the



a. ACQUISITION WINDOW



b. TRACKING WINDOW

FIG. 1. TRACK WHILE SCAN VOLUMETRIC WINDOWS

same manner as the acquisition window. Although Fig. 1b shows only the very small, 120 yards, 1.5° , 1.5° tracking window, in actual practice intermediate window sizes are generated until a smooth track is achieved.

3. Track Initiation

Concurrent with the generation of the acquisition window a track file is generated in order to store the position and window data for each track. In addition to the basic position and window data, calculated target velocities and accelerations are also stored in each track file. Track files are stored within the digital computer (or processor) subsystems memory and the data is used to perform the various calculations necessary to maintain the track.

Each track file occupies a discrete position of the digital computer's (or processor's) high speed memory. As data are needed for computation or new data are to be stored, the portion of memory which is allocated for the required data will be accessed by the system programs (software). In this manner a diversity of data in addition to the tracking data may be stored in the "track" file, for example, ESM data, IFF information. The generation of the track file begins with the initial storage of position data along with a code to indicate that an acquisition window has been established. If target position data is obtained on subsequent scans of the radar, the file is updated with the coordinates; the velocities and accelerations are computed and stored, and the acquisition window code is canceled.

The acquisition window is then decreased in size to the tracking window and the track code is stored which indicates an active track file.

As the radar continues to scan, each input of data is compared with the window positions of active track files until the proper file is found and updated. However, it should be noted that the search for the proper track file is generally not a sequential one-to-one comparison. This method is much too slow to be used in a system where speed of operation is one of the primary goals.

This idea of comparing output data with window positions leads us to the problem of correlation of data input to track files and what to do if correlation is ambiguous.

4. Resolution of Track Ambiguity

Track ambiguity arises when either multiple targets appear within a single track window or two or more windows overlap on a single target.

This occurrence can cause the system to generate erroneous tracking data and ultimately lose the ability to maintain a meaningful track. If the system is designed so that an operator initiates the track and monitors its progress, the solution is simply for the operator to cancel the erroneous track and initiate a new one.

For systems which are to be automatic, software (programming) decision rules must be established which will enable the tracking program to maintain accurate track files. Decision

rules as to target input data and track correlation can be logically developed with an understanding of the definition of the track ambiguity problem.

5. Track Window Prediction, Smoothing, and Positioning

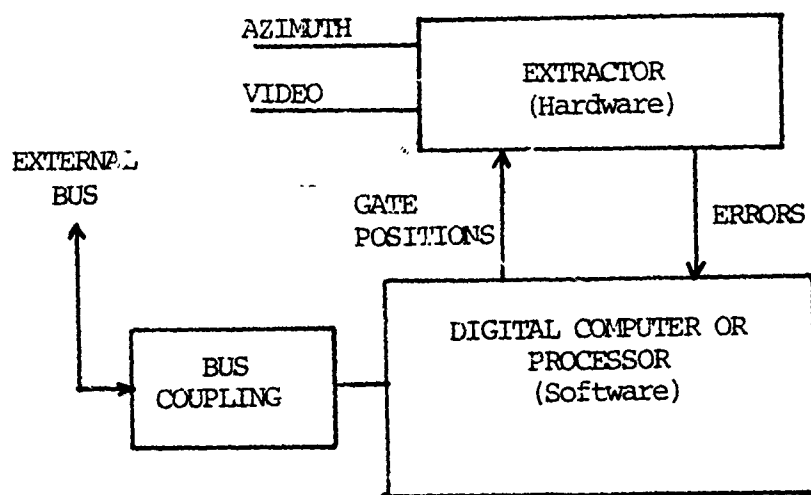
In a track-while-scan system tracking errors also exist due to target motion. The tracking window now has replaced the "tracking antenna" and this window must be positioned dynamically on the target in a similar manner as was the "tracking antenna". However, there is no "servo" system to reposition and smooth the tracking window's motion. This repositioning and smoothing must be done mathematically within the TWS algorithm. To this end, smoothing and prediction equations (Eqs. 2.1-2.3) are employed to calculate the changing position of the tracking window. Instead of the system "lagging" the target the tracking window is made to "lead" the target and smoothing is accomplished by comparing predicted parameters with observed (measured) parameters and making adjustments based upon the errors derived from this comparison.

Figs. 2 a-b and 3, illustrate the TWS principle, track positioning and the TWS general processing loop of the alpha-beta type, respectively.

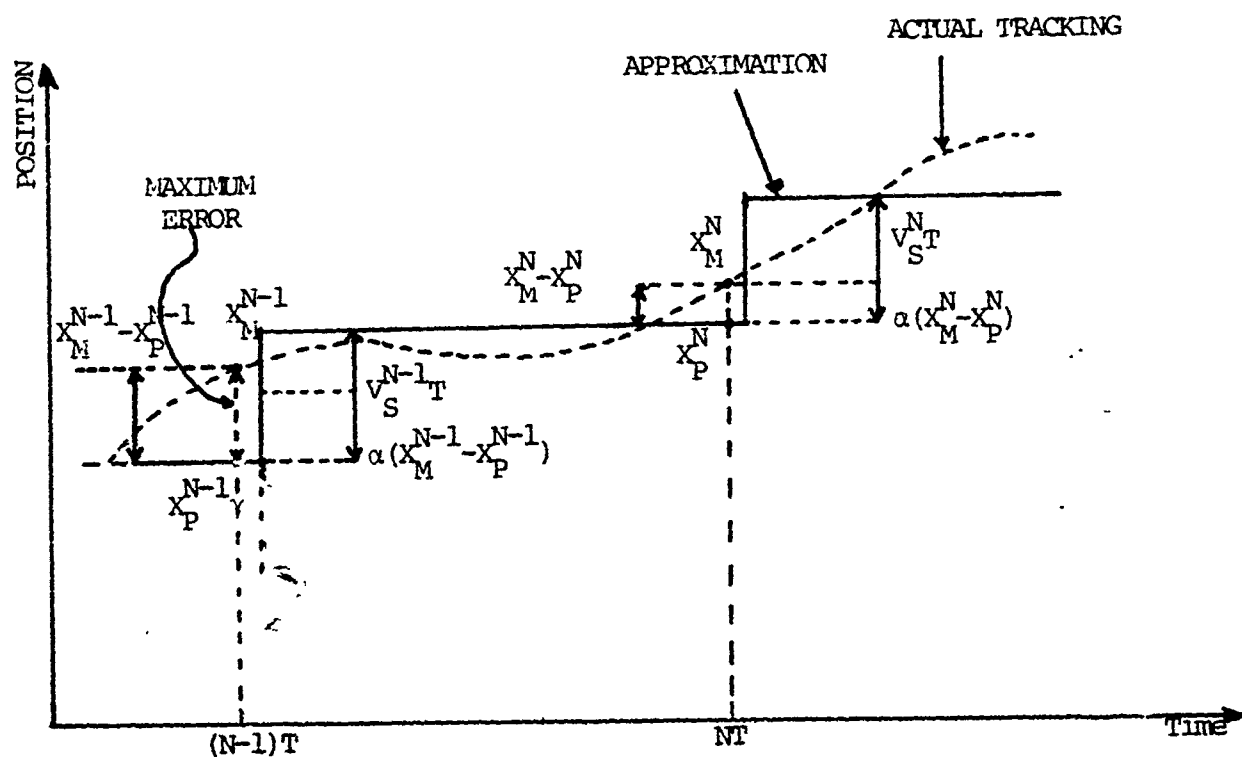
B. DEFINITION OF TRACKING EQUATIONS FOR α - β FILTER

Tracking in a track-while-scan (TWS) system consists basically of two functions:

- a. Smoothing
- b. Correlation

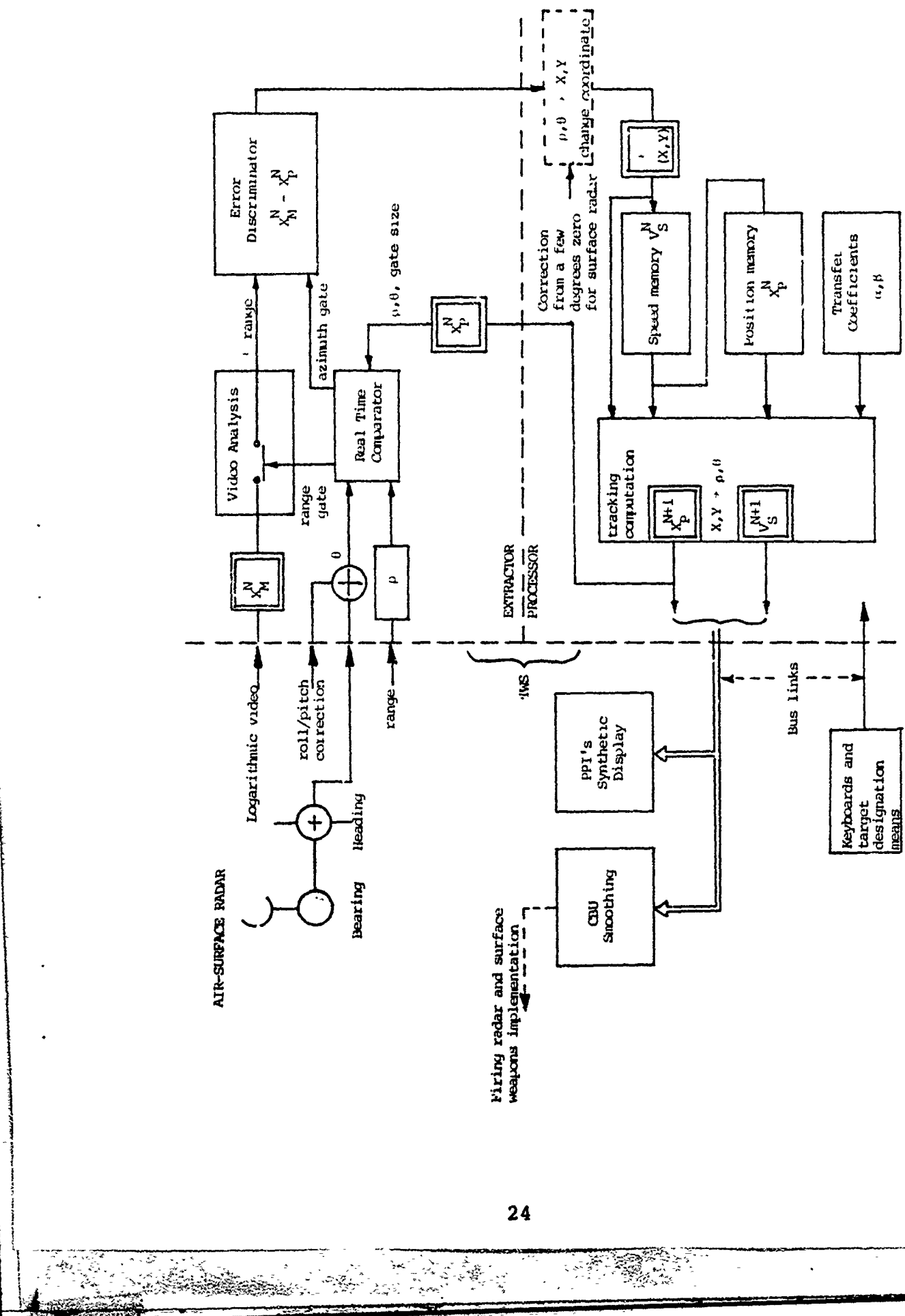


a. TWS PRINCIPLE



b. TWS POSITION TRACKING

FIG. 2. TWS PRINCIPLE AND POSITION TRACKING



Smoothing is the processing of the sensor reports to derive an estimate of both target velocity and position.

Correlation is the sorting of sensor reports into groups, to determine which belong to which target then predicting a new coordinate on which to center the correlation region.

The constants of proportionality, α and β , used in correcting the position and velocity, respectively, of the estimated target course, completely characterize the performance of the TWS system. These constants are the dynamic parameters or so-called "smoothing constants" of the system.

Finally, the simplest case target tracks are based on smoothing and prediction of an alpha (α) - beta (β) tracker operating in a cartesian coordinate reference frame. The information is ordinarily obtained from a coordinate converter operating on the raw polar to cartesian transform. The α - β filter described by the well-known α - β tracking equations [6,7]:

$$x_s^N = x_p^N + \alpha(x_m^N - x_p^N) \quad \text{smoothing Equation (2.1)}$$

$$v_s^N = v_s^{N-1} + \frac{\beta(x_m^N - x_p^N)}{T} \quad \text{prediction Equation (2.2)}$$

$$x_p^N = x_s^{N-1} + v_s^{N-1} T \quad \text{prediction Equation (2.3)}$$

where:

x_s = smoothed position

x_p = predicted position

v_s = smoothed velocity

x_m = measured position

α, β = filter parameters or filter gains

T = sampling time or time between detections

Substituting Eq. (2.3) into Eqs. (2.1) and (2.2) yields

$$x_s^N = (1-\alpha)x_s^{N-1} + (1-\alpha)Tv_s^{N-1} + \alpha x_m^N \quad (2.4)$$

$$v_s^N = -\frac{\beta}{T}x_s^{N-1} + (1-\beta)v_s^{N-1} + \frac{\beta}{T}x_m^N \quad (2.5)$$

$$x_p^{N+1} = x_s^N + v_s^N T \quad (2.6)$$

or

$$\begin{bmatrix} x_s \\ v_s \end{bmatrix}^N = \begin{bmatrix} (1-\alpha) & (1-\alpha)T \\ -\frac{\beta}{T} & (1-\beta) \end{bmatrix} \begin{bmatrix} x_s \\ v_s \end{bmatrix}^{N-1} + \\ + \begin{bmatrix} \alpha \\ \frac{\beta}{T} \end{bmatrix} [x_m]^N \quad (2.7)$$

and

$$[x_p]^{N+1} = [1 \quad T] \begin{bmatrix} x_s \\ v_s \end{bmatrix}^N \quad (2.8)$$

These equations represented in block diagram form appear in Fig. 4.

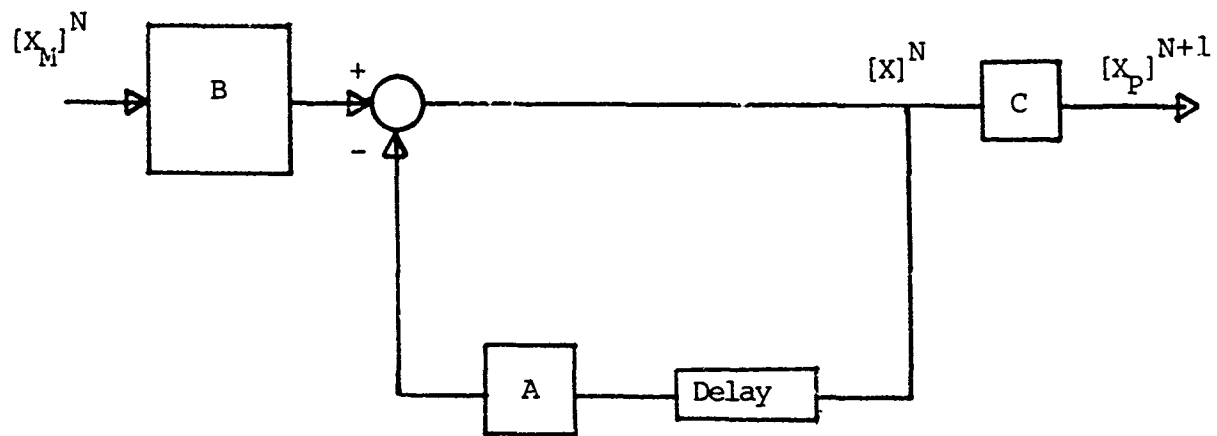


Fig. 4. Block Diagram of an α - β Tracker

where the following matrices and vectors are defined:

$$A = \begin{bmatrix} (1-\alpha) & (1-\alpha)T \\ -\beta/T & (1-\beta) \end{bmatrix} \quad B = \begin{bmatrix} \alpha \\ \beta/T \end{bmatrix}$$

$$C = [1 \quad T] \quad \bar{x} = \begin{bmatrix} x_S \\ v_S \end{bmatrix}$$

1. Stability Analysis

Since the system characteristic equations are in the form of difference equations, Z-transform theory is helpful in determining filter transfer functions and stability criteria.

For the system of the form:

$$\bar{X}_{N+1} = A\bar{X}_N + B(X_M - CX_N)$$

or

$$\bar{X}_{N+1} = (A - BC)\bar{X}_N + BX_M$$

thus,

$$G(z) = \frac{\bar{X}(z)}{X_M(z)} = [zI - (A-BC)]^{-1} B \quad (2.9)$$

Using Eq. (2.9), the Z-transform for each of the several components of Eq. (2.7) and (2.8) has been computed and is given below. Hence, the $\alpha-\beta$ tracker transfer functions:

$$G_{XS}(z) = \frac{X_S(z)}{X_M(z)} = \frac{z[\alpha(z-1) + \beta]}{D(z)} \quad \text{Smoothed position} \quad (2.10)$$

$$G_{VS}(z) = \frac{V_S(z)}{X_M(z)} = \frac{\frac{\beta}{T}z(z-1)}{D(z)} \quad \text{Smoothed velocity} \quad (2.11)$$

$$G_{XP}(z) = \frac{X_P(z)}{X_M(z)} = \frac{\alpha(z-1) + \beta z}{D(z)} \quad \text{Predicted position} \quad (2.12)$$

$$G_{VP}(z) = \frac{V_P(z)}{X_M(z)} = \frac{\frac{\beta}{T}(z-1)}{D(z)} \quad \text{Predicted velocity} \quad (2.13)$$

where the characteristic equation of the system is

$$D(z) = |zI - A| = 0$$

or

$$D(z) = z^2 - (2 - \alpha - \beta)z + (1 - \alpha) = 0 \quad (2.14)$$

The stability of the system can be determined from the location of the roots of the characteristic equation above.

A few methods are available for determining whether or not a polynomial in z contains a root or roots on or outside the unit circle. One method is to modify the Routh-Hurwitz stability criterion. The Routh stability criterion tells whether or not any of the roots of a polynomial lie in the right half of the complex plane.

Since the following transformation

$$z = \frac{r+1}{r-1}$$

maps the interior of the unit circle in the z plane to the left-half r plane, with this transformation, permits the application of the Routh stability criterion to the polynomial in r as in continuous-time systems.

Now Eq. (2.14) becomes a polynomial in r , in the form

$$\beta r^2 + 2\alpha r + 4 - 2\alpha - \beta = 0 \quad (2.15)$$

So, the resulting requirements for stability are

$$\alpha > 0, \quad \beta > 0 \quad \text{and} \quad (2\alpha + \beta) < 4 \quad (2.16)$$

An additional stable condition exists when $\beta = 0$. Thus the resulting necessary and sufficient conditions for the stability of the track-while-scan system are

$$\alpha > 0, \quad \beta \geq 0, \quad \text{and} \quad (2\alpha + \beta) \leq 4 \quad (2.17)$$

These inequalities determine a "stability triangle" in the $\alpha-\beta$ plane, for which all internal points and all points on the base ($\beta = 0$) in the interval $0 < \alpha < 2$ correspond to a stable system. This triangle is shown in Fig. 5.

The conditions for underdamped, critically damped, and overdamped transient response are found by inspecting the sign of the discriminant of Eq. (2.14). The resulting conditions are:

$$(\alpha + \beta)^2 < 4\beta \iff \text{underdamped} \quad (2.18)$$

$$\beta \leq 1, (\alpha + \beta)^2 = 4\beta \iff \text{critically damped} \quad (2.19)$$

$$\alpha \leq 1, \beta < 1, (\alpha + \beta)^2 > 4\beta \iff \text{overdamped} \quad (2.20)$$

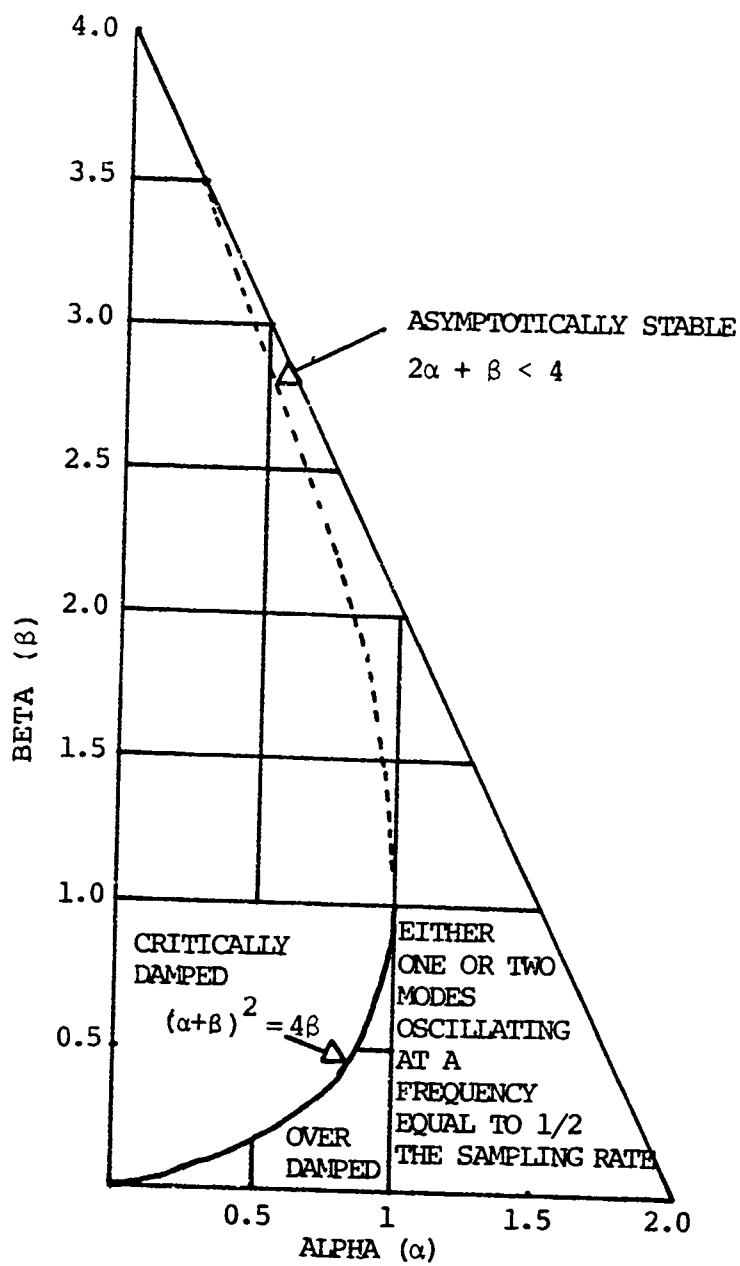


FIG. 5. THE STABILITY TRIANGLE

All other values of
 (α, β) inside the stability
triangle and on the base
 $(\beta = 0)$ in the interval
 $0 < \alpha < 2$

\Leftrightarrow
The transient response
contains at least one
damped oscillatory natural
mode with a rate of
oscillation equal to one
half the sampling frequency

The permissible values of α and β are shown in Fig. 6

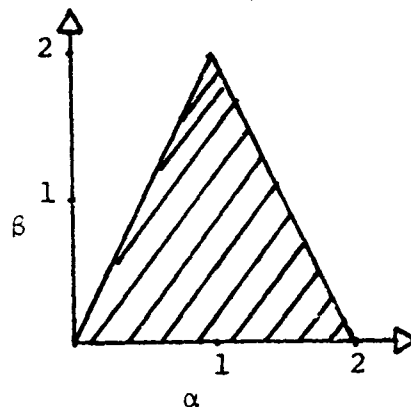


Fig. 6. Allowable Values of α and β in α - β Tracker

Further restrictions will be placed on this region, when the frequency response characteristics of the system are examined.

2. Frequency Response Characteristics

In this section, the frequency response characteristics of the α - β filter are formed. This approach has not been done before, in detail.

The frequency response of the filter can be found by placing $Z = e^{j\omega T}$ and $e^{j\omega T} = \cos \omega T + j \sin \omega T$ into Eqs. (2.10) - (2.13). These equations are now in the form:

$$G_{XS}(e^{j\omega T}) = \frac{[\alpha(\cos 2\omega T - \cos \omega T) + \beta \cos \omega T] + j[\alpha(\sin 2\omega T - \sin \omega T) + \beta \sin \omega T]}{D(e^{j\omega T})} \quad (2.21)$$

$$G_{VS}(e^{j\omega T}) = \frac{[\frac{\beta}{T}(\cos 2\omega T - \cos \omega T)] + j[\frac{\beta}{T}(\sin 2\omega T - \sin \omega T)]}{D(e^{j\omega T})} \quad (2.22)$$

$$G_{XP}(e^{j\omega T}) = \frac{[(\alpha+\beta)\cos \omega T - \alpha] + j[(\alpha+\beta)\sin \omega T]}{D(e^{j\omega T})} \quad (2.23)$$

$$G_{VP}(e^{j\omega T}) = \frac{[\frac{\beta}{T}(\cos \omega T - 1)] + j[\frac{\beta}{T}\sin \omega T]}{D(e^{j\omega T})} \quad (2.24)$$

where

$$D(e^{j\omega T}) = [\cos 2\omega T - (2-\alpha-\beta)\cos \omega T + (1-\alpha)] + j[\sin 2\omega T - (2-\alpha-\beta)\sin \omega T]$$

The amplitude and phase characteristics of G_{XS} (smoothed position) and G_{XP} (predicted position) are plotted and shown in Figs. 7-16, for several values of α and β . Also the amplitude and phase characteristics of G_{VS} (smoothed velocity) and G_{VP} (predicted velocity) are shown in Figs. 17-26. All the amplitudes and phases are plotted as a function of α , β and ωT .

Observing these figures and Eqs. (2.7) - (2.8) one finds that x_S^N is the result of passing x_M^N through a low pass filter, v_S^N is the result of differentiating x_M^N , and α should never be larger than one.

It may be seen also, for positional smoothing, if $\alpha = 0$, all sensor information is ignored whereas if $\alpha = 1$, there is no smoothing of positional information. Similarly $\beta = 0$ causes sensor information to be ignored in the estimation of velocity whereas $\beta > 1$ will cause overcorrection.

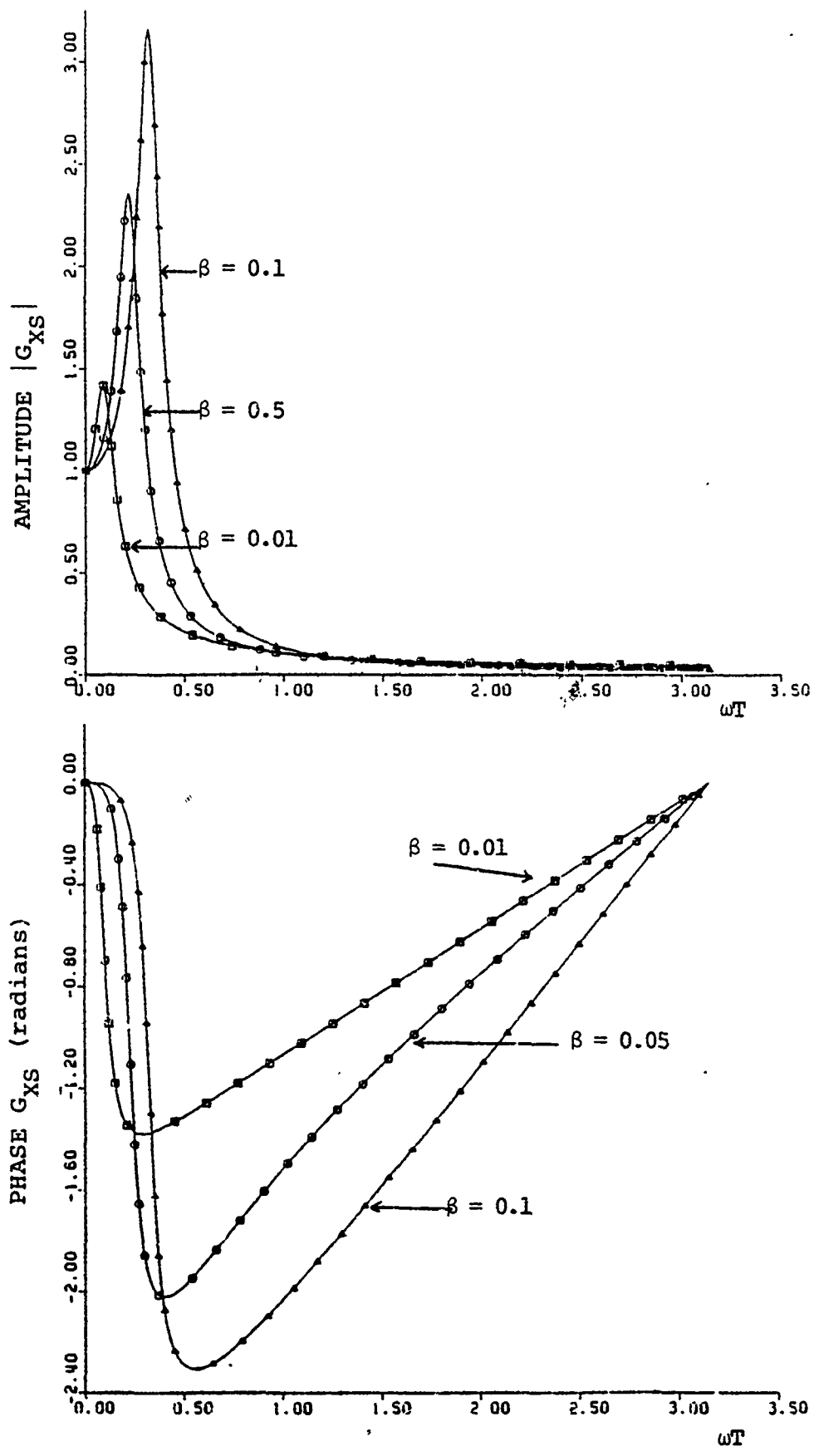


FIG. 7. AMPLITUDE AND PHASE OF SMOOTHED POSITION G_{XS} FOR $\alpha = 0.1$

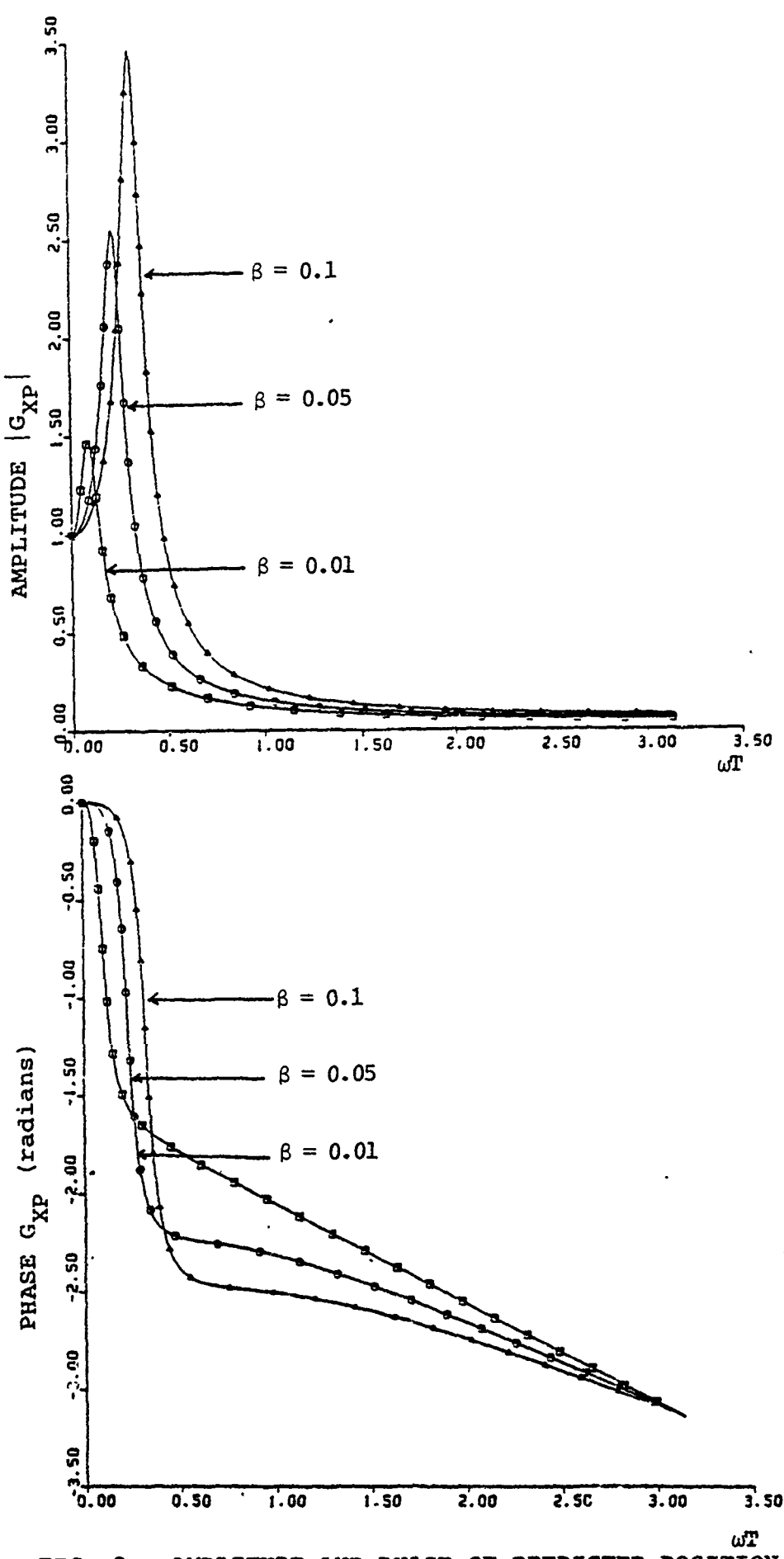


FIG. 8. AMPLITUDE AND PHASE OF PREDICTED POSITION G_{XP}
FOR $\alpha = 0.1$

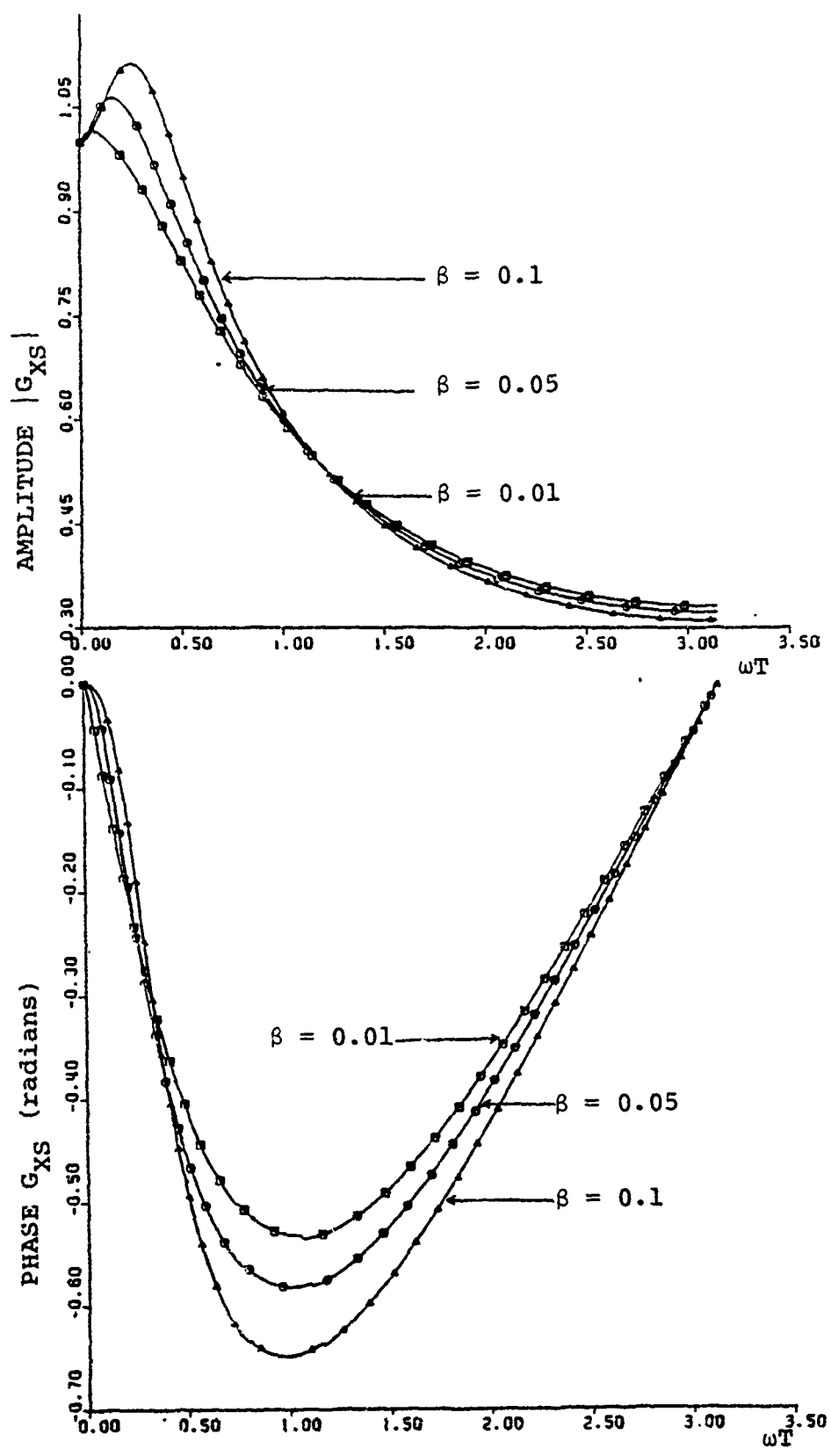


FIG. 9. AMPLITUDE AND PHASE OF SMOOTHED POSITION G_{xs}
FOR $\alpha = 0.5$

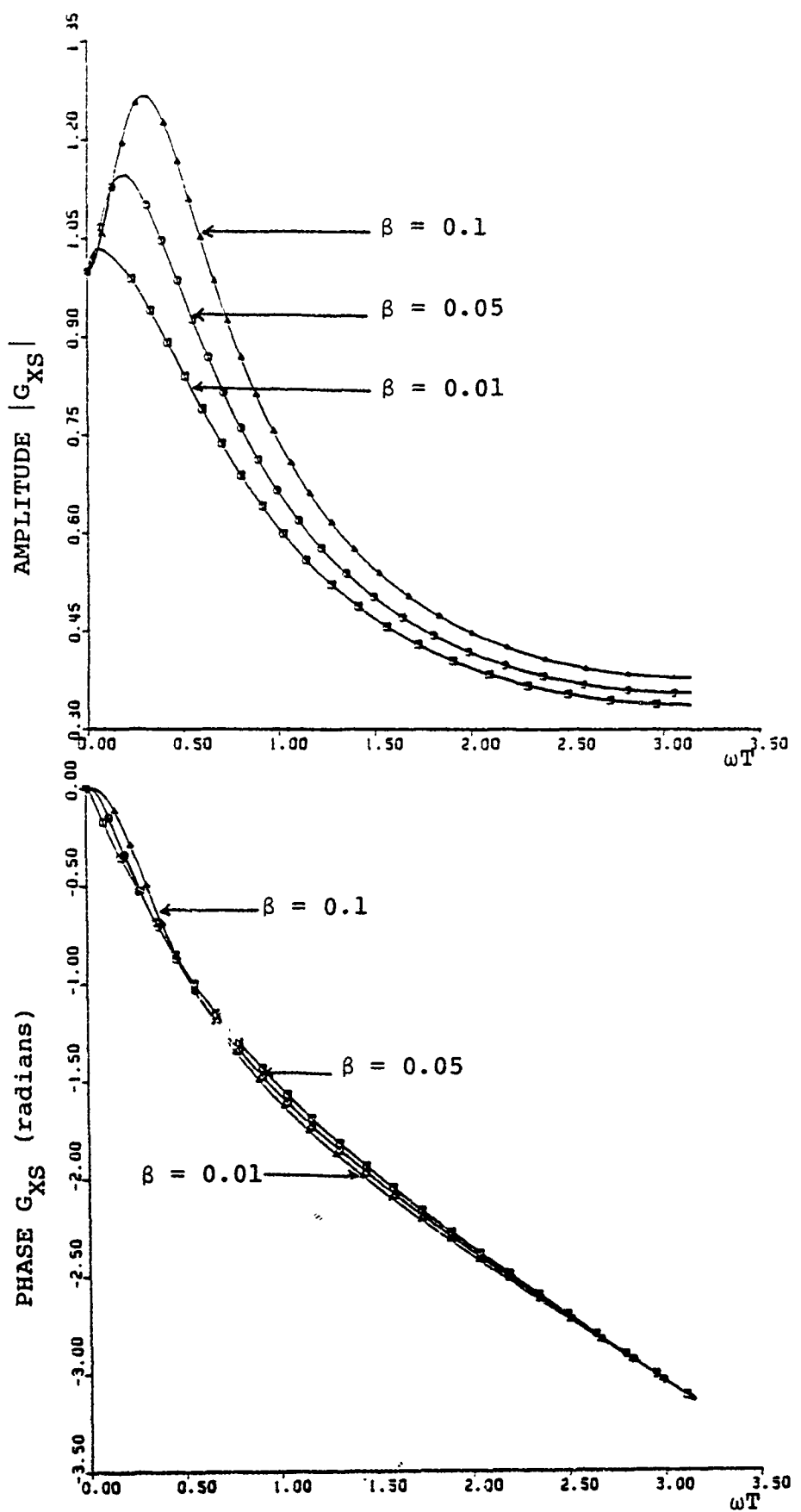


FIG. 10. AMPLITUDE AND PHASE OF PREDICTED POSITION G_{XP} FOR $\alpha = 0.5$

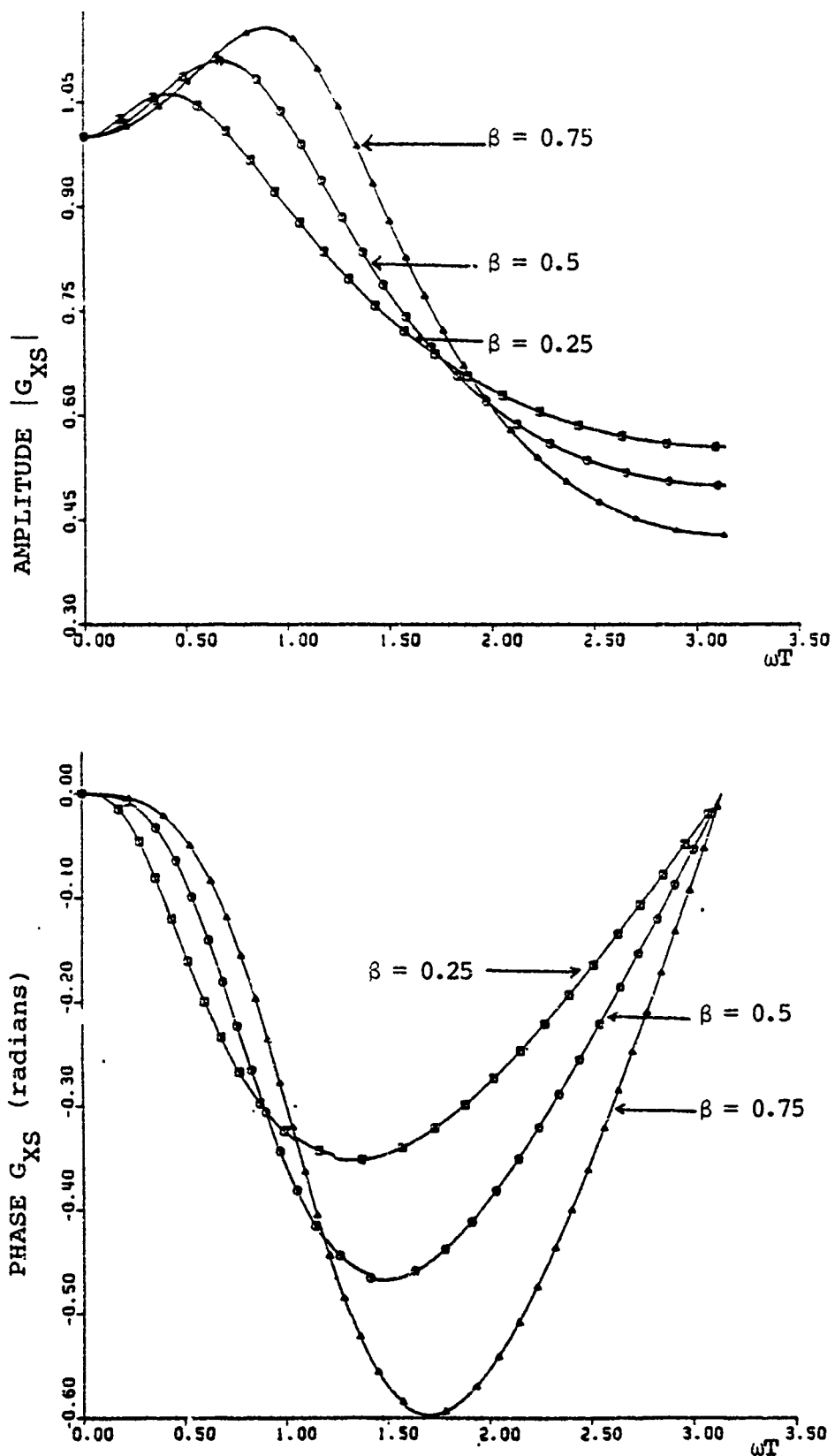


FIG. 11. AMPLITUDE AND PHASE OF SMOOTHED POSITION G_{XS}
FOR $\alpha = 0.75$

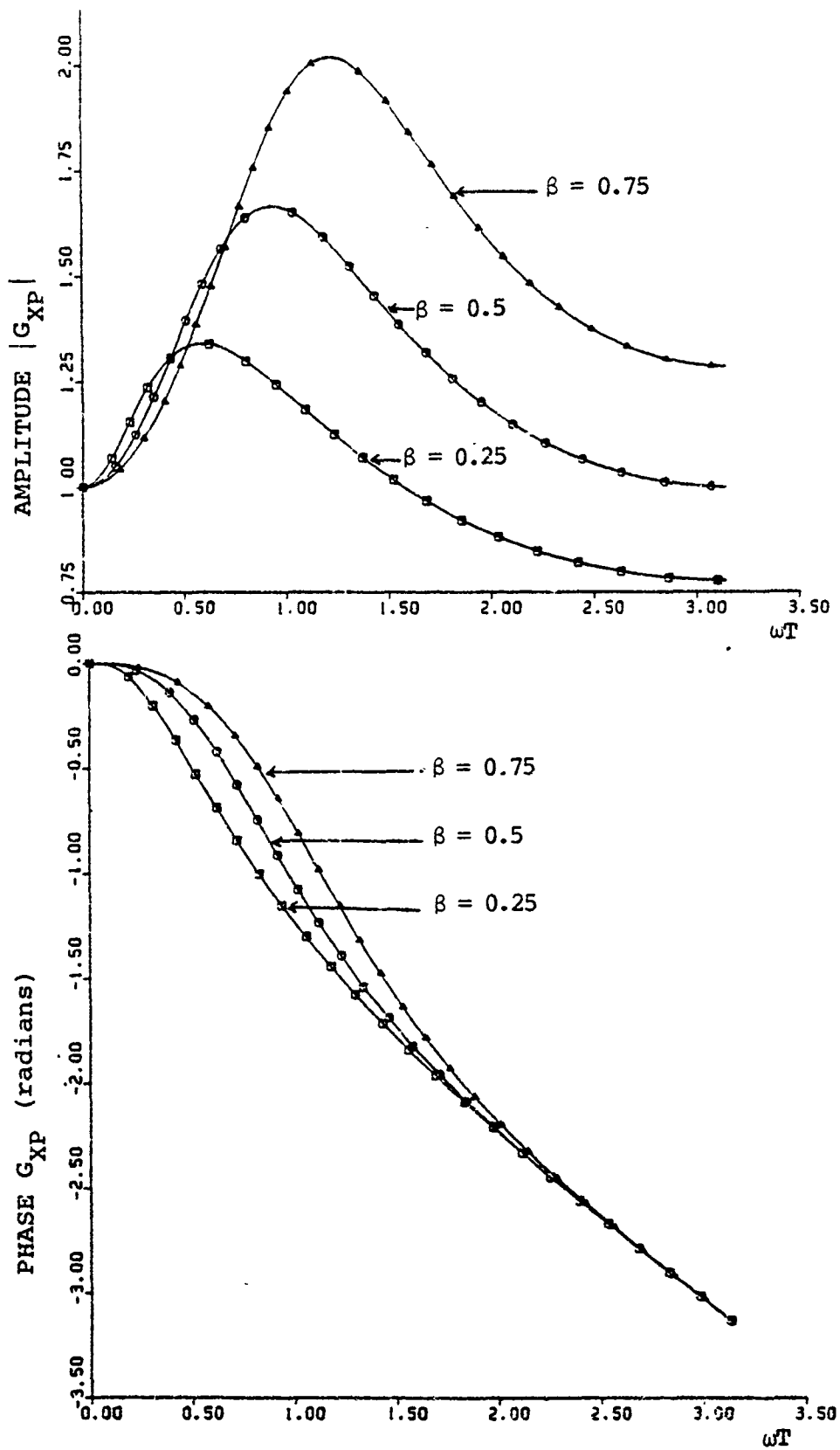


FIG. 12. AMPLITUDE AND PHASE OF PREDICTED POSITION G_{XP}
FOR $\alpha = 0.75$

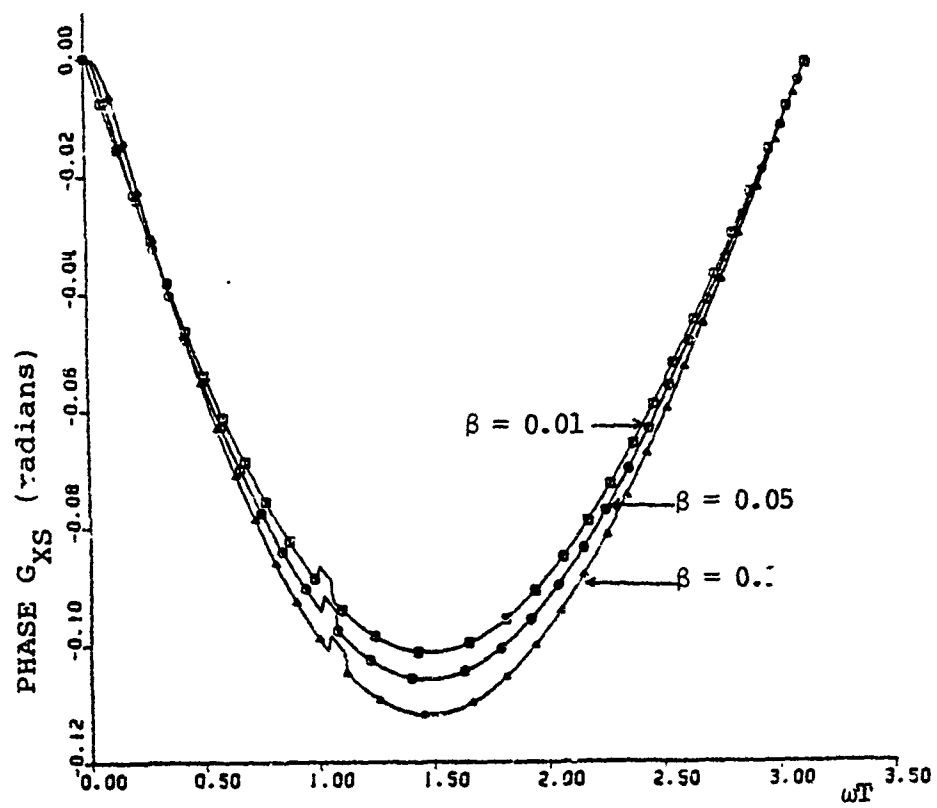
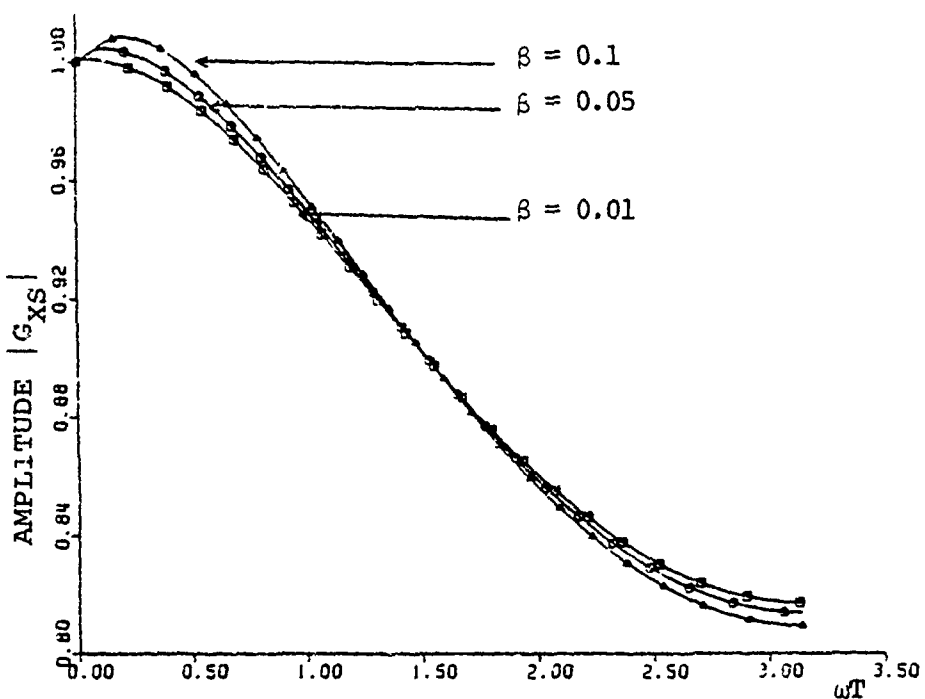


FIG. 13. AMPLITUDE AND PHASE OF SMOOTHED POSITION G_{XS}
FOR $\alpha = 0.9$

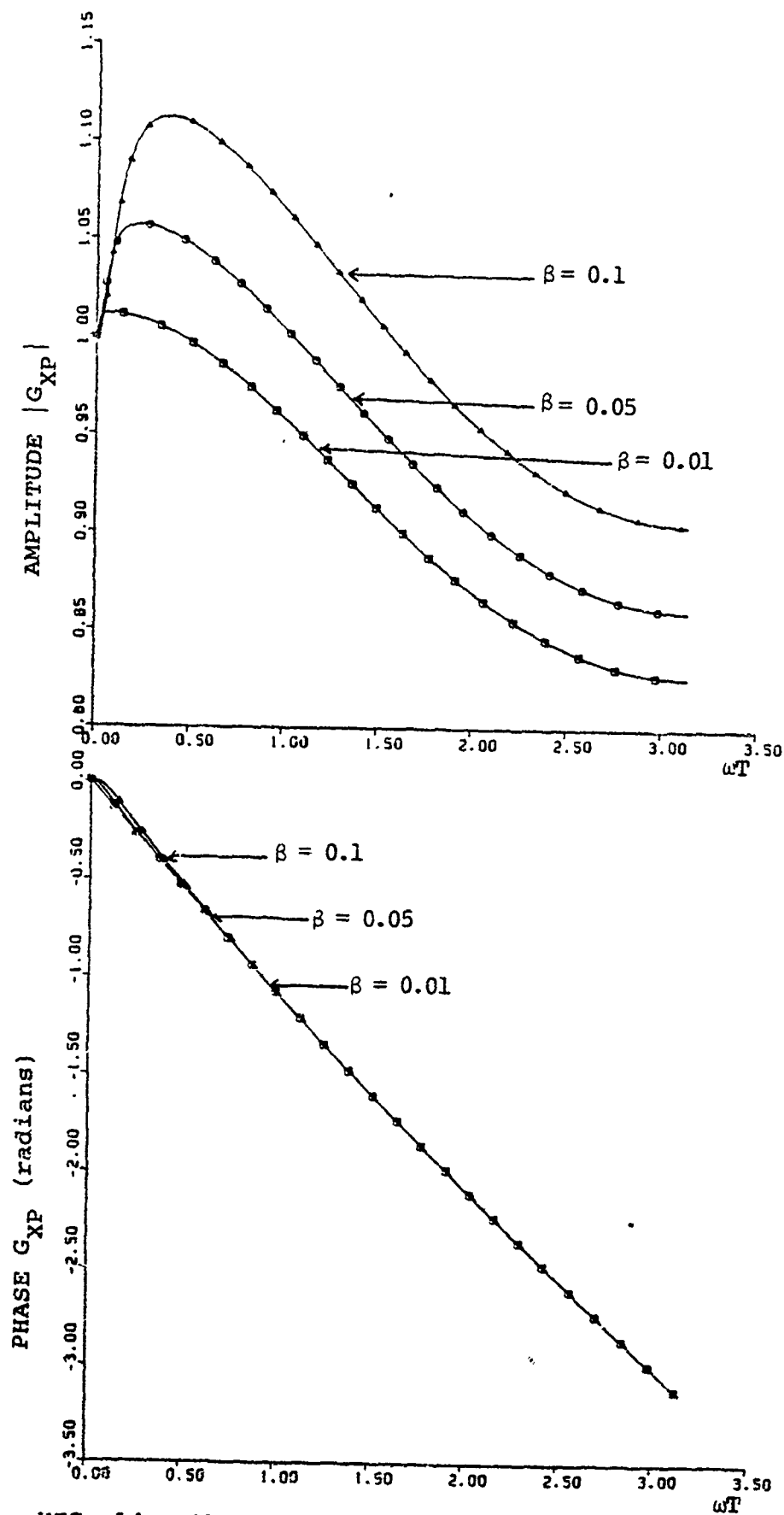


FIG. 14. AMPLITUDE AND PHASE OF PREDICTED POSITION G_{XP}
FOR $\alpha = 0.9$

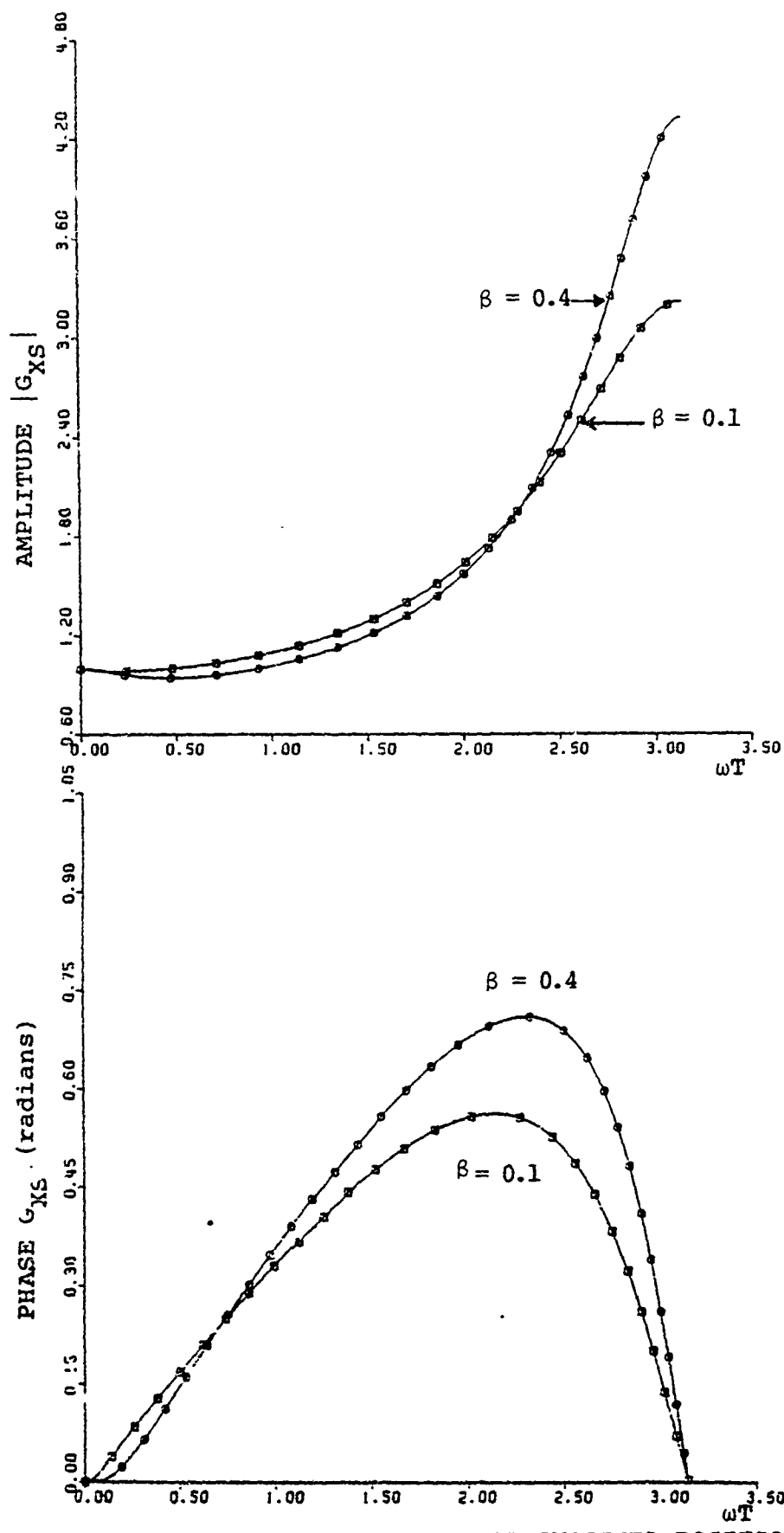


FIG. 15. AMPLITUDE AND PHASE OF SMOOTHED POSITION G_{XS}
FOR $\alpha = 1.5$

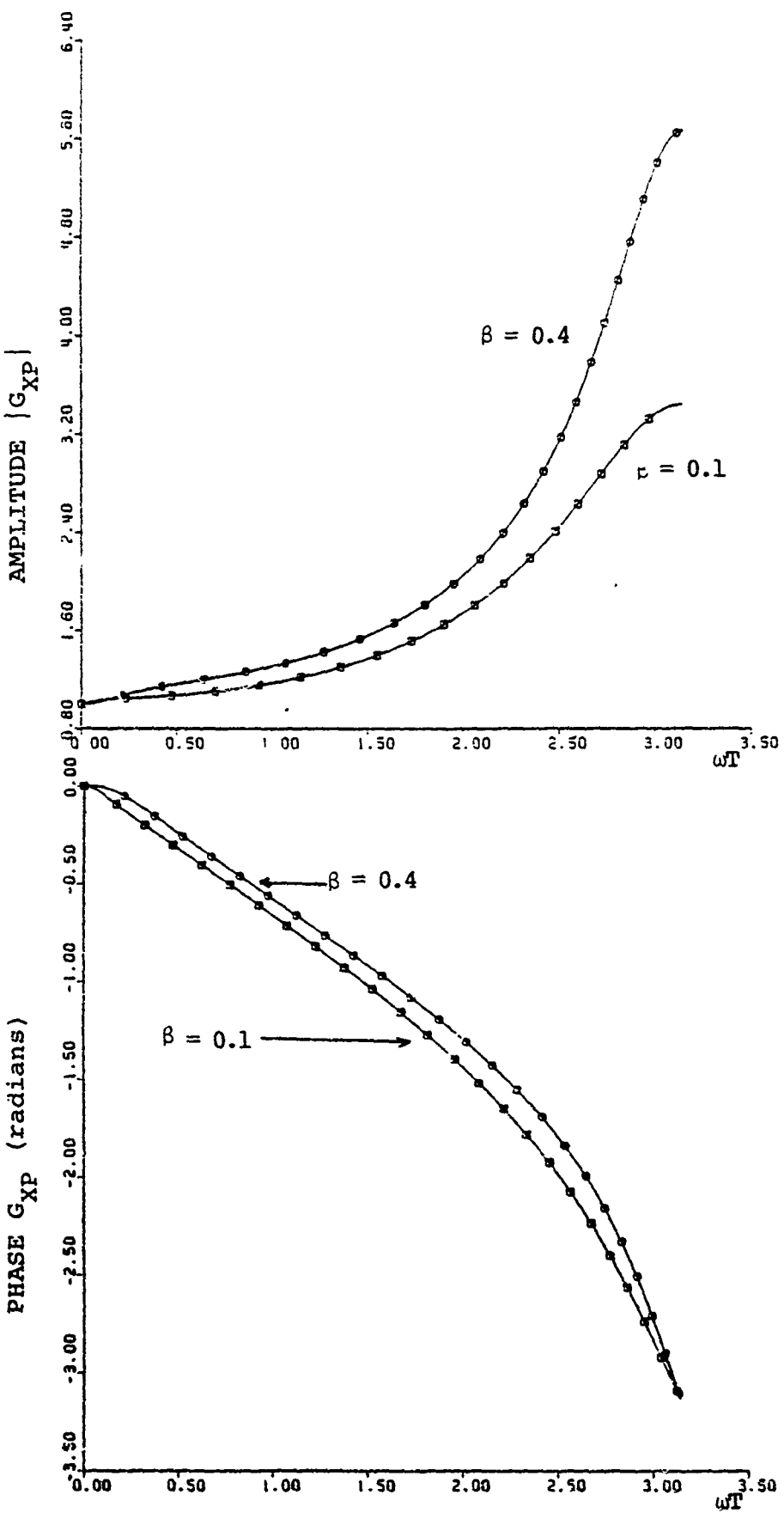


FIG. 16. AMPLITUDE AND PHASE OF PREDICTED POSITION G_{XP}
FOR $\alpha = 1.5$

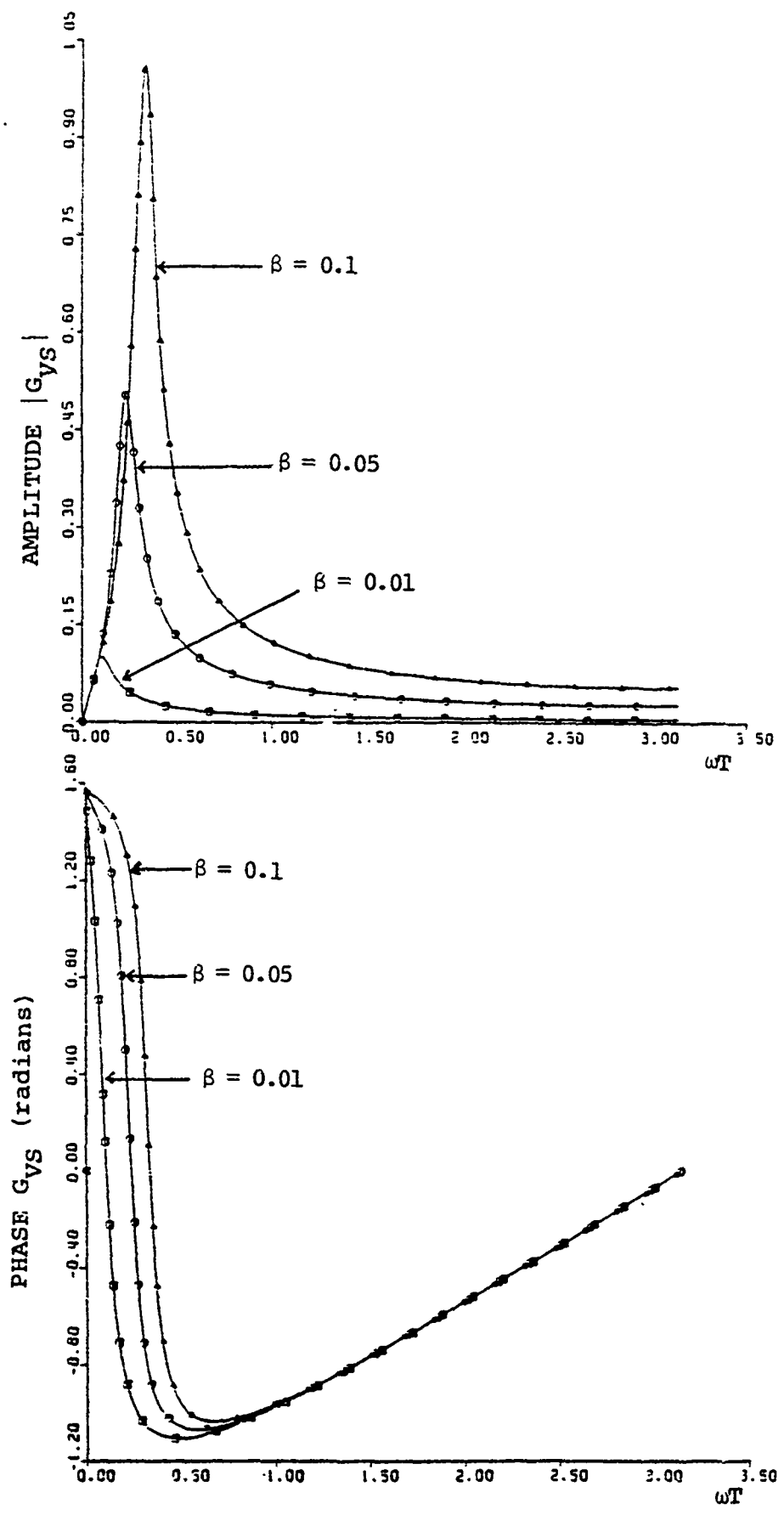


FIG. 17. AMPLITUDE AND PHASE OF SMOOTHED VELOCITY G_{VS} FOR $\alpha = 0.1$

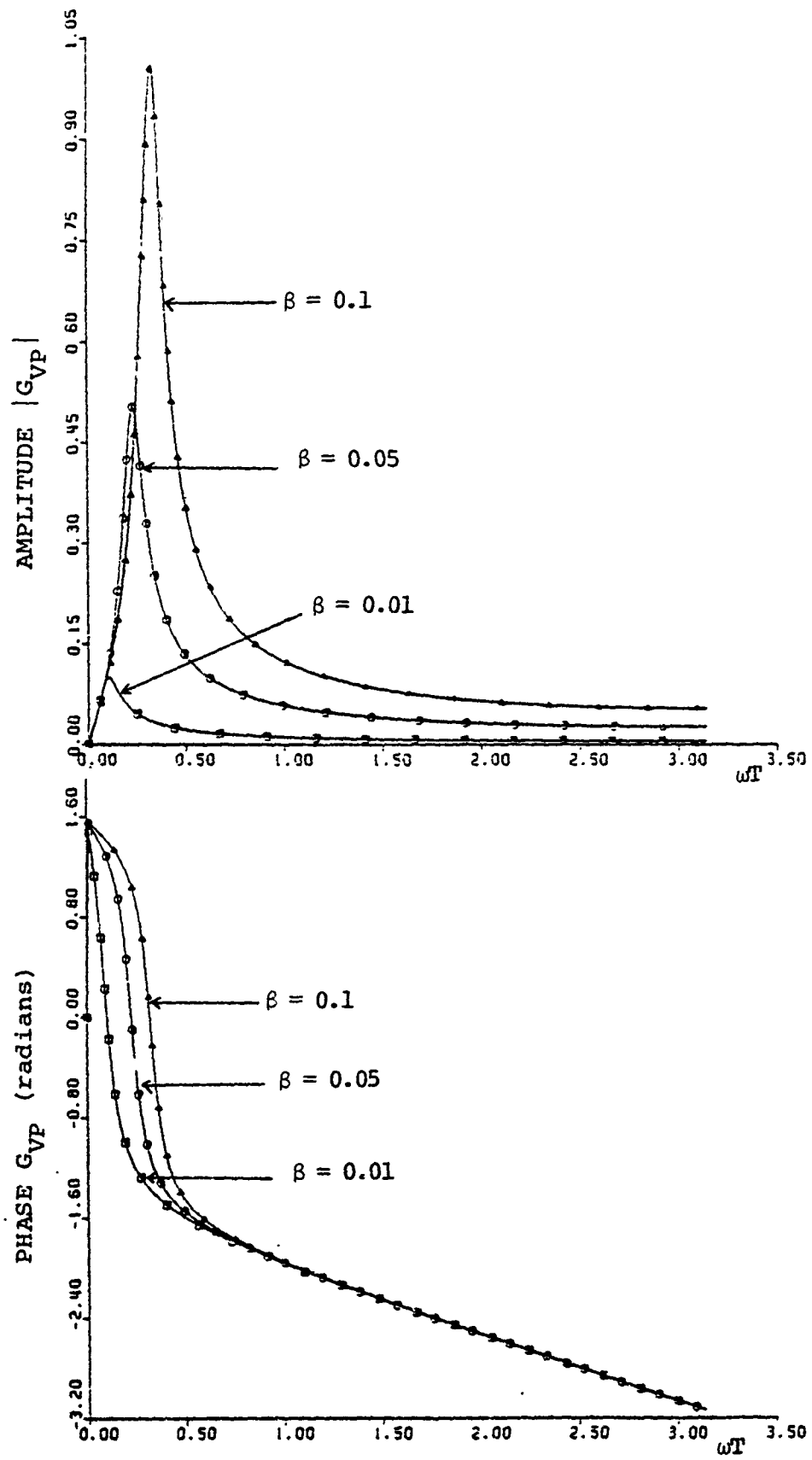


FIG. 18. AMPLITUDE AND PHASE OF PREDICTED VELOCITY G_{VP}
FOR $\alpha = 0.1$

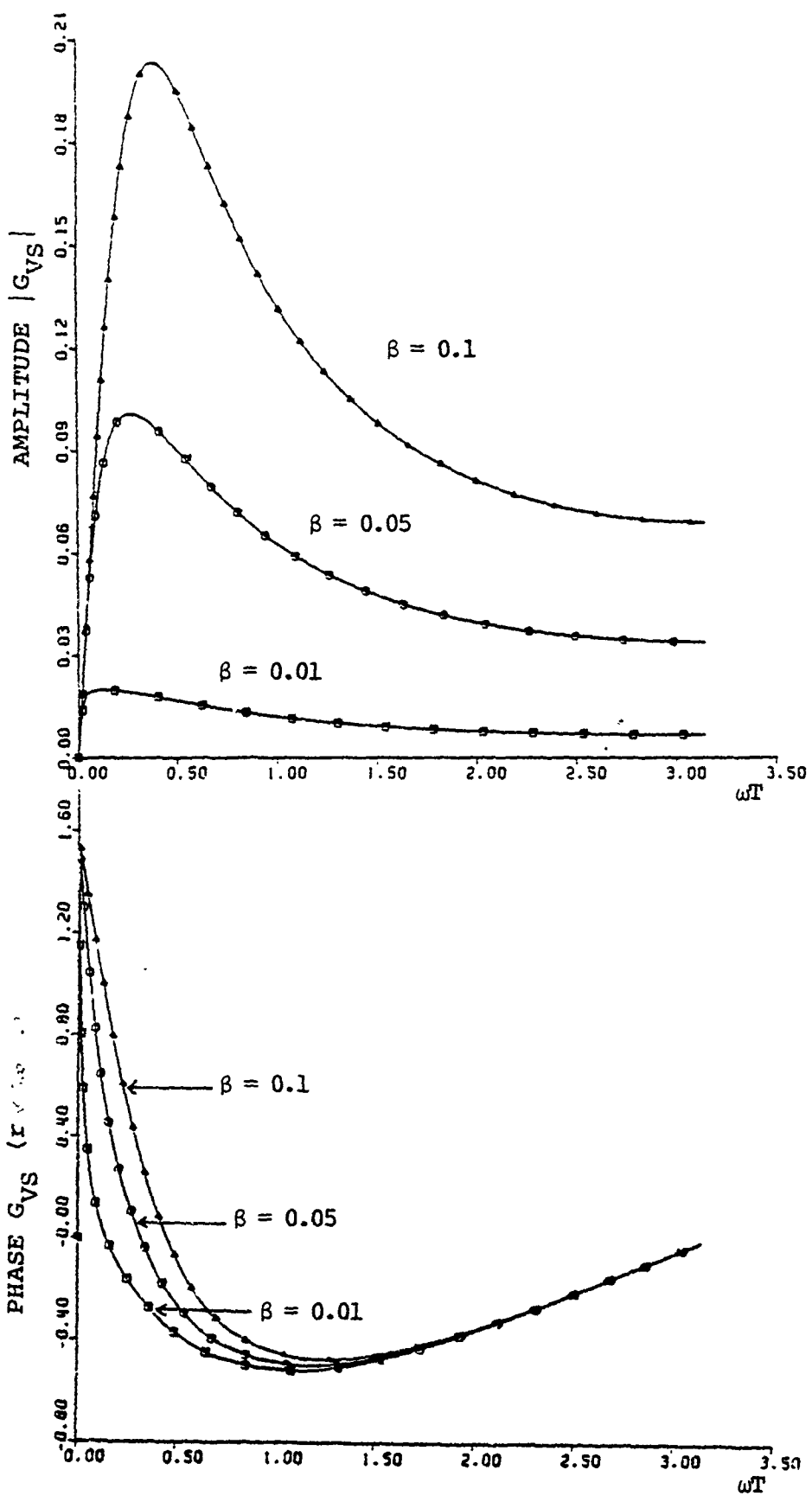


FIG. 19. AMPLITUDE AND PHASE OF SMOOTHED VELOCITY G_{VS} FOR $\alpha = 0.5$

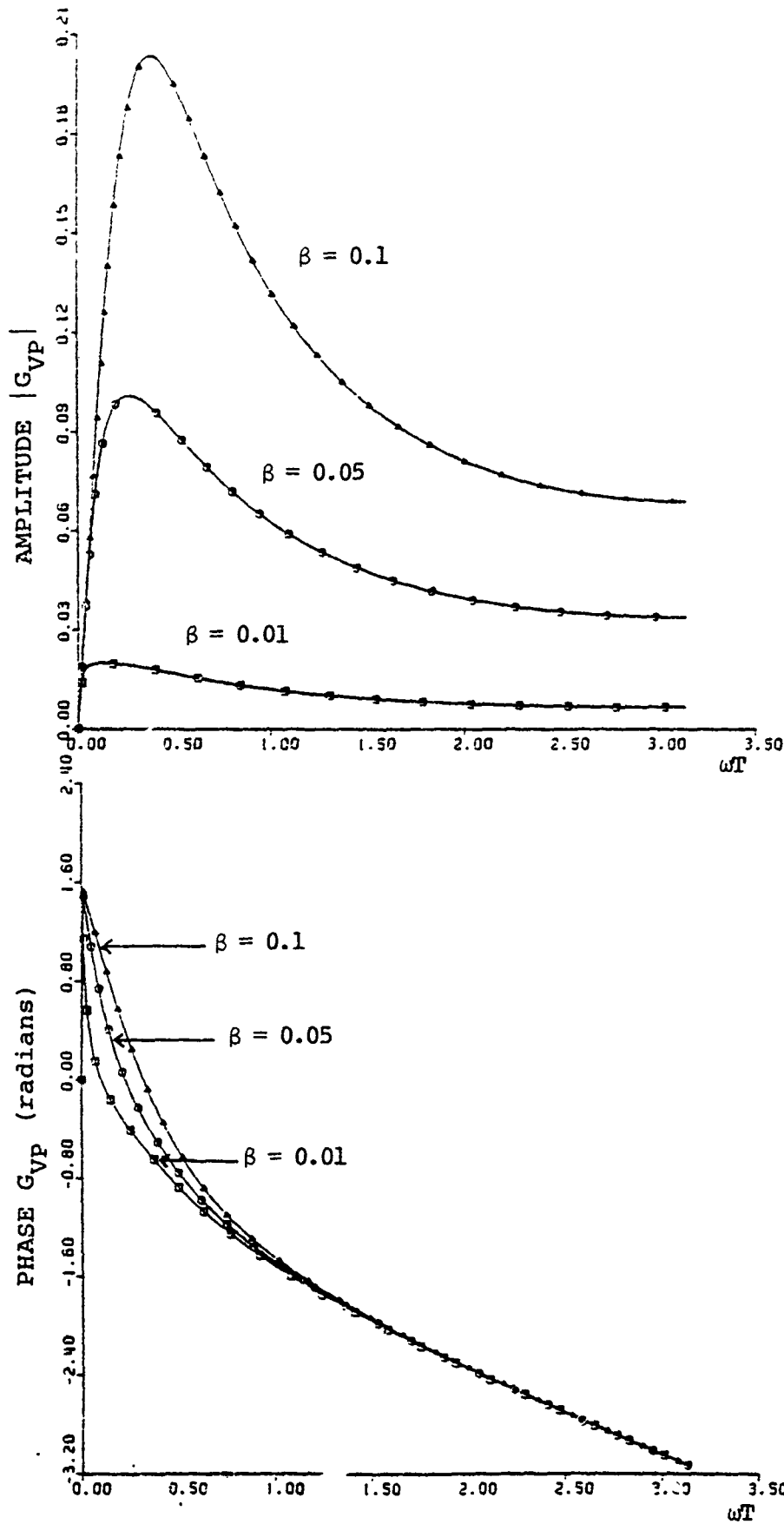


FIG. 20. AMPLITUDE AND PHASE OF PREDICTED VELOCITY G_{VP}
FOR $\alpha = 0.5$

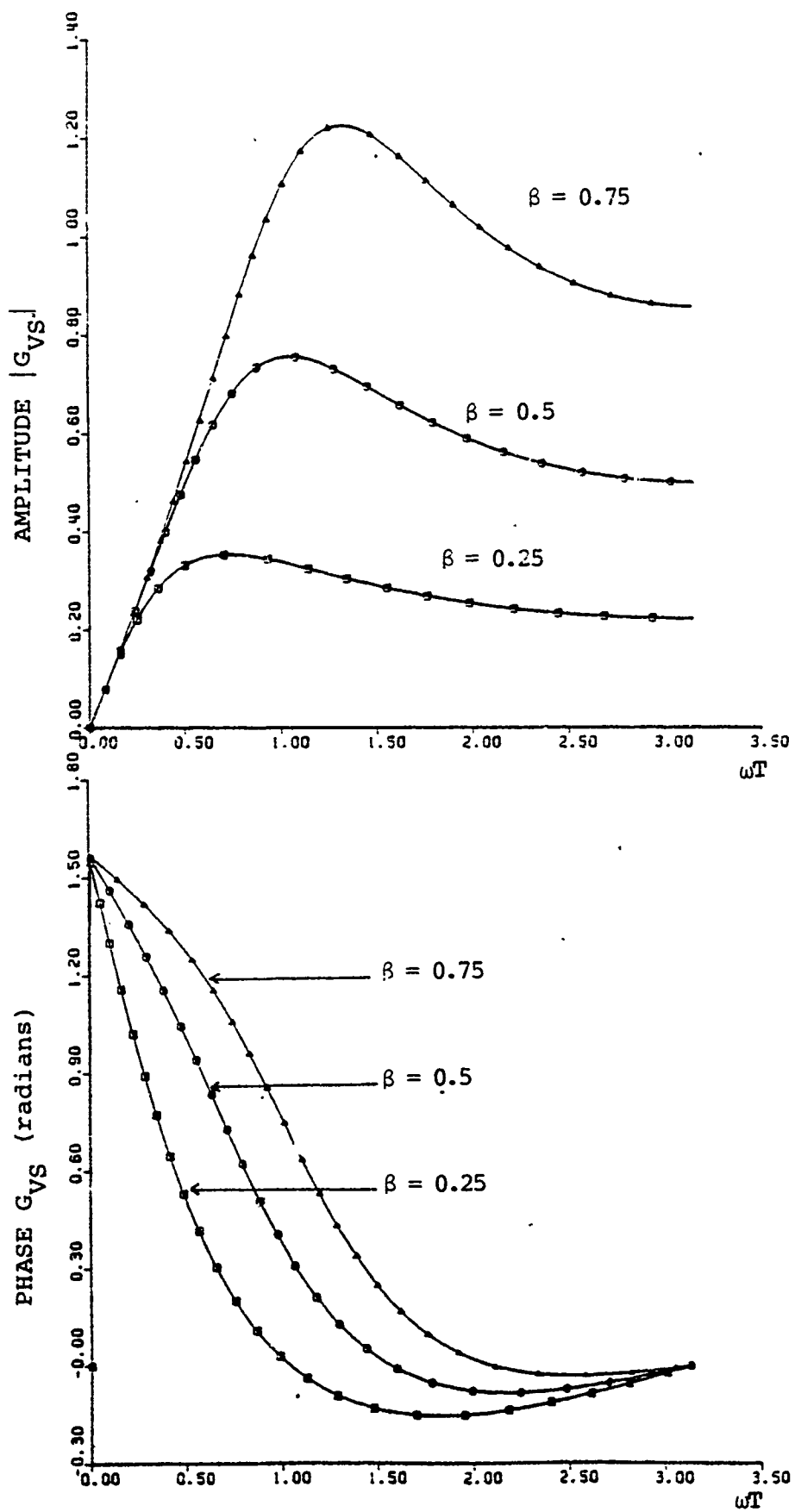


FIG. 21. AMPLITUDE AND PHASE OF SMOOTHED VELOCITY G_{VS}
FOR $\alpha = 0.75$

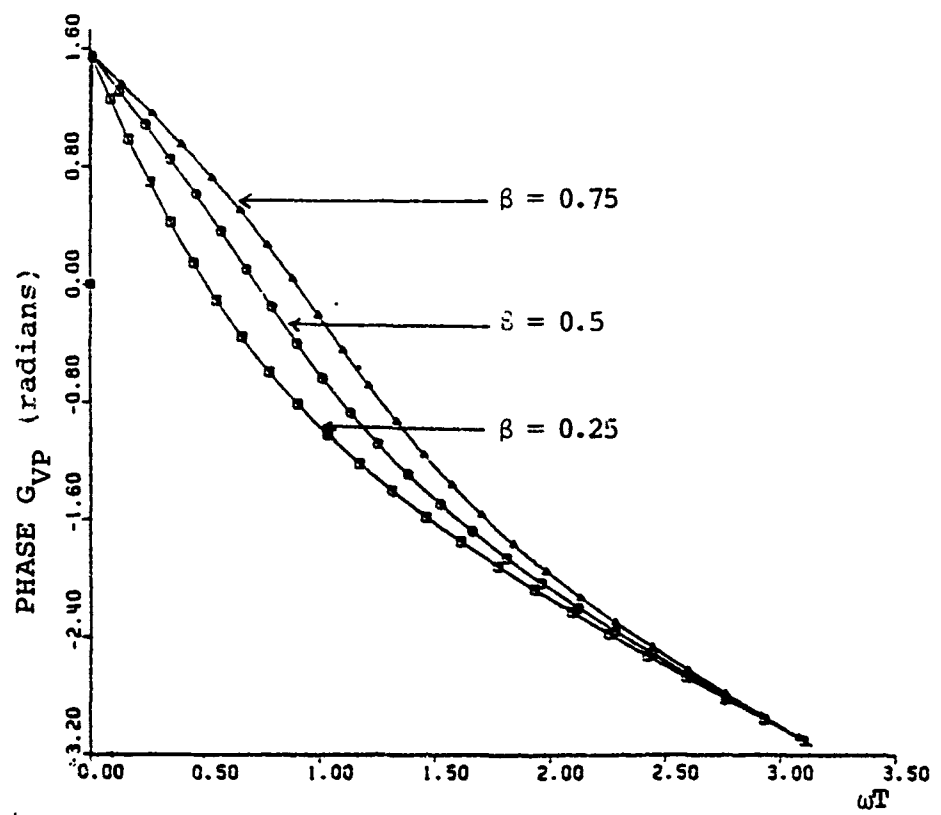
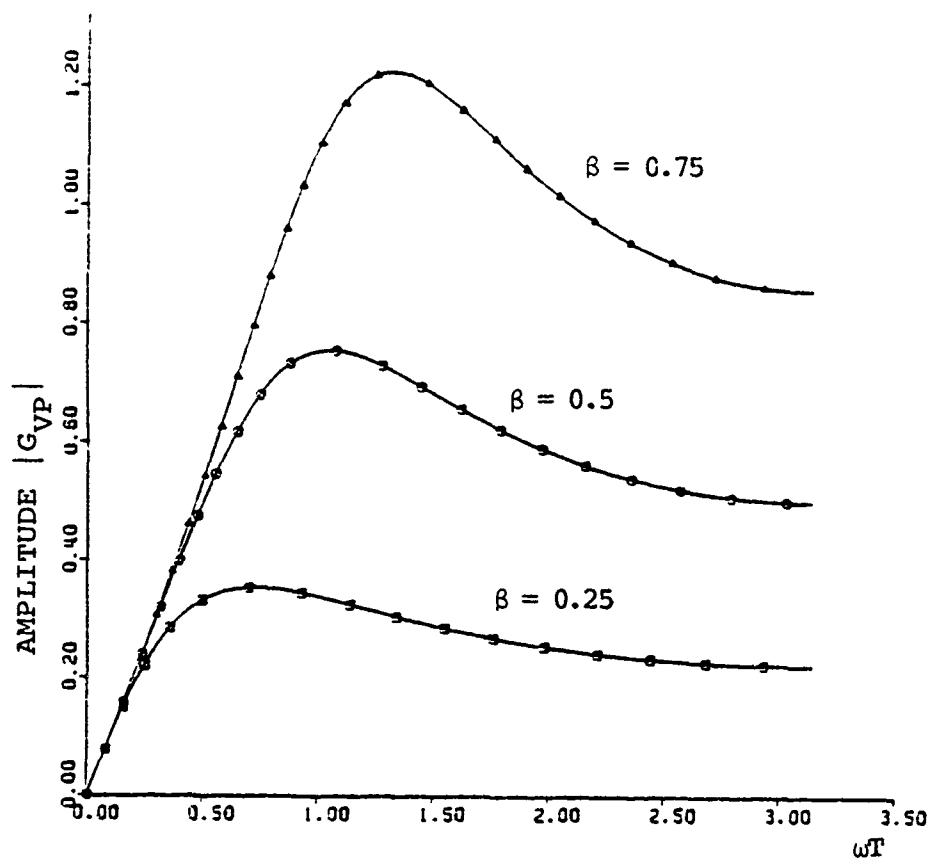


FIG. 22. AMPLITUDE AND PHASE OF PREDICTED VELOCITY G_{vp} FOR $\alpha = 0.75$

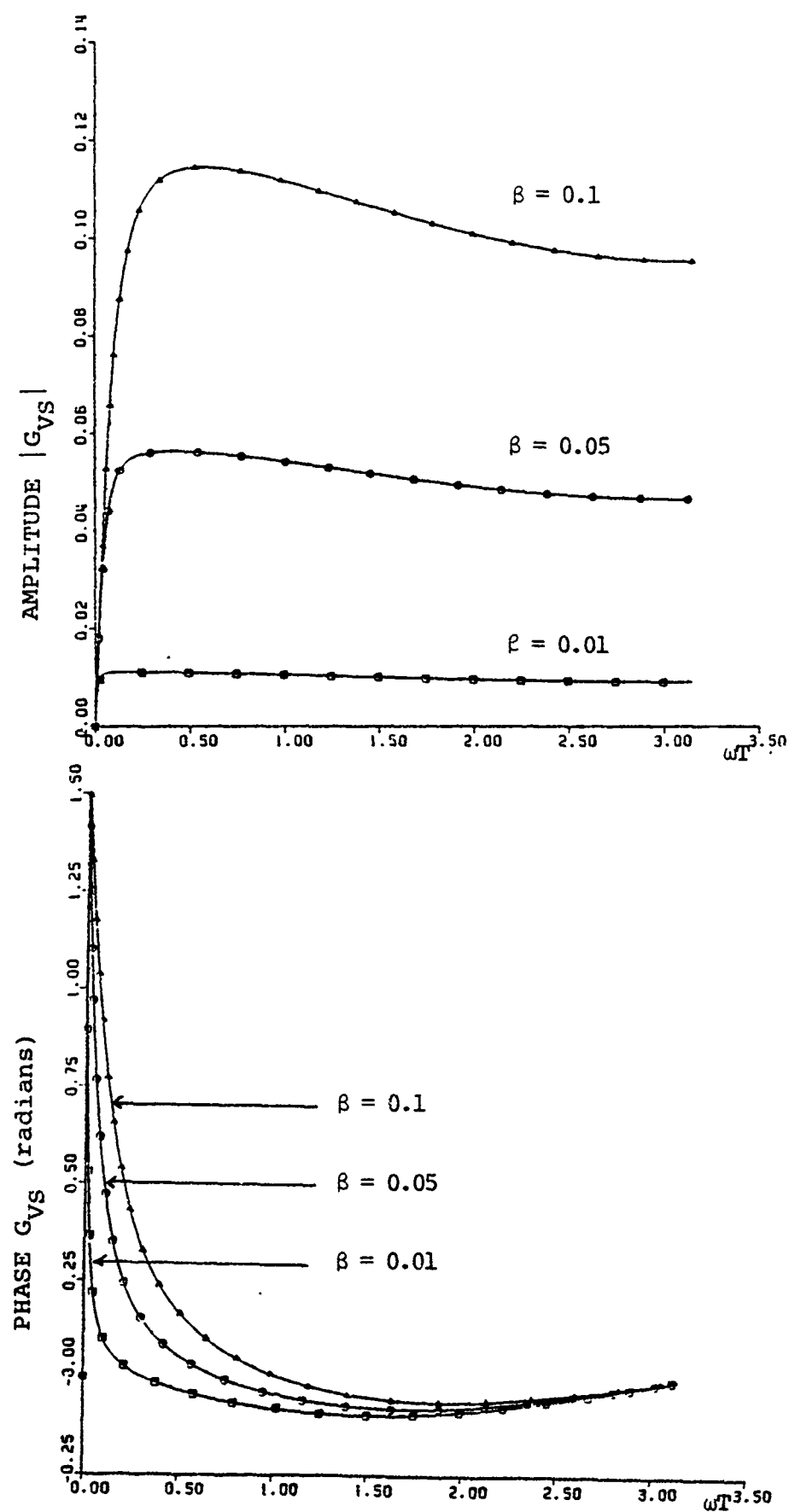


FIG. 23. AMPLITUDE AND PHASE OF SMOOTHED VELOCITY G_{VS} FOR $\alpha = 0.9$

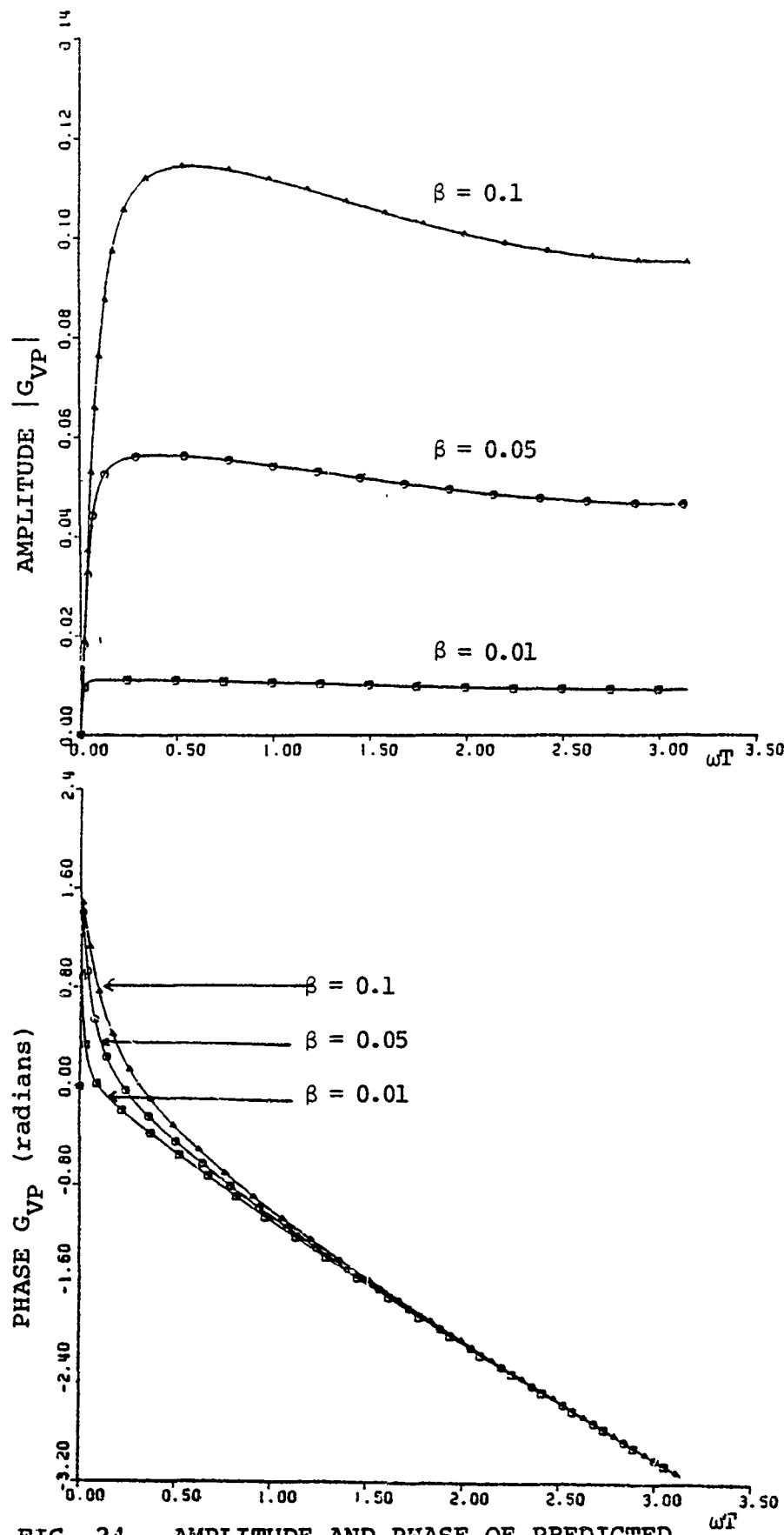


FIG. 24. AMPLITUDE AND PHASE OF PREDICTED VELOCITY G_{vp} FOR $\alpha = 0.9$

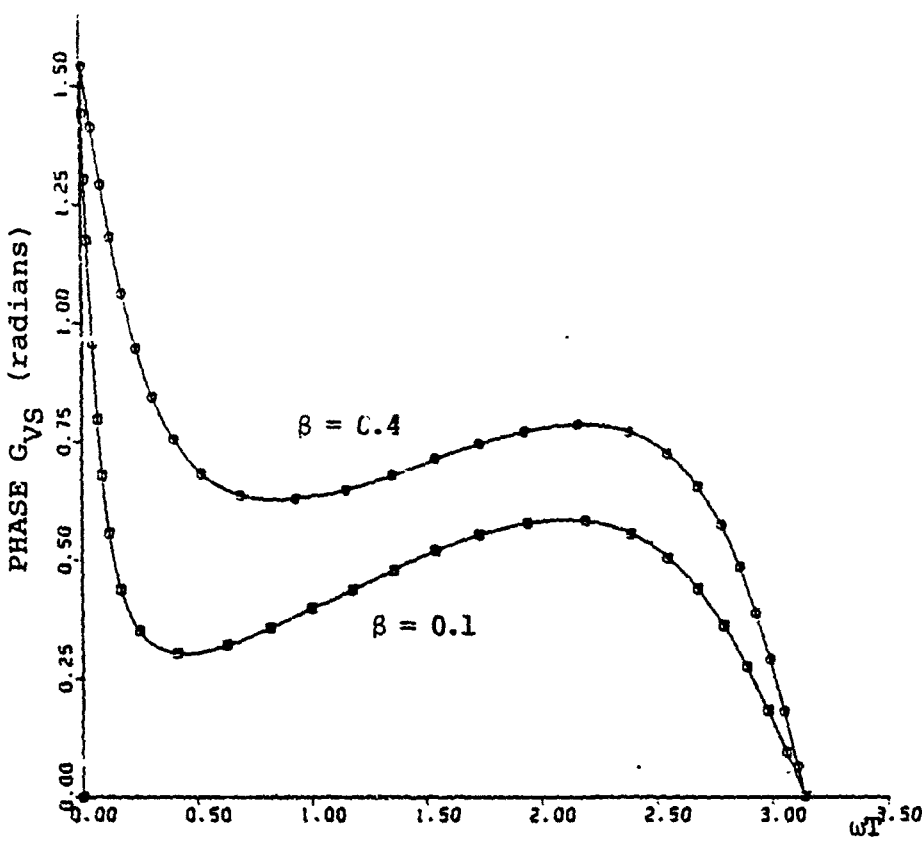
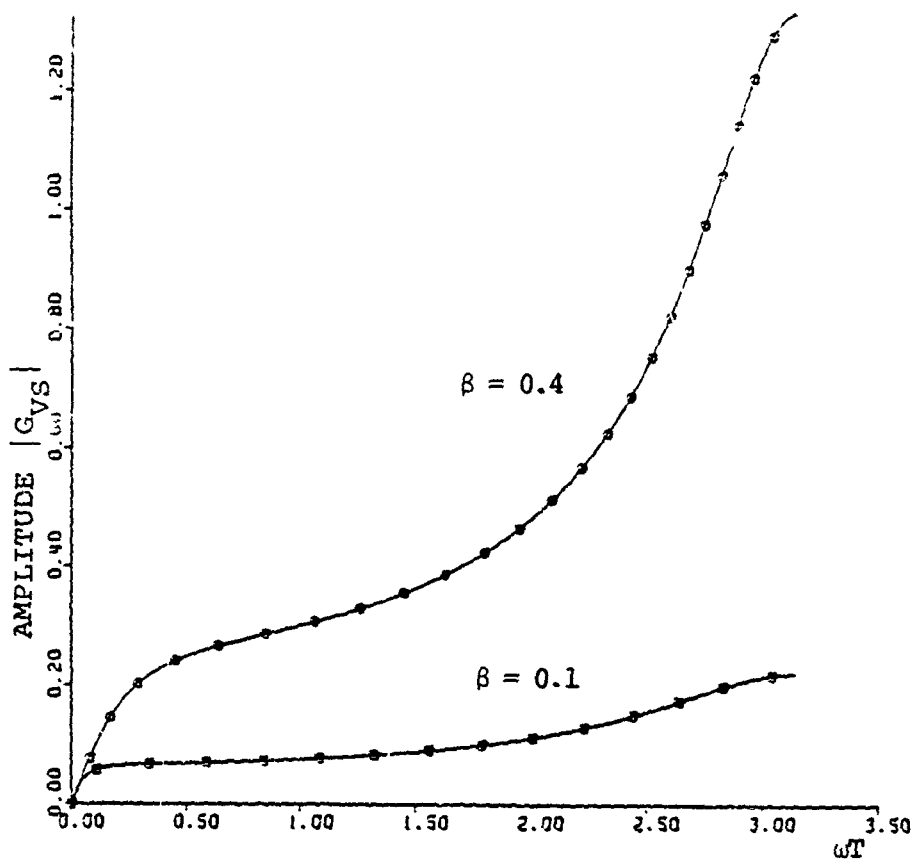


FIG. 25. AMPLITUDE AND PHASE OF SMOOTHED VELOCITY G_{VS}
FOR $\alpha = 1.5$

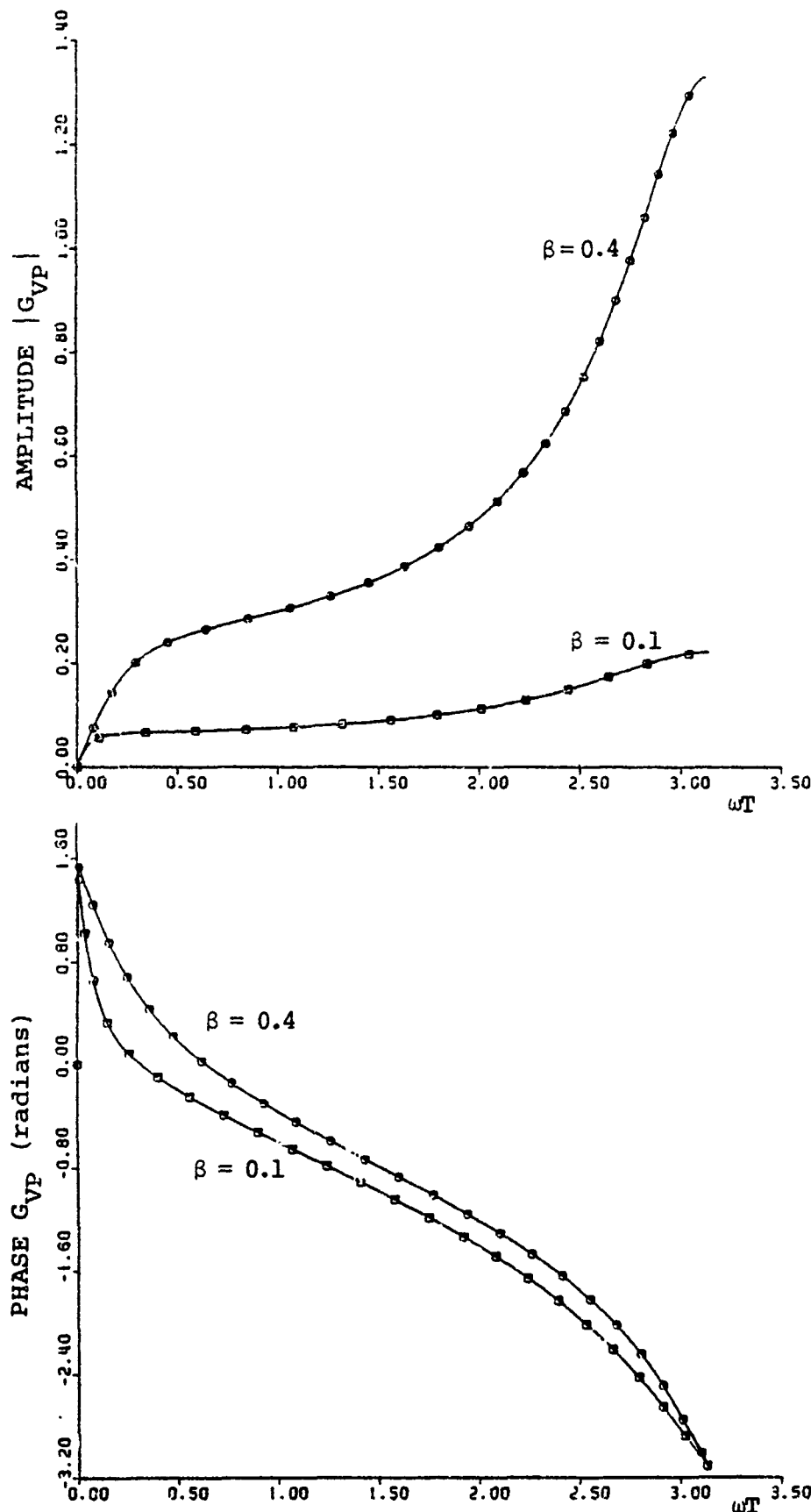


FIG. 26. AMPLITUDE AND PHASE OF PREDICTED VELOCITY G_{VP}
FOR $\alpha = 1.5$

Considering the figures for several values of $\alpha < 1$, α seems to control the bandwidth of the low-pass filter and β has more control over the damping. In fact β should be somewhat smaller than α such that resonant spikes do not occur.

Better accuracy occurs between smoothed and predicted positions, when α has very large values compared with β .

Table I, which follows, summarizes the accuracy and provides an important design tool. In general the frequency of the input signal, the sampling time T , and the filter parameters α and β control the filter's response.

A. ACCURACY (0-1) BETWEEN SMOOTHED AND PREDICTED POSITION FOR $\omega T = 0$ to $\omega T = \pi$

β	α	0.1	0.5	0.75	0.9
0.01		1.0-0.90	1.0-0.98		1.0-0.99
0.05		1.0-0.60	1.0-0.90		1.0-0.94
0.10		1.0-0.33	1.0-0.82		1.0-0.89
0.25				1.0-0.71	
0.50				1.0-0.50	
0.75				1.0-0.33	

B. ACCURACY (0-1) BETWEEN SMOOTHED AND PREDICTED VELOCITY FOR $\omega T = 0$ to $\omega T = \pi$

β	α	0.1	0.5	0.75	0.9
0.01		1.0*	1.0*		1.0
0.05		1.0	1.0		1.0
0.10		1.0	1.0		1.0
0.25				1.0	
0.50				1.0	
0.75				1.0	

*As we expect 100% accuracy, since the vehicle was generally assumed to follow straight line constant velocity, when an α - β filter is used.

TABLE I. ACCURACY BETWEEN SMOOTHED AND PREDICTED, POSITION AND VELOCITY

III. NOISE CHARACTERISTICS OF α - β FILTER-ERRORS-CRITERIA

In the study of any filter it is essential to know the characteristics of the desired signals and the noise which excites the filter. It is desirable also to know how the choice of α and β affects the degree to which the noise is smoothed or exaggerated by the system. The description of the noise processes, prediction errors and methods (criteria) for designing an α - β filter, proceeds as follows:

A. NORMALIZED NOISE POWER OF PREDICTED POSITION

By making the following change of variable:

$$\Delta X = V_S T \quad (3.1)$$

Equations (2.7) and (2.8) describing the filter can be rewritten as:

$$\begin{bmatrix} X_S \\ \Delta X \end{bmatrix}^N = \begin{bmatrix} (1-\alpha) & (1-\alpha) \\ -\beta & (1-\beta) \end{bmatrix} \begin{bmatrix} X_S \\ \Delta X \end{bmatrix}^{N-1} + \begin{bmatrix} \alpha \\ \beta \end{bmatrix} [X_M]^N \quad (3.2)$$

$$[X_P]^{N+1} = [1 \quad 1] \begin{bmatrix} X_S \\ \Delta X \end{bmatrix} \quad (3.3)$$

where now

$$A' = \begin{bmatrix} (1-\alpha) & (1-\alpha) \\ -\beta & (1-\beta) \end{bmatrix} \quad B' = \begin{bmatrix} \alpha \\ \beta \end{bmatrix}$$

$$C' = [1 \quad 1] \quad X = \begin{bmatrix} X_S \\ \Delta X \end{bmatrix}$$

The mean and covariance equations are defined as

$$[\bar{X}]^N = A' \bar{X}^{N-1} + B' X_M^N \quad (3.4)$$

$$P^N = A' P^{N-1} A'^T + B' \sigma^2 B'^T \quad (3.5)$$

where

$$[\bar{X}]^N = E[X^N], \text{ the expected value,}$$

$$P = \begin{bmatrix} P_{11} & P_{12} \\ P_{21} & P_{22} \end{bmatrix}$$

$$P_{11} = E[(X_S - \bar{X}_S)(X_S - \bar{X}_S)]$$

$$P_{12} = E[(X_S - \bar{X}_S)(\Delta X - \bar{\Delta X})] = P_{21}$$

$$P_{22} = E[(\Delta X - \bar{\Delta X})(\Delta X - \bar{\Delta X})]$$

σ_{XM} = standard deviation of measurement error.

The covariance equation for the filter becomes

$$\begin{bmatrix} P_{11} \\ P_{12} \\ P_{22} \end{bmatrix}^N = \begin{bmatrix} (1-\alpha)^2 & 2(1-\alpha)^2 & (1-\alpha)^2 \\ -\beta(1-\alpha) & (1-2\beta)(1-\alpha) & (1-\beta)(1-\alpha) \\ \beta^2 & -2\beta(1-\beta) & (1-\beta)^2 \end{bmatrix} \begin{bmatrix} P_{11} \\ P_{12} \\ P_{22} \end{bmatrix}^{N-1} + \begin{bmatrix} \alpha^2 \\ \alpha\beta \\ \beta^2 \end{bmatrix} [\sigma_{XM}^2] \quad (3.6)$$

The variance of the predicted position is easily computed in terms of the variances from Eq. (3.6)

$$\sigma_{XP}^2 = P_{11} + 2P_{12} + P_{22} \quad (3.7)$$

The steady state solution of Eq. (3.6) is computed by letting $P(N)$ equal $P(N-1)$ and the resulting algebraic equations are solved;

$$\frac{P_{11}}{\sigma_{XM}^2} = \frac{2\beta - 3\alpha\beta + 2\alpha^2}{\alpha(4 - 2\alpha - \beta)} \quad (3.8)$$

$$\frac{P_{12}}{\sigma_{XM}^2} = \frac{\beta(2\alpha - \beta)}{\alpha(4 - 2\alpha - \beta)} \quad (3.9)$$

$$\frac{P_{22}}{\sigma_{XM}^2} = \frac{\beta(2\alpha^2 - \alpha^3 + 2\beta - \alpha\beta)}{\alpha(4 - 2\alpha - \beta)} \quad (3.10)$$

The predicted noise power is normalized

$$R = \sigma^2 = \frac{\sigma_{XP}^2}{\sigma_{XM}^2} \quad (3.11)$$

Substituting Eqs. (3.7) - (3.10) into Eq. (3.11) yields

$$R = \frac{\sigma_{XP}^2}{\sigma_{XM}^2} = \frac{a^2(2 + 2\beta - \alpha\beta) + \beta(2 + a - a\beta)}{a(4 - 2a + \beta)} \quad (3.12)$$

Hence, the predicted noise power is plotted as a function of α and β in Fig. 27. This figure shows that by appropriately adjusting α and β the input noise power can be reduced. One also finds that the parameter β greatly affects the predicted noise power, as expected, since differentiated noise is quite "noisy" and β affects this quantity.

An interesting phenomenon occurs for small values of α and large values of β . The noise power increases sharply. The reason for this may most easily be seen by looking at the frequency responses in Figs. 7-16. The large resonant peaks in the response allow a lot of noise to come through.

B. PREDICTION ERROR DUE TO MEASUREMENT ADDITIVE NOISE ERRORS

In the $\alpha-\beta$ tracker the observations are in the form

$$x_M^N = x_M^N + v^N \quad (3.13)$$

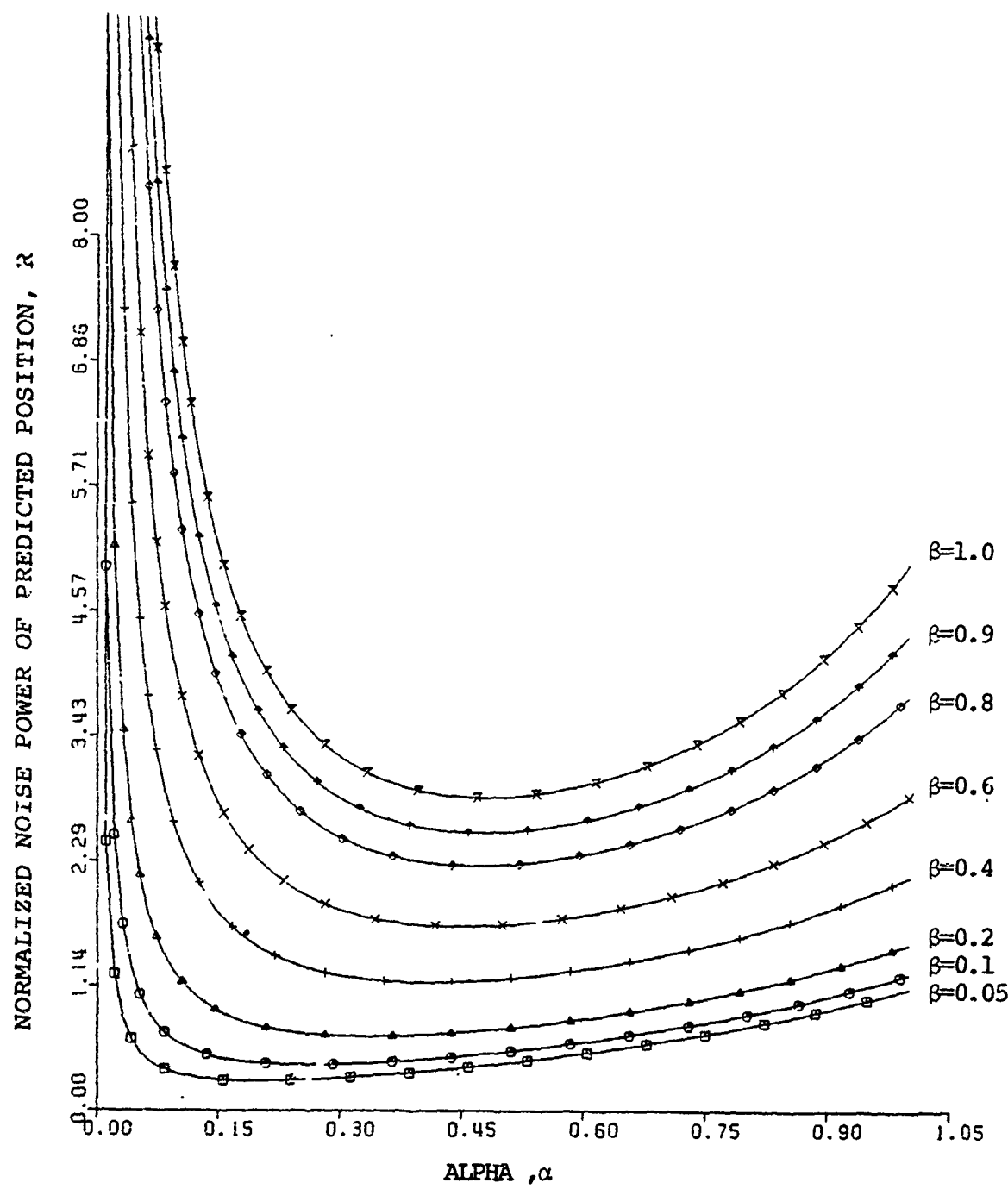


FIG. 27. PREDICTED POSITION NOISE POWER AS A FUNCTION OF α AND β

where:

$$\begin{aligned}\sigma_v^N &= \text{additive measurement noise} \\ \sigma_v^2 &= \frac{\sqrt{NM}}{\sqrt{v}} = \sigma_R^2 \quad \text{for } N = M \\ &= 0 \quad \text{for } N \neq M\end{aligned}$$

and by letting

$$\text{Variance } (x_p^{N+1}) = \text{VAR}(x_p^{N+1})$$

$$\text{Variance Reduction Factor} = \text{VRF}$$

hence

$$\text{VRF}(x_p^{N+1}) = \frac{\text{VAR}(x_p^{N+1})}{\sigma_v^2} \quad (3.14)$$

or

$$\text{VRF}(x_p^{N+1}) = \frac{\text{VAR}(x_p^{N+1})}{\sigma_R^2} = \frac{2\alpha^2 + 2\beta + \alpha\beta}{\alpha(4 - 2\alpha - \beta)} \quad (\text{Steady state}) \quad (3.15)$$

The VRF is plotted in Fig. 28 as a function of α and β . Comparing this figure with Fig. 27 (normalized noise power of predicted position), the two figures look alike, but this is not true, when both graphs are plotted together in Fig. 29.

C. PREDICTION ERROR DUE TO CONSTANT ACCELERATION

Constant acceleration $\ddot{x}(t)$ results in fixed error in predicted position x_p^{N+1} on reaching steady state, i.e., for $N \rightarrow \infty$.

NORMALIZED PREDICTION ERROR DUE TO ADDITIVE NOISE, VRF
(VARIANCE REDUCTION FACTOR)

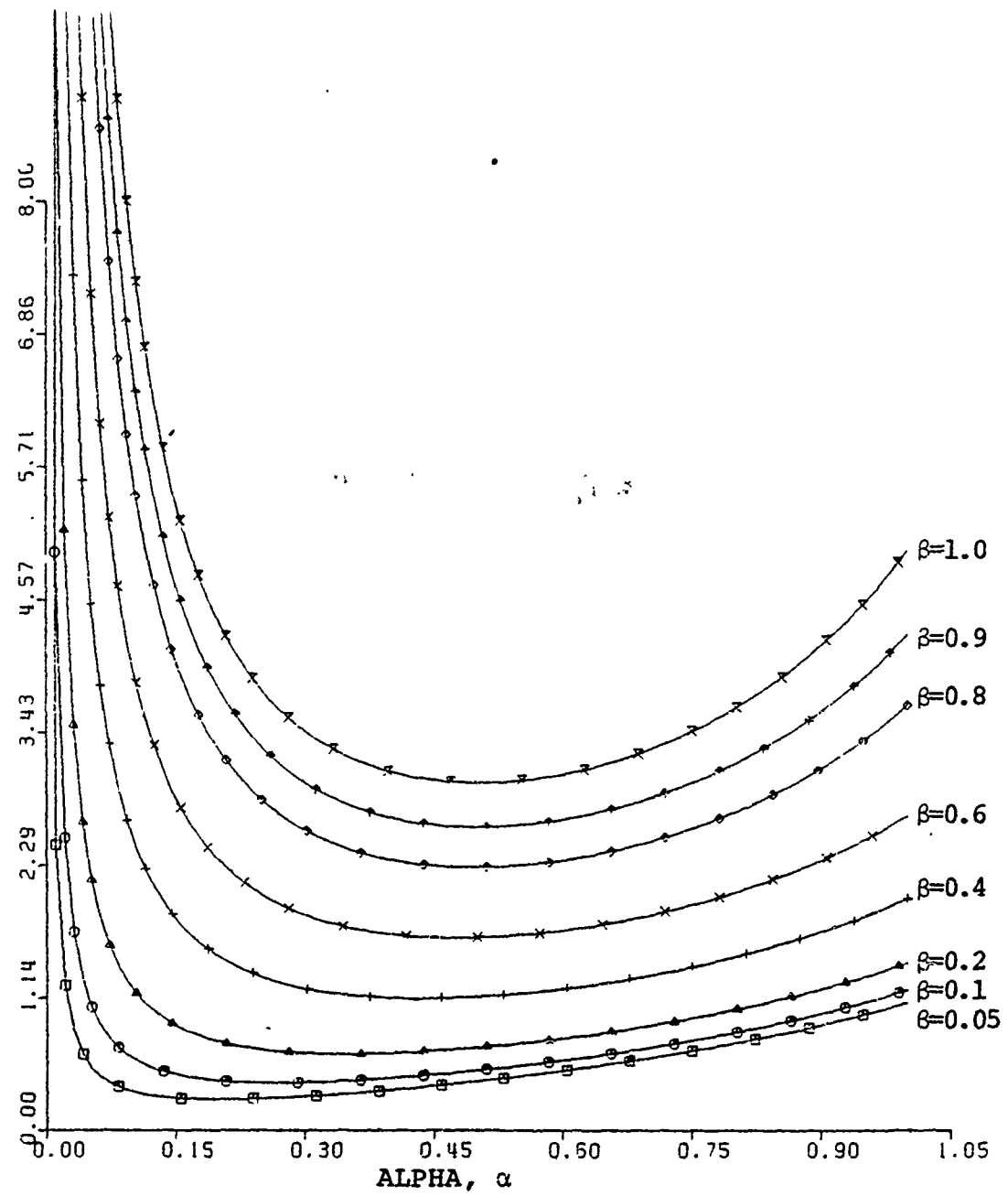


FIG. 28. PREDICTION ERROR DUE TO ADDITIVE NOISE AS A
FUNCTION OF α AND β

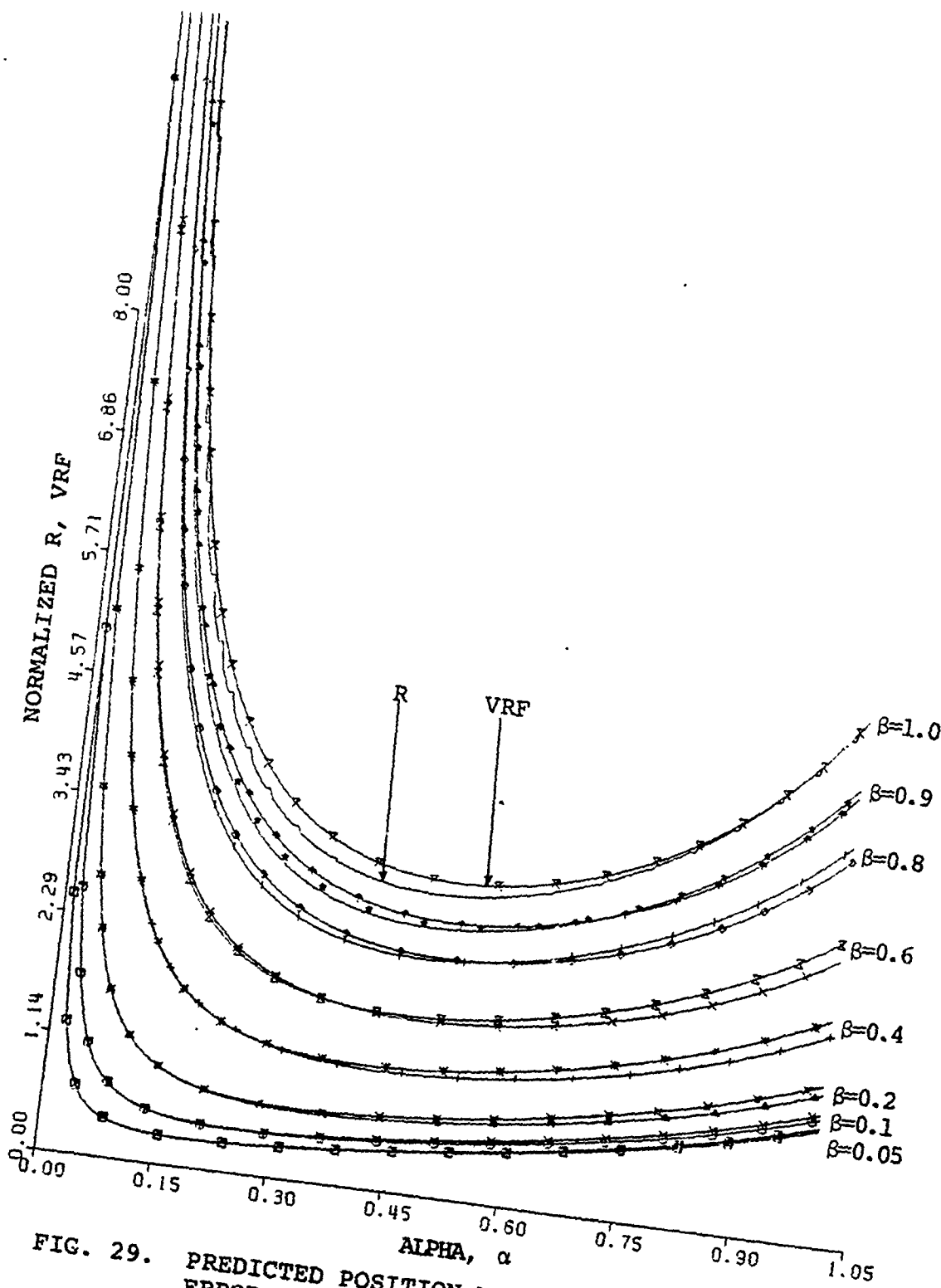


FIG. 29. PREDICTED POSITION NOISE (R) AND PREDICTION
ERROR DUE TO ADDITIVE NOISE (VRF) AS A
FUNCTION OF α AND β

Specifically for noiseless constant acceleration trajectories,

$$x_M^N = \frac{(NT)^2}{2} \ddot{x} \quad (3.16)$$

the steady state prediction error becomes

$$\epsilon^* = \lim_{N \rightarrow \infty} (x_M^N - x_P^{N+1}) = -\frac{\ddot{x}T^2}{\beta} \quad (3.17)$$

Common names for steady state prediction error ϵ^* due to constant acceleration are:

- (i) Dynamic error
- (ii) Truncation error
- (iii) Systematic error
- (iv) Bias error

Typical design procedure for balanced dynamic and random errors is

$$3(\text{Standard deviation of random error}) = (\text{Dynamic error})$$

that is

$$3 \sqrt{\text{VAR}(x_P^{N+1})} = \epsilon^* \quad (3.18)$$

D. TRANSIENT ERROR

The transient error of the system becomes significant when the input is switched from one time-shared target to another

or when the target makes a sharp maneuver. Since α - β trackers are initialized by original estimates of position and velocity and in many applications these estimates are so inaccurate that the filter exhibits transient errors before settling to a steady-state solution. In the transient phase, when the estimates are poor, one would like to rely on the measurements and thus weight the errors more heavily. After several measurements have been made, the accuracy in prediction increases.

So, the transient error yields

$$D_{x_p^{N+1}} = \sum_{n=0}^{\infty} (x_p^{N+1} - x_m^n)^2 = \frac{T^2(2-\alpha)}{\alpha\beta(4-2\alpha-\beta)} \quad (3.19)$$

The transient error $D_{x_p^{N+1}}$ is plotted and shown in Figs. 30-32, as a function of α , β and T . Observing these figures, one finds, that the sampling time T greatly affects the transient error. For large values of T the transient error increases. An interesting phenomenon occurs for small values of α and small values of β . The transient error increases sharply.

E. OPTIMAL STEADY STATE RELATIONS FOR THE α - β TRACKER

The simplest possible system is one in which α and β are fixed constants. The theory of such systems has been studied in [8]. For such systems, T.R. Benedict and G.W. Bordner [1] applied the calculus of variations to derive the following relationship:

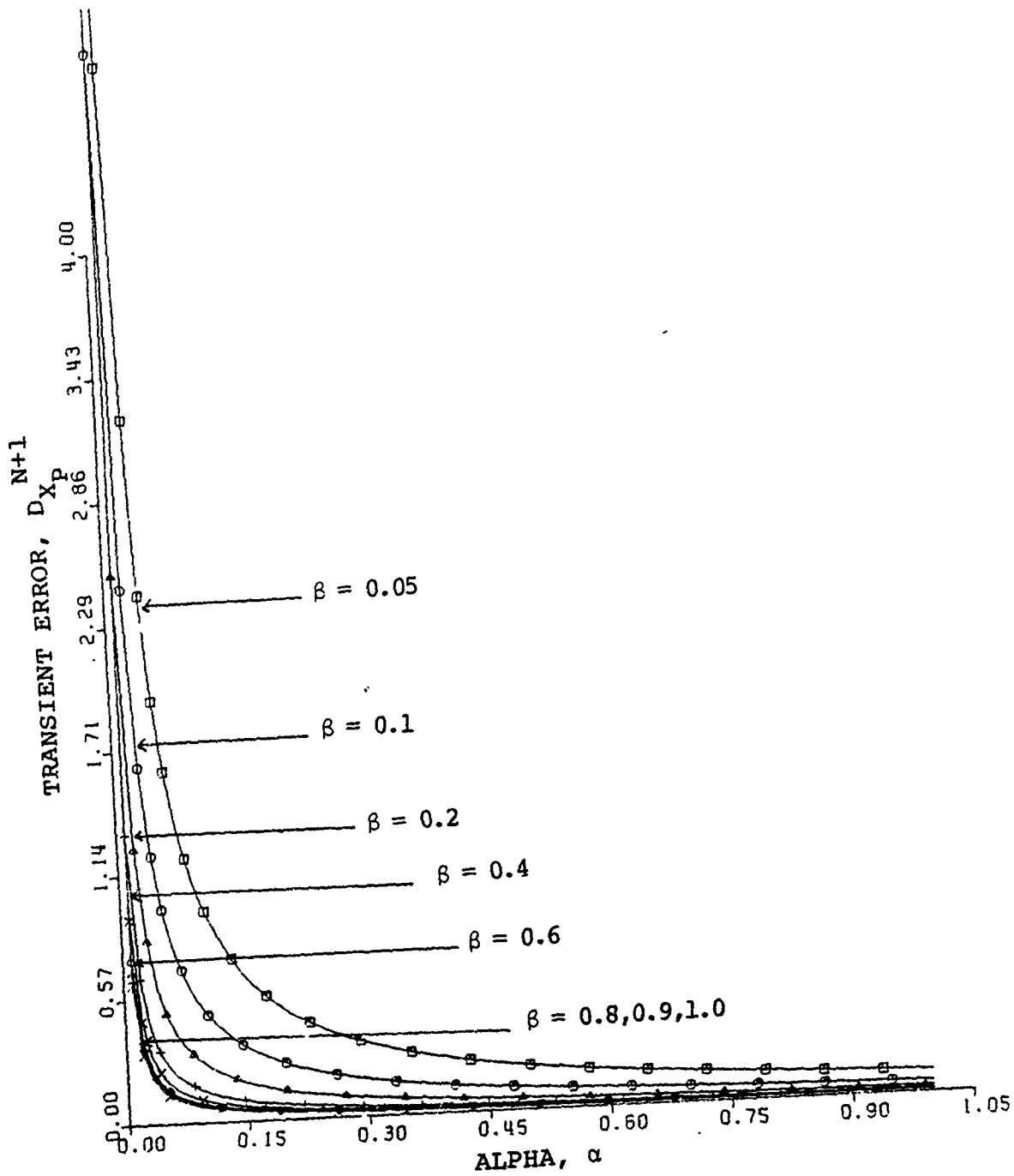


FIG. 30. TRANSIENT ERROR FOR $T = 0.1$ AS A FUNCTION
OF α AND β

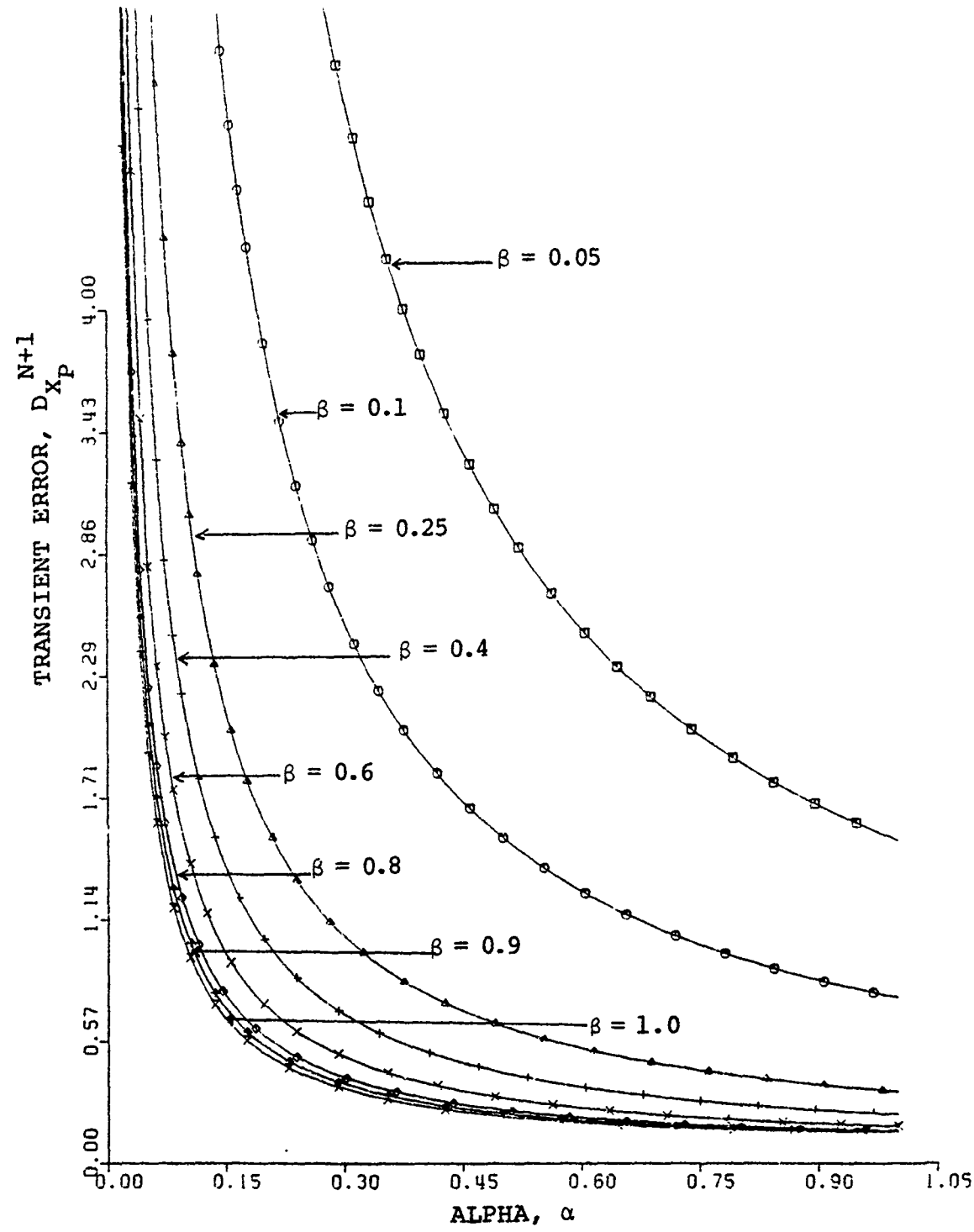


FIG. 31. TRANSIENT ERROR FOR $T = 0.3848$ AS A FUNCTION OF α AND β

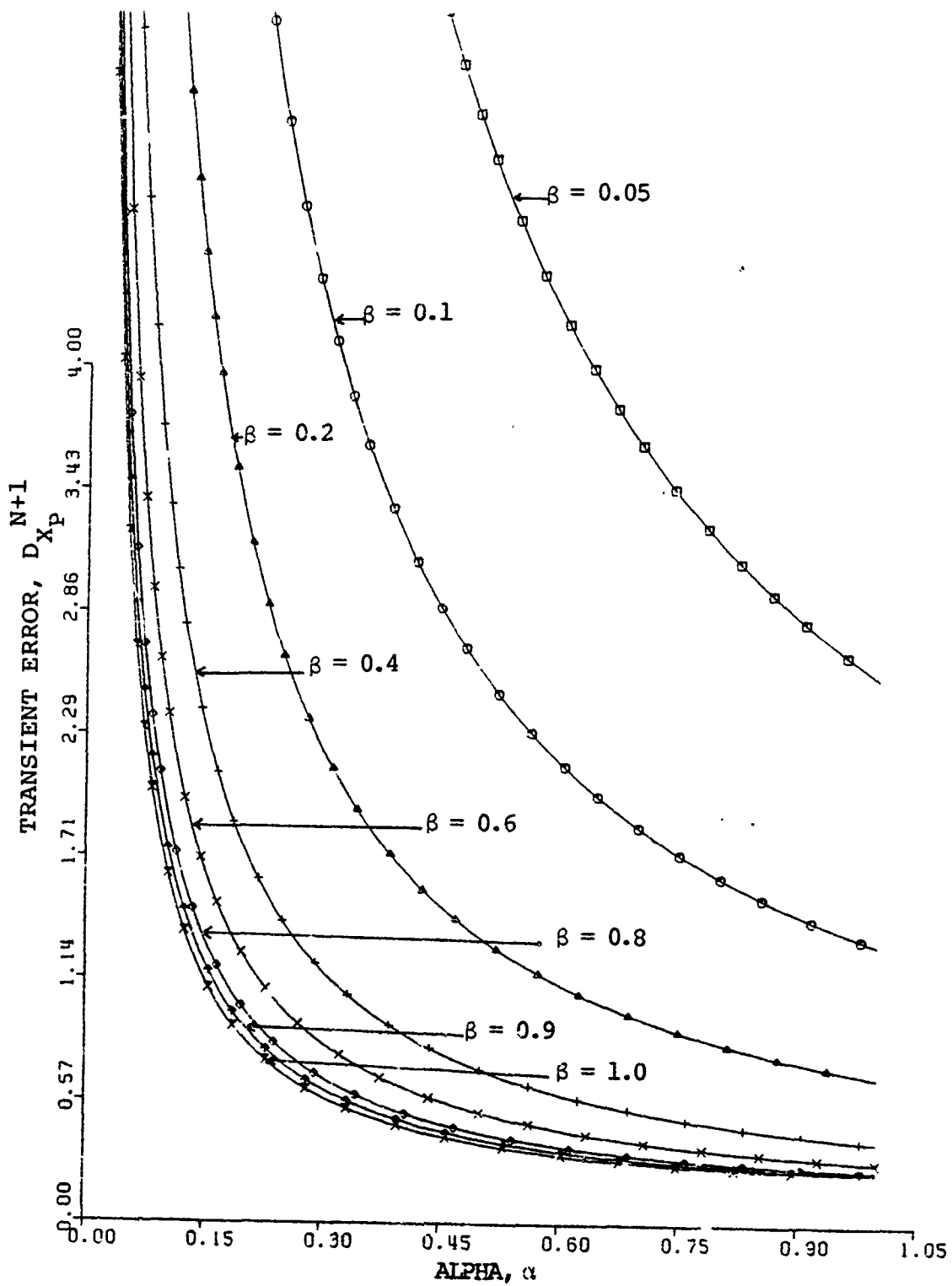


FIG. 32. TRANSIENT ERROR FOR $T = 0.5$ AS A FUNCTION OF α AND β

$$\beta = \frac{\alpha^2}{(2-\alpha)} \quad (3.20)$$

A few years later S.R. Neal [7] used the results of linear estimation theory to derive the relation:

$$(2\alpha + \beta)^2 = 8\beta \quad (3.21)$$

As a matter of interest, the above Eqs. are plotted and compared in Fig. 33. Observing these figures it is interesting to note that the relations (3.20) and (3.21) are quite similar for $0 \leq \alpha \leq 0.4$ and $0 \leq \beta \leq 0.1$.

Constant parameter systems suffer from the incompatible demands that good smoothing requires heavy damping (i.e., small values of α and β - small noise response, Figs. 27-28), while good response to maneuvers requires light damping (i.e., large values of α and β - small transient error, Figs. 30-32). Light damping and therefore large noise response, can lead to low probabilities of weapon sensor acquisition and problems of plot-to-track association. Heavy damping, implying poor maneuver response (large transient error), can cause sudden loss of tracks (sometimes termed track death) through failure to associate with subsequent plots.

These limitations led some workers to optimize for variable parameter systems, where α and β are varied according to the state of the track. Some systems have been developed wherein α and β were initially selected arbitrarily and changed

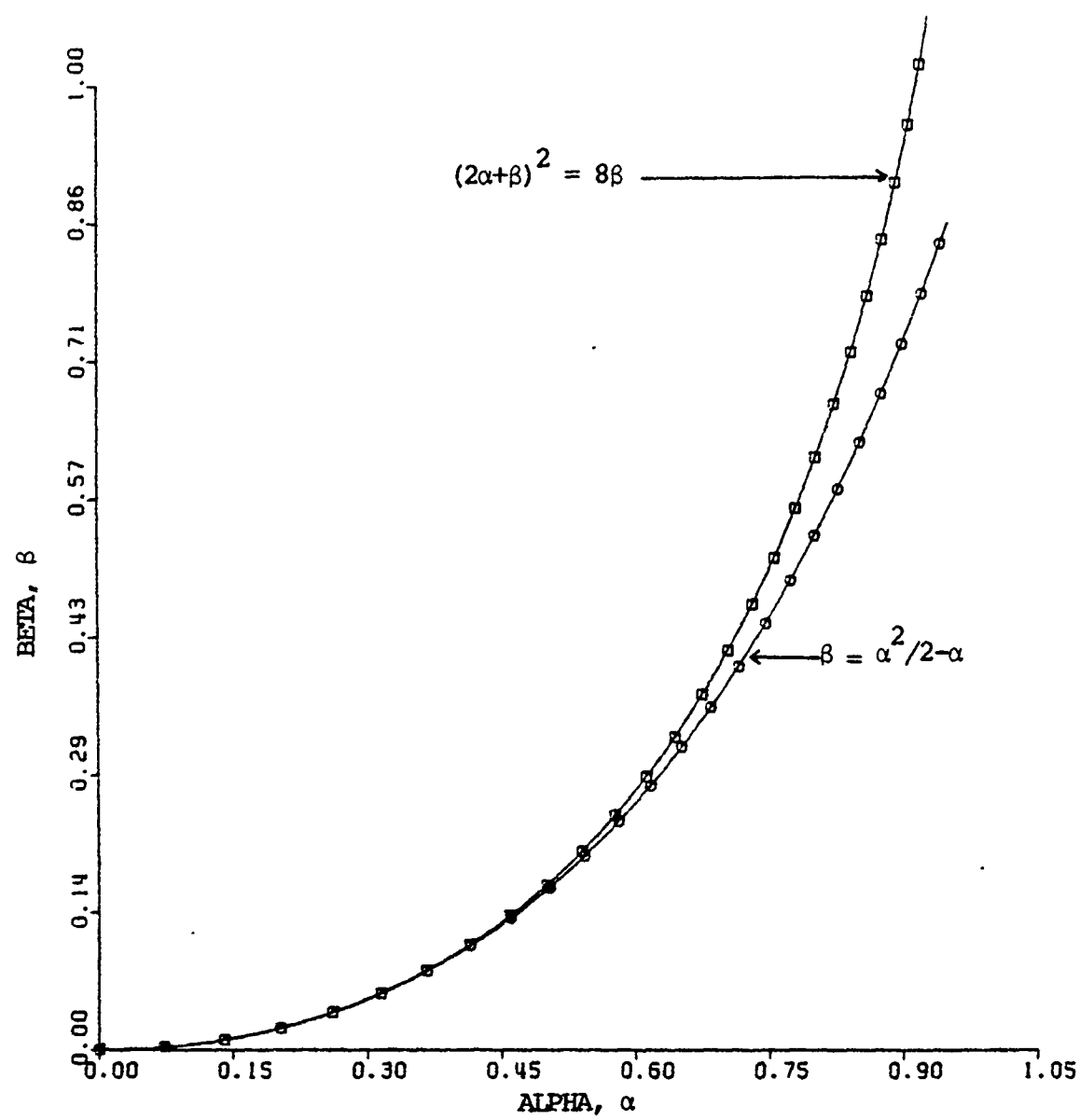


FIG. 33. STEADY STATE FILTER GAIN RELATIONS

during program development by trial and error. Various operational sets of values being derived for various states of track. Such methods are adaptive and are usually economical in computer use, both in terms of required storage and run time, but generally have no theoretically optimum adaptation.

F. DISCOUNTED LEAST-SQUARES CRITERION

To find linear trajectory

$$x_p^N = x_p^0 + N T v_p^0 \quad (3.22)$$

which minimizes sum of weighted errors between x_p^N and $x_m^N, x_m^{N-1}, x_m^{N-2}, \dots$, i.e.,

$$e_N = \sum_{r=0}^{\infty} (x_m^{N-r} - x_p^N)^2 \theta^r \quad (3.23)$$

where $0 \leq \theta < 1$, still too many degrees of freedom for selecting gain terms, α and β . Minimize

$$\{e_N\} = (x_m^N - x_p^N)^2 \theta^0 + (x_m^{N-1} - x_p^{N-1})^2 \theta^1 + (x_m^{N-2} - x_p^{N-2})^2 \theta^2 + \dots \quad (3.24)$$

by solving the above equation in order to weight the difference between measured and predicted values. This yields in simple gain terms

$$\alpha = (1 - \theta^2) \quad (3.25)$$

$$\beta = (1 - \theta)^2 \quad (3.26)$$

Common names for discounted least-squares α - β filter are

(i) Critically damped α - β filter

(ii) Fading-memory polynomial filter of degree 1

Equations (3.25)-(3.26) are plotted as a function of θ (theta) in Fig. 34.

More recently, processes have been developed in which α and β are made to change with time in order to continually compute the least-squares line through the observations. Such approaches assumed that errors are equally distributed in x and y and had a constant standard deviation. The formulae for changing α and β in this manner were worked out in [9].

For the incorporation of the n th measurement:

$$\alpha = \frac{2(2N - 1)}{N(N + 1)} \quad (3.27)$$

$$\beta = \frac{6}{N(N + 1)} \quad (3.28)$$

The above equations are plotted as a function of the number of measurements N , in Fig. 35.

It is clear that, for large N , α and β tend to zero, i.e., observations will be increasingly ignored. This suggests that there should be some maximum value of N . The maximum value used is generally 7 to 15. Such a method may be made adaptive if a means of detecting changes in motion

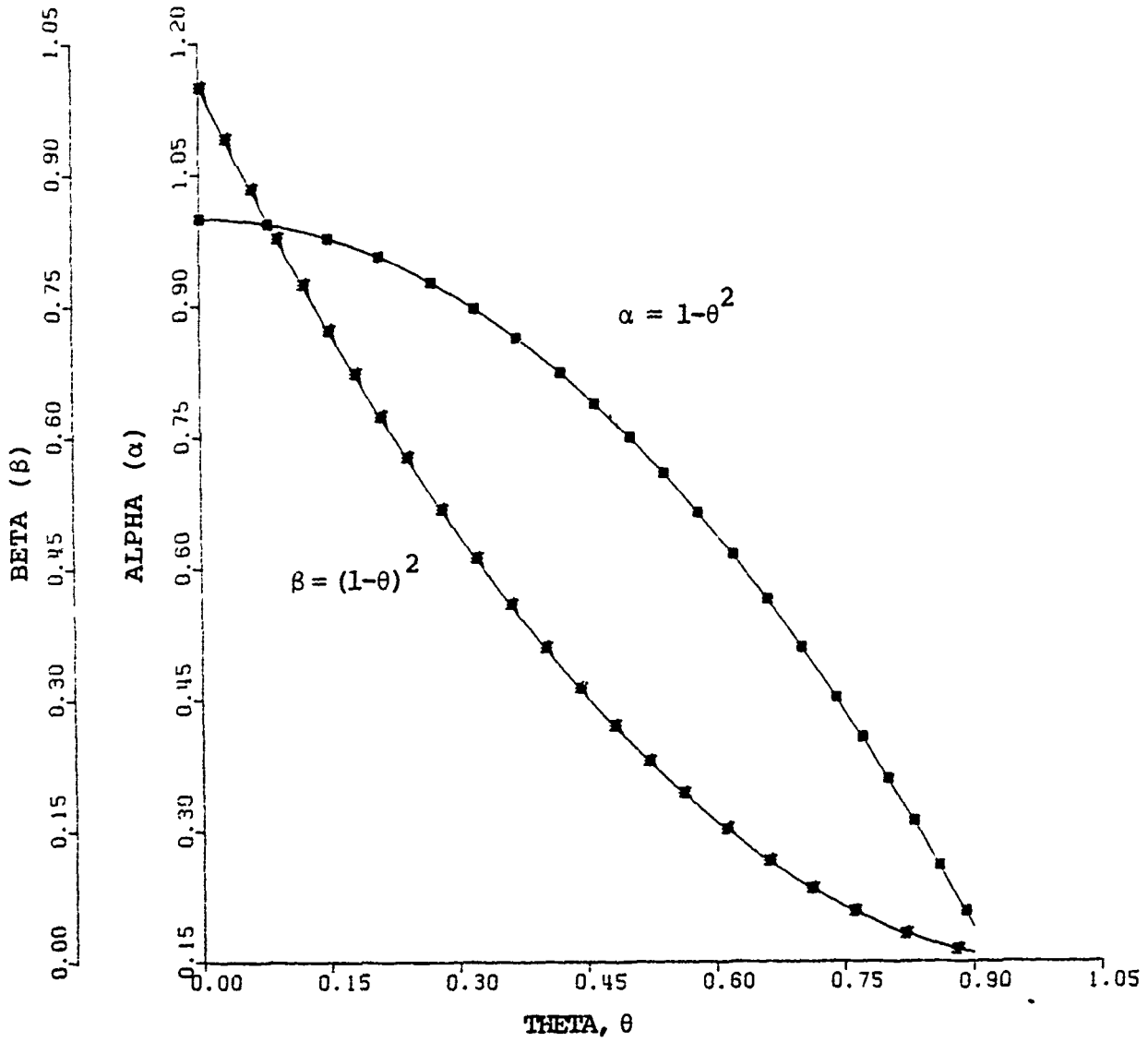


FIG. 34. $\alpha-\beta$ GAIN FOR LEAST-SQUARE CRITERION AS A FUNCTION OF THETA

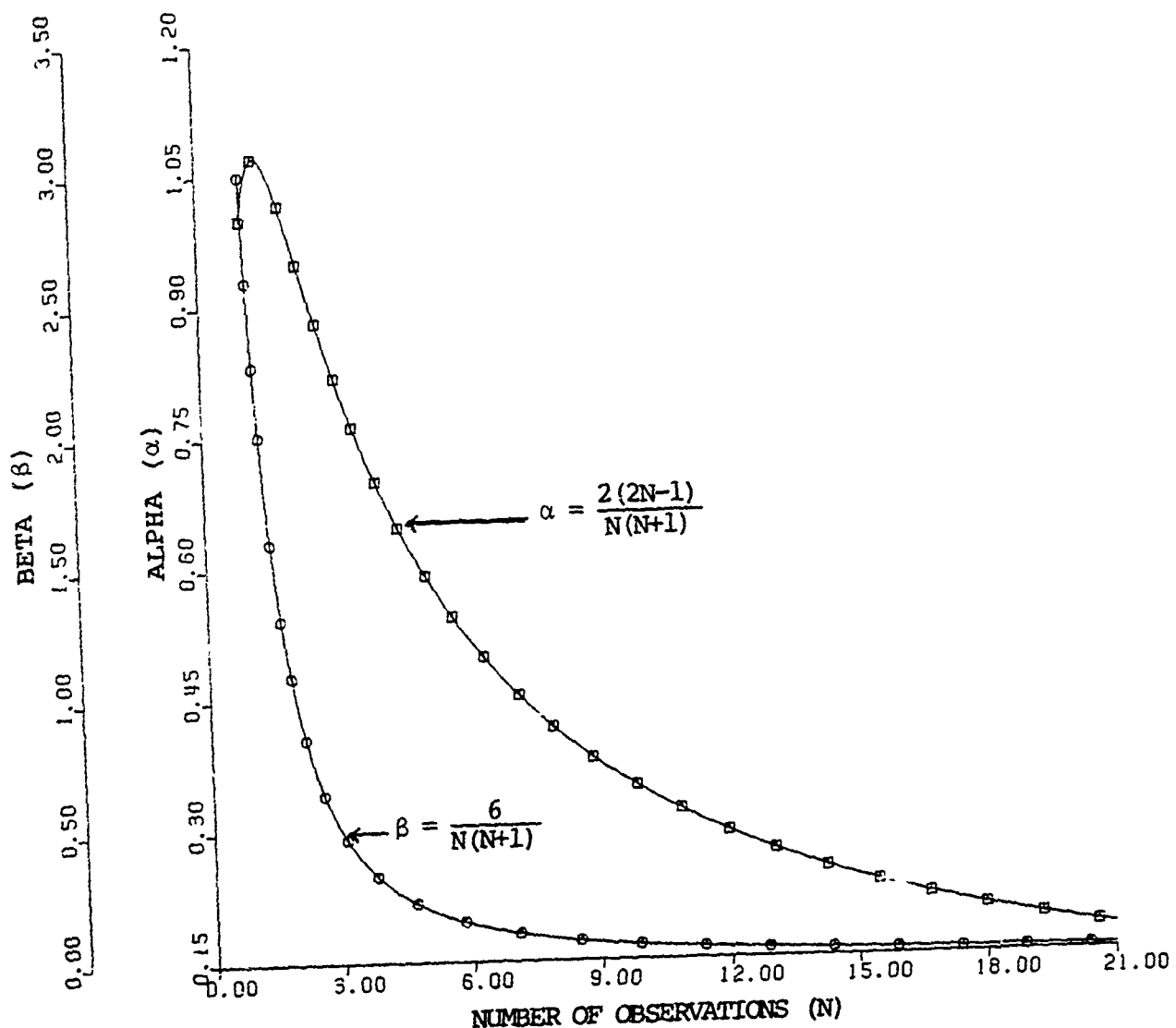


FIG. 35. α - β GAIN FOR CONTINUALLY COMPUTE THE LEAST-SQUARES LINE AS A FUNCTION OF OBSERVATIONS (N)

is used, i.e., if turn detection is provided. Then, if a turn is detected, the values of α and β may be raised simply by lowering N. Doing this will improve the turn following capability.

1. Numerical Example

Assume the following;

$$\text{Range measurement} = \sigma_R = 30.5 \text{ ft}$$

$$\ddot{x}_{\max} = 5g = 150 \text{ ft/sec}$$

$$\text{Desire } \sqrt{\text{VAR}(x_p^{N+1})} = 31.6 \text{ ft}$$

Find suitable critically damped α - β filter design.

By substituting Eqs. (3.25) and (3.26)

$$\alpha = 1 - \theta^2$$

$$\beta = (1 - \theta)^2$$

in Eq. (3.15)

$$\text{VRF} = \frac{\text{VAR}(x_p^{N+1})}{\sigma_R^2} = \frac{2a^2 + a\beta + 2\beta}{\alpha(4 - 2a - \beta)}$$

and letting

$$\text{VAR}(x_p^{N+1}) = (31.6)^2, \quad \sigma_R^2 = (30.5)^2,$$

yields

$$VRF = 1.074$$

$$\theta = 0.5$$

hence

$$\alpha = 0.75$$

$$\beta = 0.25$$

From Eq. (3.18)

$$\epsilon^* = 3 \sqrt{VAR(x_p^{N+1})} = 3 \sqrt{(31.6)^2} = 94.8 \text{ ft}$$

but from Eq. (3.17)

$$\epsilon^* = - \frac{\ddot{x} T^2}{\beta}$$

hence

$$T = 0.3848 \text{ sec.}$$

Finally, from Eq. (3.19)

$$\frac{D}{x_p^{N+1}} = \frac{T^2(2-\alpha)}{\alpha\beta(4-2\alpha-\beta)}$$

yields

$$D_{x_p^{N+1}} = D = 0.439 \text{ ft}^2$$

The values for $\alpha = 0.75$ and $\beta = 0.25$ satisfy the critically damped Eq. (2.19)

$$(\alpha + \beta)^2 = 4\beta \quad \text{and} \quad \beta \leq 1$$

The above values for $\alpha-\beta$, VRF and D can also be determined by using Figs. 27-31-34.

IV. ESTIMATING OPTIMAL TRACKING FILTER FOR MANEUVERING TARGET

The work which follows is an attempt to apply optimum filter theory to the tactical radar environment. There it is desired to obtain optimal estimates of target positions and their predicted tracks.

There are several possibilities for structuring a digital filter. From the work of Kalman [3], the filter should contain the same dynamic model as that of the incoming signal shown in Fig. 36.

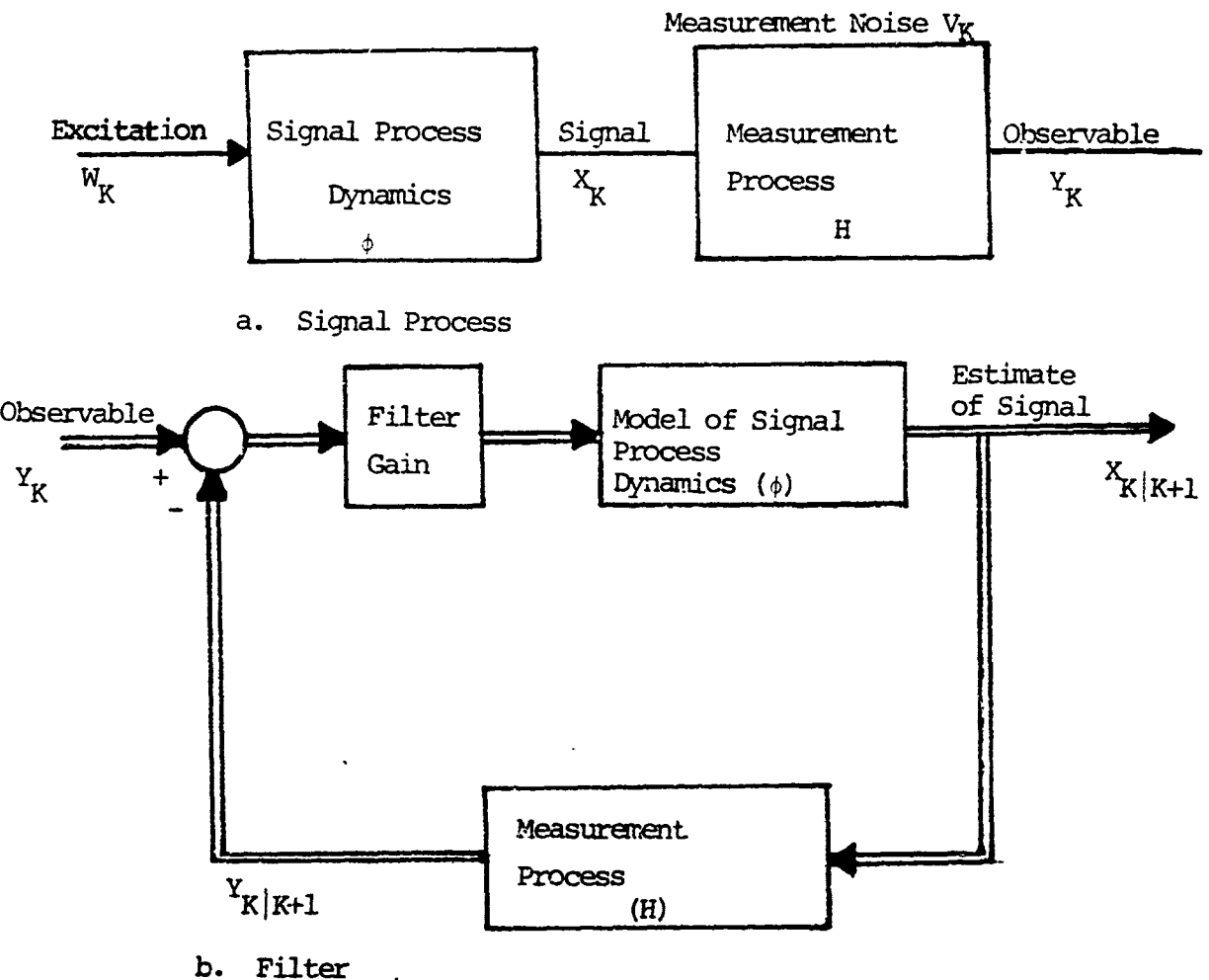


Fig. 36. Schematic of Filter Structure in Relation to Signal Process

The modeling of the various system components involved in a tactical weapon system, such as the radar measurement process and the target itself, is essential in the design of practical tracking and control algorithm. By modeling the target to be tracked and the accuracy of the radar's measurements [10], then a practical tracking procedure, consistent with the computer limitations and weapon system requirements, can be designed.

A. SENSOR AND VEHICLE MODELING - DYNAMIC EQUATIONS

The tracking systems under consideration utilize sensors that provide measurements of range and bearing. The selection is intended to reflect that this pair of measurements is most common, however, other output measurements as elevation and range rate (Doppler) are often available.

The vehicles to be tracked can be modeled by the state equations:

$$X(K+1) = \phi X(K) + G u(K) \quad (4.1)$$

where

$$X(K) = \begin{bmatrix} Y(K) \\ \dot{Y}(K) \\ \theta(K) \\ \dot{\theta}(K) \end{bmatrix} = \begin{bmatrix} \text{range at time } K \\ \text{range rate at time } K \\ \text{bearing at time } K \\ \text{bearing rate at time } K \end{bmatrix}$$

= vehicle state vector at time $t = KT$

$$u(K) = \begin{bmatrix} u_1(K) \\ u_2(K) \end{bmatrix} = \begin{bmatrix} \text{change in vehicle range rate between time } K \text{ and time } K+1 \\ \text{change in vehicle bearing rate between time } K \text{ and time } K+1 \end{bmatrix}$$

$$\phi = \begin{bmatrix} 1 & T & 0 & 0 \\ 0 & 1 & 0 & 0 \\ 0 & 0 & 1 & T \\ 0 & 0 & 0 & 1 \end{bmatrix} = \text{state transition matrix} \quad (4.2)$$

$$G = \begin{bmatrix} 0 & 0 \\ 1 & 0 \\ 0 & 0 \\ 0 & 1 \end{bmatrix}$$

and

T = sampling period.

The tracking sensor measures target position, range and bearing or elevation and provides the following output equation:

$$Y(K) = HX(K) + V(K) = \begin{bmatrix} \text{measured range at time } K \\ \text{measured bearing at time } K \end{bmatrix} \quad (4.3)$$

where

$$H = \begin{bmatrix} 1 & 0 & 0 & 0 \\ 0 & 0 & 1 & 0 \end{bmatrix} \quad \text{and} \quad V(K) = \begin{bmatrix} v_1(K) \\ v_2(K) \end{bmatrix} \quad (4.4)$$

The measurement noise covariance matrix $R(K)$, satisfies

$$R(K) = E[V(K)V^T(K)] = \begin{bmatrix} \sigma_{R(K)}^2 & 0 \\ 0 & \sigma_{\theta(K)}^2 \end{bmatrix} \quad (4.5)$$

assuming the noise $V_1(K)$ and $V_2(K)$ are independent. The selection of sensor coordinates (R, θ) , at this point, for the covariance matrix $R(K)$ has been made because the output matrix H assumes the extremely simple form shown, and the $R(K)$ becomes diagonal. When Doppler measurements are available, this selection of sensor coordinates becomes extremely advantageous because the cartesian forms for H and $R(K)$ becomes complex and time varying and often impose computational penalties for real-time implementation.

Consider the following polar to cartesian transformation (i.e., from R, θ to X, Y)

$$\begin{aligned} X &= R \sin \theta \\ (4.5a) \end{aligned}$$

$$Y = R \cos \theta$$

For the Kalman filter in XY coordinates, the measurement covariance matrix $R(K)$ is a function of the radar-target geometry. Therefore, the elements of the covariance matrix

$$R(K) = \begin{bmatrix} \sigma_{XX}^2 & \sigma_{XY}^2 \\ \sigma_{XY}^2 & \sigma_{YY}^2 \end{bmatrix} \quad (4.5b)$$

are

$$\sigma_{XX}^2 = \sigma_R^2 \cos^2 \theta + R^2 \sigma_\theta^2 \sin^2 \theta$$

$$\sigma_{YY}^2 = \sigma_R^2 \sin^2 \theta + R^2 \sigma_\theta^2 \cos^2 \theta \quad (4.5c)$$

$$\sigma_{XY}^2 = [\sigma_R^2 - R^2 \sigma_\theta^2] \sin \theta \cos \theta$$

where σ_R^2 and σ_θ^2 are the variances of the range (R) and bearing (θ) measurement errors, respectively. It is interesting to note that in general, the coordinates after the transformation (X and Y) are not independent. The singular cases where they are independent occur for $\theta = 0^\circ, 90^\circ, 180^\circ, \dots$ or for $R = \frac{\sigma_R}{\sigma_\theta}$. These special cases are easily explained from the assumption that the measurement errors are Gaussian, with typical contours of equal probability, which are ellipses.

Hence, if the axes lie in the directions of the axes of the frame of reference, the covariance terms $R(T)_{12}, R(K)_{21}$ are zero and the independence of X,Y errors for $\theta = 0^\circ, 90^\circ, \dots$

When $R = \sigma_R/\sigma_\theta$, these ellipses reduce to circles which may be considered as limiting ellipses whose major and minor

axes lie along the axes of the reference frame. Finally, since the observation $y(K)$ consists of x and y position measurements, hence, the observation $V(K)$ can be assumed to have covariance

$$R(K) = \begin{bmatrix} \sigma_u^2 & 0 \\ 0 & \sigma_v^2 \end{bmatrix} \quad (4.5d)$$

B. STATISTICAL DESCRIPTION OF TARGET MANEUVER

The input sequence $u(K)$ is additive state (or maneuver) noise that results in the vehicle deviating from a constant velocity trajectory.

Although the maneuver history and observation noise are not independent, the covariance $E[u(K)V^T(j)]$ is zero. Indeed, the radar cross section of a piloted vehicle changes during a maneuver, causing the radar observation noise to depend on the particular maneuver being exercised by the vehicle.

The maneuver noise is neither Gaussian nor white. For example, the pilot of an aircraft moving at constant velocity will generally not maneuver unless threatened by either radar detection or attacking vehicles. His maneuver will then often be a turn or an increase or decrease in his forward velocity.

A typical maneuver probability density is shown in Fig. 37.

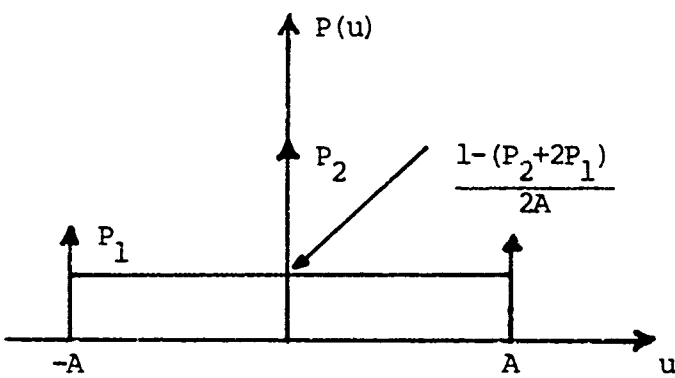


Fig. 37. Typical Probability Density of Target Maneuver

The quantity A is the maximum acceleration which the plane-pilot combination can withstand. Values of the density between non-maneuver ($u = 0$) and maximum ($u = \pm A$) are non zero because:

- (i) The vehicle may not be accelerating at its maximum rate
- (ii) The projection of a circular maneuver on any dimension can give values of u from $-A$ to A .

Clearly, then, the maneuver density is not Gaussian.

C. DISCRETE TIME EQUATIONS OF MOTION

It is often desirable to whiten the maneuver noise so that system equations to which optimal filtering theory applies can be obtained. This is done, as in [4]. The whitening procedure for a discrete signal is analogous to the procedure developed by Wiener and Kolmogorov to white continuous signals [11]. So, $u(k)$ may be expressed recursively in terms of the white noise sequence $w(k)$ by

$$u(K+1) = \rho u(K) + w(K) \quad (4.6)$$

Using the above equation, the following set of system equations are obtained having white noise sequences $w_1(K)$ and $w_2(K)$ as their only inputs:

$$x(K+1) = \phi x(K) + gw(K) \quad (4.7)$$

$$y(K) = hx(K) + v(K) \quad (4.8)$$

where

$$x(K) = \begin{bmatrix} r(K) \\ \dot{r}(K) \\ u_1(K) \\ \theta(K) \\ \dot{\theta}(K) \\ u_2(K) \end{bmatrix} \quad (4.9)$$

and

$$w(K) = \begin{bmatrix} w_1(K) \\ w_2(K) \end{bmatrix} \quad (4.10)$$

Also

$$\phi = \begin{bmatrix} 1 & T & 0 & 0 & 0 & 0 \\ 0 & 1 & 1 & 0 & 0 & 0 \\ 0 & 0 & \rho & 0 & 0 & 0 \\ 0 & 0 & 0 & 1 & T & 0 \\ 0 & 0 & 0 & 0 & 1 & 1 \\ 0 & 0 & 0 & 0 & 0 & \rho \end{bmatrix} = \begin{bmatrix} \text{State Transition} \\ \text{Matrix} \end{bmatrix} \quad (4.11)$$

$$G = \begin{bmatrix} 0 & 0 \\ 0 & 0 \\ 1 & 0 \\ 0 & 0 \\ 0 & 0 \\ 0 & 1 \end{bmatrix} \quad (4.12)$$

$$H = \begin{bmatrix} 1 & 0 & 0 & 0 & 0 & 0 \\ 0 & 0 & 0 & 1 & 0 & 0 \end{bmatrix} = [\text{Observation matrix}] \quad (4.13)$$

and where

$$\begin{aligned} Q(K) &= E[W(K)W^T(K)] = \begin{bmatrix} \sigma_{M1}^2(1-\rho^2) & 0 \\ 0 & \sigma_{M2}^2(1-\rho^2) \end{bmatrix} \\ &= \begin{bmatrix} \text{Covariance of} \\ \text{the measured} \\ \text{noise} \end{bmatrix} \quad (4.14) \end{aligned}$$

The values for the maneuver variances σ_{Mi}^2 and the correlation coefficient, ρ , depend on the maneuver characteristics of the vehicles being tracked.

Hence, the variances, σ_{Mi}^2 , of target acceleration are calculated using the model illustrated in Fig. 37. The target can accelerate at a maximum rate A ($-A$) and will do each with a probability P_1 and a probability P_2 of not accelerating at all, with an assumed uniform probability distribution of amplitude:

$$P(u) = \frac{1 - (2P_1 + P_2)}{2A} \quad (4.15)$$

of accelerating between $-A$ and $+A$.

The acceleration variable, therefore, has mean zero and variance

$$\sigma_{Mi}^2 = \frac{A^2(1 + 4P_1 - P_2)}{3} \quad (4.16)$$

Consequently, the variables u_1 and u_2 , which are assumed independent, have zero means and u_1 has variance

$$\sigma_{M1}^2 = \frac{A^2 T^2 (1 + 4P_1 - P_2)}{3} \quad (4.17)$$

while u_2 has variance

$$\sigma_{M2}^2 = \frac{A^2 T^2 (1 + 4P_1 - P_2)}{3R^2} \quad (4.18)$$

where R is the target range from the sensor and where all these quantities have appropriate units.

The correlation coefficient ($|\rho| \leq 1$) can be modelled by

$$\rho = \frac{E[u(K)u(K-1)]}{\sigma_{Mi}^2} = \begin{cases} 1 - \mu T & T \leq \frac{1}{\mu} \\ 0 & T > \frac{1}{\mu} \end{cases} \quad (4.19)$$

The quantity, μ , is essentially the inverse of the average maneuver duration. This correlation model is analogous to that in [4], which has the discrete time form $r(K) = \sigma_{Mi}^2 e^{-aT}$, where a is the inverse of the continuous maneuver time constant of the target. Hence, ρ equals e^{-aT} . When aT is small, ρ can be approximated closely by $1-aT$, so that a and μ become identical.

The two extreme cases occur when ρ is unity and when ρ approaches zero. So, the first case represents the completely correlated case, and the second is the completely uncorrelated case, namely white noise.

D. FILTER DESCRIPTION

Three types of filters are considered as potential candidate algorithms for tracking vehicles that are described by the model just discussed. These filters are the Kalman, the simplified Kalman and an $\alpha-\beta$ filter.

1. The Kalman Filter

The Kalman filter uses the augmented version of the model presented earlier in order to obtain white excitation (maneuver) noise.

The method of computing the optimum estimate (the filter) is as follows:

$$X(K|K-1) = \hat{X}(K-1|K-1) \quad (4.20)$$

$$\begin{aligned} X(K|K) &= \hat{X}(K|K-1) + P(K|K-1)H^T [HP(K|K-1)H^T + R(K)]^{-1} \\ &\quad \cdot [y(K) - H\hat{X}(K|K-1)] \end{aligned} \quad (4.21)$$

where

$$P(K|K-1) = \phi P(K-1|K-1) \phi^T + GQ(K-1)G^T \quad (4.22)$$

$$P(K|K) = P(K|K-1) - P(K|K-1)H^T [HP(K|K-1)H^T + R(K)]^{-1} HP(K|K-1) \quad (4.23)$$

In these equations

- (i) The double argument always denotes an estimate
- (ii) $\hat{X}(K|K)$ = Filtered estimate of $X(K)$
- (iii) $\hat{X}(K|K-1)$ = one-step predicted estimate of $X(K)$
- (iv) $P(K|K)$ = Covariance of filtered estimate
- (v) $P(K|K-1)$ = Covariance of predicted estimate
- (vi) $[y(K) - H\hat{X}(K|K-1)]$ = Error in the predicted observations

- (vii) $G(K) = P(K|K-1)H^T [HP(K|K-1)H^T + R(K)]^{-1}$
- = Kalman Gain Matrix
- = Is a matrix of adjustment coefficients.
The matrix, $G(K)$, reflects the relative confidence one should have in the observed data as compared to the predicted estimate.

The filter is initialized on the basis of two observations as follows:

$$\hat{x}(2|2) = \begin{bmatrix} y_1(2) \\ \frac{1}{T}[y_1(2)-y_1(1)] \\ 0 \\ y_2(2) \\ \frac{1}{T}[y_2(2)-y_2(1)] \\ 0 \end{bmatrix} \quad (4.24)$$

The elements of the corresponding covariance matrix, $P(2|2)$, are:

$$P(2|2) = \begin{bmatrix} \sigma_R^2 & \sigma_R^2/T & 0 & 0 & 0 & 0 \\ \sigma_R^2/T & \sigma_{M1}^2 + \frac{2\sigma_R^2}{T^2} & \rho\sigma_{M1}^2 & 0 & 0 & 0 \\ 0 & \rho\sigma_{M1}^2 & \sigma_{M1}^2 & 0 & 0 & 0 \\ 0 & 0 & 0 & \sigma_\theta^2 & \sigma_\theta^2/T & 0 \\ 0 & 0 & 0 & \sigma_\theta^2/T & \sigma_{M2}^2 + \frac{2\sigma_\theta^2}{T^2} & \rho\sigma_{M2}^2 \\ 0 & 0 & 0 & 0 & \rho\sigma_{M2}^2 & \sigma_{M2}^2 \end{bmatrix}$$

(4.25)

The quantities σ_{M1}^2 , σ_{M2}^2 should be calculated as discussed previously (Eq. 4.17-4.18).

A block diagram of the discrete Kalman filter is shown in Fig. 38.

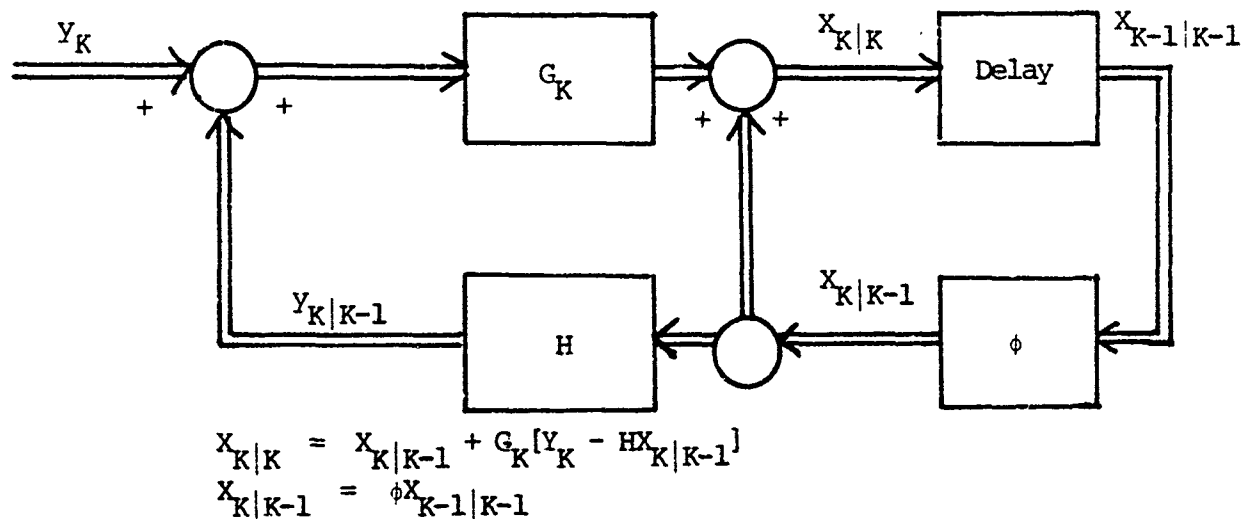


Fig. 38. Block Diagram and Equations of the Discrete Kalman Filter

2. The Simplified Kalman Filter

By simplifying the maneuver model used in the Kalman filter, the state vector can be reduced from six to four elements, and the number of independent components of the covariance matrix from ten to six. The model simplification is achieved by assuming (incorrectly) that the vehicle's change in velocity is uncorrelated between samples, i.e., the maneuver is white.

The regular Kalman filter requires two augmented state variables in order to whiten the target maneuver. If the maneuver is assumed white, no augmentation need be performed and the simplification just discussed occurs. This simplified Kalman filter can therefore also be referred to, as an unaugmented Kalman filter.

The utility of this filter is greatest, therefore, when either sensitivity of tracking performance to assumed maneuver correlation is small, or when the target maneuver approaches whiteness relative to the sensor data rate.

The equations for this filter and all quantities except the following have previously been defined:

$$Q(K) = \begin{bmatrix} \sigma_{M1}^2 & 0 \\ 0 & \sigma_{M2}^2 \end{bmatrix} = \begin{bmatrix} \text{Covariance of} \\ \text{"assumed white"} \\ \text{maneuver noise} \end{bmatrix} \quad (4.26)$$

and the elements of the corresponding covariance matrix, $P(2|2)$, are:

$$P(2|2) = \begin{bmatrix} \sigma_R^2 & \sigma_R^2/T & 0 & 0 \\ \sigma_R^2/T & \sigma_{M1}^2 + \frac{2\sigma_R^2}{T^2} & 0 & 0 \\ 0 & 0 & \sigma_\theta^2 & \sigma_\theta^2/T \\ 0 & 0 & \sigma_\theta^2/T & \sigma_{M2}^2 + \frac{2\sigma_\theta^2}{T^2} \end{bmatrix} \quad (4.27)$$

3. Recursive Algorithm

The problem is solved recursively by first assuming the problem is solved at time K-1. Specifically it is assumed that the best estimate $\hat{X}(K-1|K-1)$ at time K-1 and its error covariance matrix $P(K-1|K-1)$ are known.

(i) Calculate the one-step prediction

$$\hat{X}(K|K-1) = \phi \hat{X}(K-1|K-1) \quad (4.28)$$

(ii) Calculate the covariance matrix for the one-step prediction

$$P(K|K-1) = \phi P(K-1|K-1) \phi^T + G Q(K-1) G^T \quad (4.29)$$

(iii) Calculate the prediction observation

$$\hat{y}(K|K-1) = H \hat{X}(K|K-1) \quad (4.30)$$

(iv) Calculate the filter gain

$$G(K) = P(K|K-1)H^T [HP(K|K-1)H^T + R(K)]^{-1} \quad (4.31)$$

(v) Calculate the new smoothed estimate

$$\hat{X}(K|K) = \hat{X}(K|K-1) + G(K)[Y(K) - \hat{Y}(K|K-1)] \quad (4.32)$$

(vi) Calculate the new covariance matrix

$$P(K|K) = P(K|K-1) - P(K|K-1)H^T [HP(K|K-1)H^T + R(K)]^{-1}HP(K|K-1)$$

$\xleftarrow{\hspace{1cm}} G_K \xrightarrow{\hspace{1cm}}$

or

$$P(K|K) = [I - G(K)H] P(K|K-1) \quad (4.33)$$

In summary, starting with an estimate $\hat{X}(K-1|K-1)$ and its covariance matrix $P(K-1|K-1)$ after receiving a new observation $Y(K)$ and calculating the six quantities in the recursive algorithm, a new estimate $\hat{X}(K|K)$ and its covariance matrix $P(K|K)$ are obtained.

V. IMPLEMENTATION AND SIMULATION RESULTS

In order to evaluate the three filter algorithms in a variety of tactical environments, an air vehicle type, and two tracking sensors were selected for analysis.

Maneuver statistics (A , P_1 , P_2 , μ) were selected to match the vehicle, and sensor statistics (σ_R^2 , σ_θ^2 , T) were selected for each combination of sensor and data entry evaluated. One trajectory was constructed for the vehicle that consists of a straight track and a maneuvering track and is shown in Fig. 39.

The x-direction vs time of range, velocity, acceleration, bearing, bearing rate and bearing acceleration, were plotted and shown in Figs. 40-45.

For the scenario considered, an aircraft moves at 10 KM moves at 100 m/sec (200 knots), can maneuver at a maximum acceleration of $4g$ ($A = 39.24 \text{ m/sec}^2$), and has a probability of maneuvering at max 0.2 ($2P_1 = 0.2$, $P_1 = 0.1$), and a probability 0.5 of not maneuvering at all ($P_2 = 0.5$). Assume a lazy maneuver that will provide correlated acceleration inputs for periods between 10 and 30 sec. Hence, with an average maneuver duration of 20 sec, by using Eq. (4.19), $\mu = 1/20 = 0.05 = a$, and the correlation coefficient $P = 1 - aT = 1 - .005T$.

The two sensors were classified as:

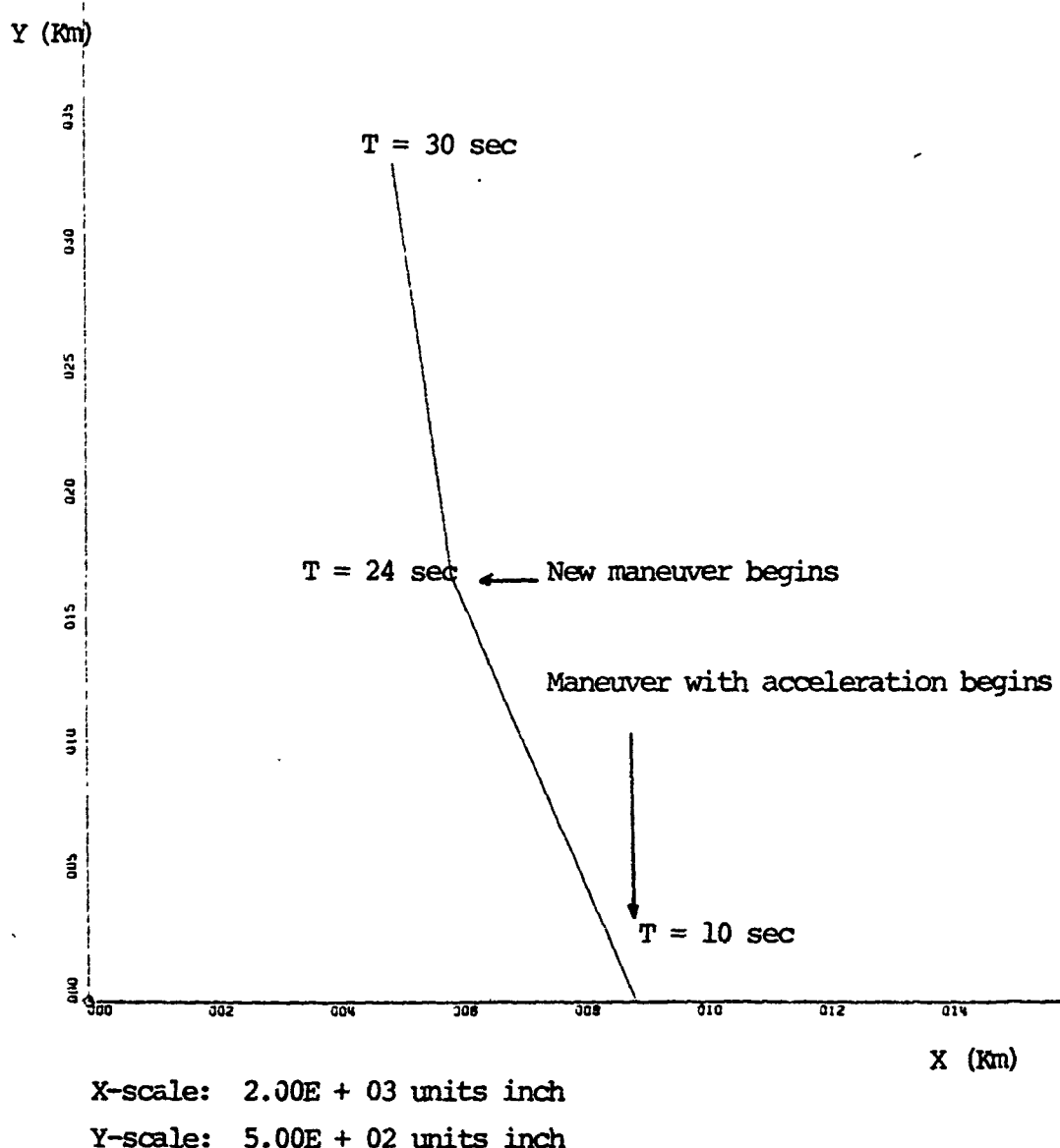
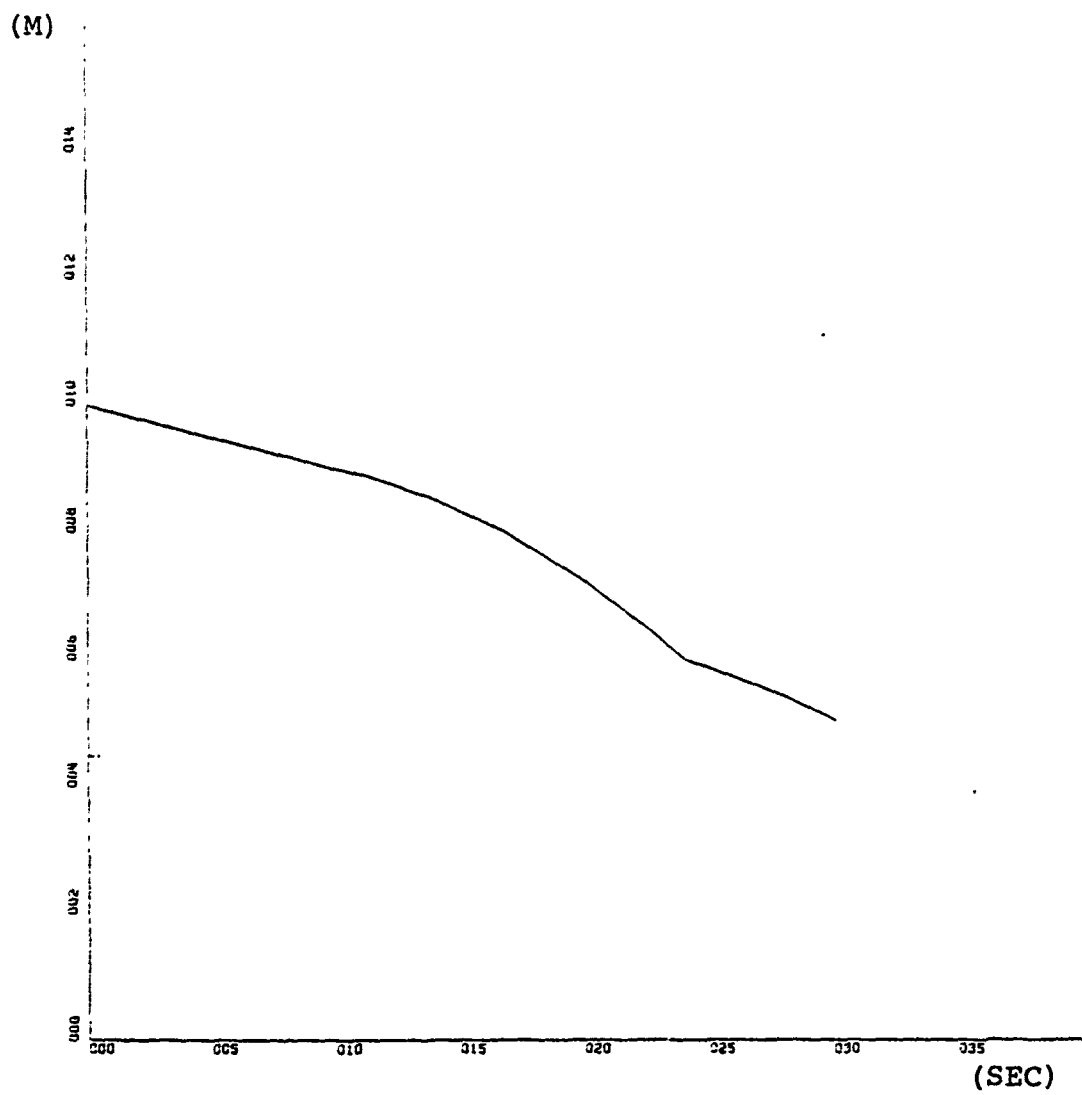


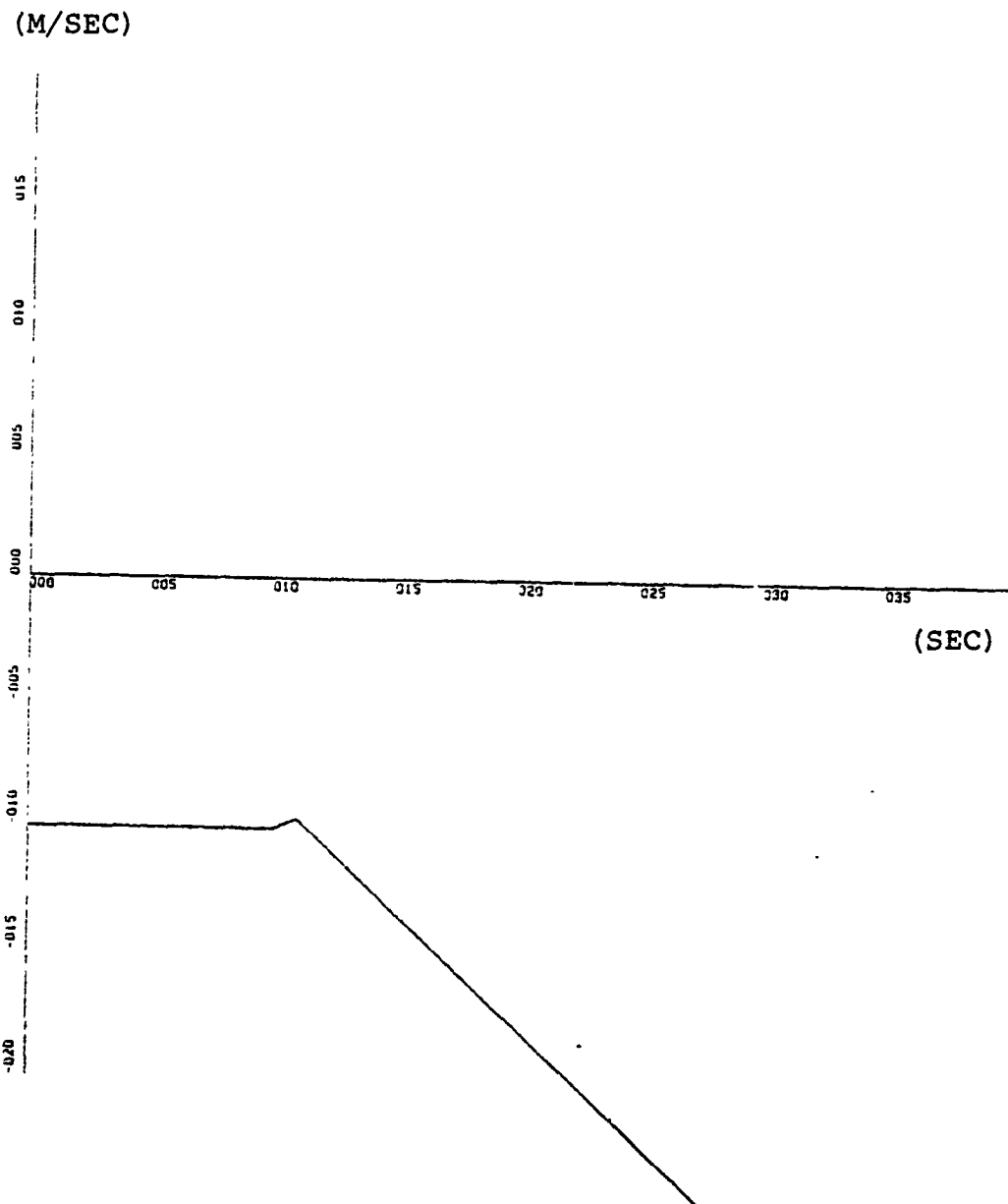
FIG. 39. VEHICLE TRAJECTORY IN X-Y



X-Scale: 5.00E + 00 units inch

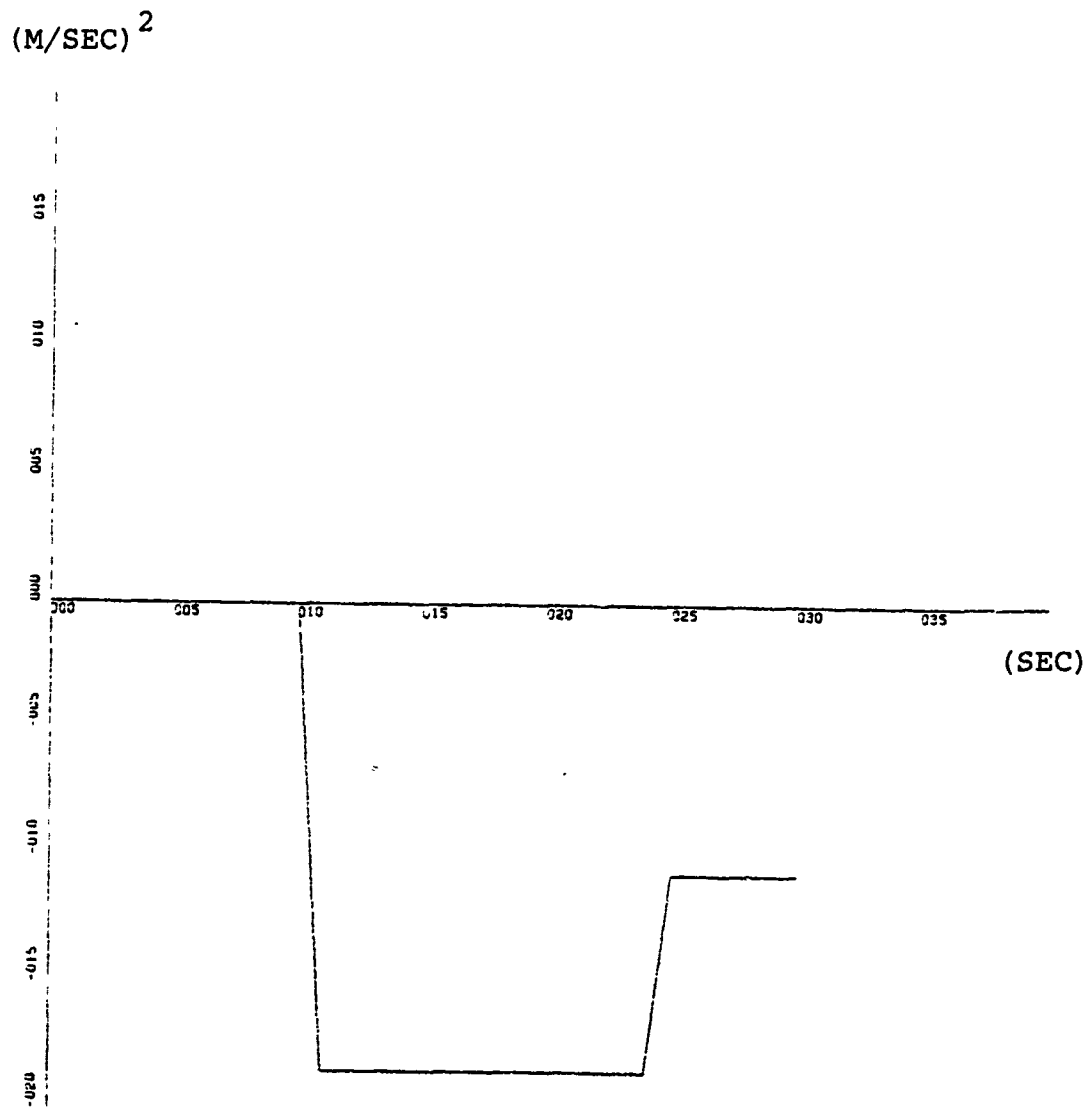
Y-scale: 2.00E + 03 units inch

FIG. 40. RANGE (X-AXIS) VS TIME



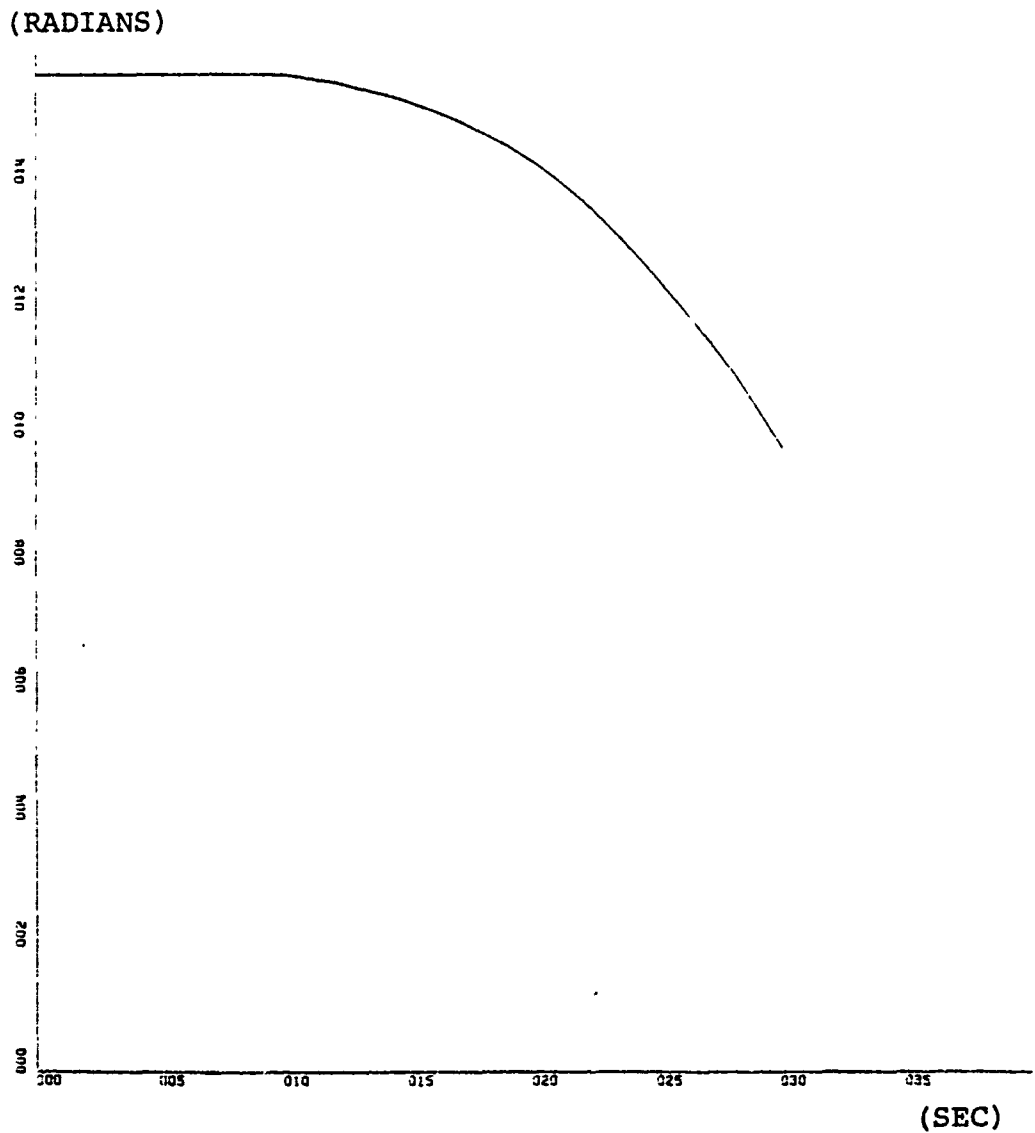
X-Scale: 5.00E + 00 units inch
Y-scale: 5.00E + 01 units inch

FIG. 41. VELOCITY (X-AXIS) VS TIME



X-Scale: 5.00E + 00 units inch
Y-Scale: 5.00E + 00 units inch

FIG. 42. ACCELERATION (X-AXIS) VS TIME

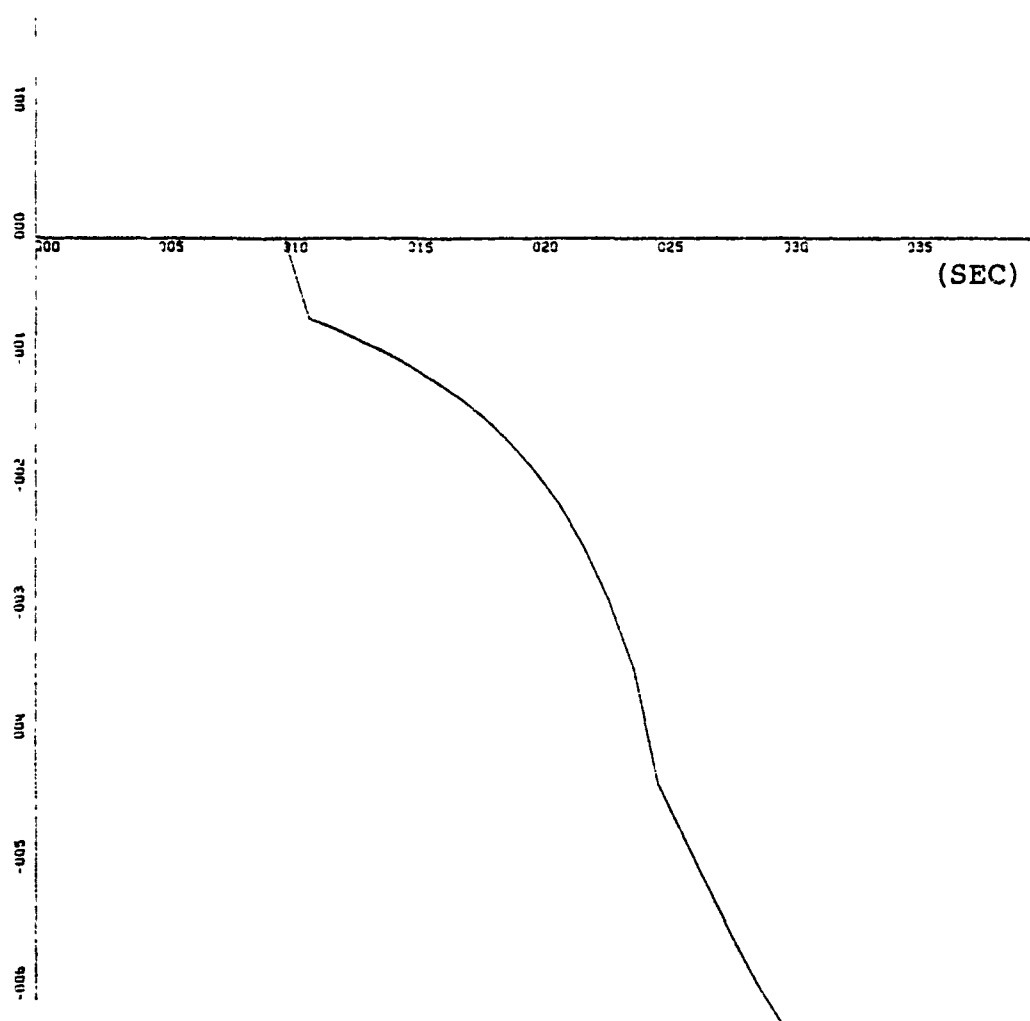


X-Scale: 5.00E + 00 units inch

Y-Scale: 2.00E - 01 units inch

FIG. 43. BEARING (X-AXIS) VS TIME

(RAD/SEC)

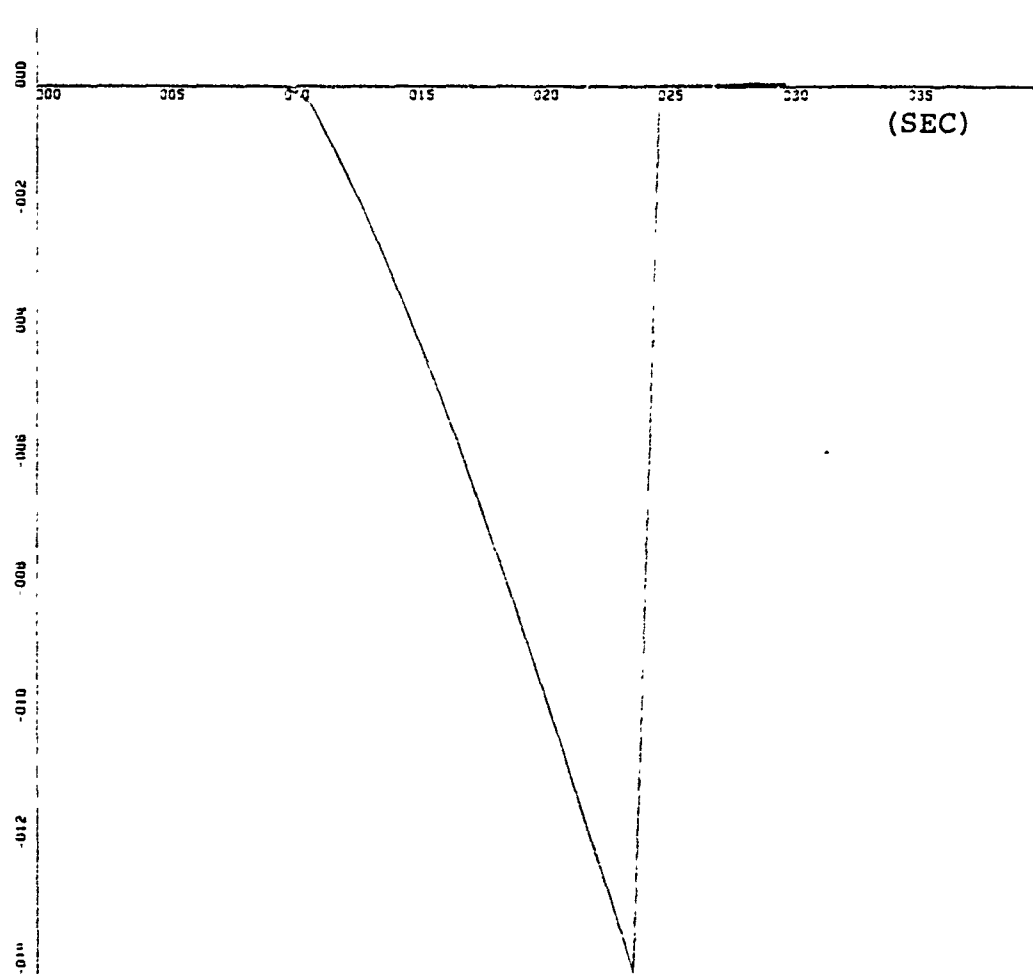


X-Scale: 5.00E + 00 units inch

Y-Scale: 1.00E - 02 units inch

FIG. 44. BEARING RATE (X-AXIS) VS TIME

(RAD/SEC)²



X-Scale: 5.00E + 00 units inch

Y-Scale: 2.00E + 00 units inch

FIG. 45. BEARING ACCELERATION (X-AXIS) VS TIME

A. EXAMPLE 1 - AIR SEARCH RADAR

The radar data rate was ten samples per second ($T = 10$ sec) hence, the correlation coefficient $\rho = 1 - 0.05(10) = 0.5$, and the sensor processing noise (measurement noise variances) has been taken into account, 500 m in range ($\sigma_R = 500$ m) and 17.4 mrad in bearing ($\sigma_\theta = 1$ degree = 17.4 mrad). The variances of maneuvering at max acceleration, and not maneuvering at all, were calculated by using Eqs. (4.17-4.18) and found to be, $\sigma_{M1}^2 = 46193$ m/sec and $\sigma_{M2}^2 = 1.346 \times 10^{-4}$ sec $^{-2}$.

1. Kalman Filter Evaluation

This model can be used with the Kalman filter Eqs. (4.29-4.31-4.33) to determine a set of filter gains.

For the model assumed, by using Eqs. (4.5, 4.11-4.14, 4.25), the following matrices were obtained:

$$\Phi = \begin{bmatrix} 1 & 10 & 0 & 0 & 0 & 0 \\ 0 & 1 & 1 & 0 & 0 & 0 \\ 0 & 0 & 0.5 & 0 & 0 & 0 \\ 0 & 0 & 0 & 1 & 10 & 0 \\ 0 & 0 & 0 & 0 & 1 & 1 \\ 0 & 0 & 0 & 0 & 0 & 0.5 \end{bmatrix} \quad G = \begin{bmatrix} 0 & 0 \\ 0 & 0 \\ 1 & 0 \\ 0 & 0 \\ 0 & 0 \\ 0 & 1 \end{bmatrix}$$

$$H = \begin{bmatrix} 1 & 0 & 0 & 0 & 0 & 0 \\ 0 & 0 & 0 & 1 & 0 & 0 \end{bmatrix}$$

$$R = \begin{bmatrix} 25 \times 10^4 & 0 \\ 0 & 3.02 \times 10^{-4} \end{bmatrix}$$

$$Q = \begin{bmatrix} 34645 & 0 \\ 0 & 10^{-4} \end{bmatrix}$$

$$P(2|2) = \begin{bmatrix} 25 \times 10^4 & 25 \times 10^3 & 0 & 0 & 0 & 0 \\ 25 \times 10^3 & 51193 & 23096.5 & 0 & 0 & 0 \\ 0 & 23096.5 & 46193 & 0 & 0 & 0 \\ 0 & 0 & 0 & 3.02 \times 10^{-4} & 3.02 \times 10^{-5} & 0 \\ 0 & 0 & 0 & 3.02 \times 10^{-5} & 1.41 \times 10^{-4} & 0.673 \times 10^{-4} \\ 0 & 0 & 0 & 0 & 0.673 \times 10^{-4} & 1.346 \times 10^{-4} \end{bmatrix}$$

2. Simplified Kalman Filter Evaluation

The simplified Kalman filter is achieved by assuming (incorrectly) that the vehicle's change in velocity is uncorrelated between samples; i.e., the maneuver is white, and $\rho = 0$. Here, for the model assumed, by using Eqs. (4.2-4.4-4.5-4.26-4.27), the following matrices are obtained.

$$\phi = \begin{bmatrix} 1 & 10 & 0 & 0 \\ 0 & 1 & 0 & 0 \\ 0 & 0 & 1 & 10 \\ 0 & 0 & 0 & 1 \end{bmatrix} \quad G = \begin{bmatrix} 0 & 0 \\ 1 & 0 \\ 0 & 0 \\ 0 & 1 \end{bmatrix}$$

$$H = \begin{bmatrix} 1 & 0 & 0 & 0 \\ 0 & 0 & 1 & 0 \end{bmatrix} \quad R = \begin{bmatrix} 25 \times 10^4 & 0 \\ 0 & 3.02 \times 10^{-4} \end{bmatrix}$$

$$Q = \begin{bmatrix} 46193 & 0 \\ 0 & 1.346 \times 10^{-4} \end{bmatrix}$$

$$P(2|2) = \begin{bmatrix} 25 \times 10^4 & 25 \times 10^3 & 0 & 0 \\ 25 \times 10^3 & 51193 & 0 & 0 \\ 0 & 0 & 3.02 \times 10^{-4} & 3.02 \times 10^{-5} \\ 0 & 0 & 3.02 \times 10^{-5} & 1.41 \times 10^{-4} \end{bmatrix}$$

B. EXAMPLE 2 - SURFACE AND AIR SEARCH RADAR

In this example, all quantities except the following, have previously been defined for the air search radar example:

Sampling time $T = 1$ sec, hence $\rho = 1-aT = 1-0.05(1) = 0.95$, the sensor processing noise (measurement noise variances) has been taken into account, $s_R = 20$ m, $\sigma_\theta = 0.1$ degree = 1.74 mrad and the variances of maneuvering were calculated and found to be, $\sigma_{M1}^2 = 461.93$ m/sec 2 , $\sigma_{M2}^2 = 1.346 \times 10^{-6}$ sec $^{-2}$.

1. Kalman Filter Evaluation

For the model assumed the following matrices were obtained.

$$\phi = \begin{bmatrix} 1 & 1 & 0 & 0 & 0 & 0 \\ 0 & 1 & 1 & 0 & 0 & 0 \\ 0 & 0 & 0.95 & 0 & 0 & 0 \\ 0 & 0 & 0 & 1 & 1 & 0 \\ 0 & 0 & 0 & 0 & 1 & 1 \\ 0 & 0 & 0 & 0 & 0 & 0.95 \end{bmatrix} \quad G = \begin{bmatrix} 0 & 0 \\ 0 & 0 \\ 1 & 0 \\ 0 & 0 \\ 0 & 0 \\ 0 & 1 \end{bmatrix}$$

$$H = \begin{bmatrix} 1 & 0 & 0 & 0 & 0 & 0 \\ 0 & 0 & 0 & 1 & 0 & 0 \end{bmatrix} \quad R = \begin{bmatrix} 400 & 0 \\ 0 & 3.02 \times 10^{-6} \end{bmatrix}$$

$$Q = \begin{bmatrix} 45.04 & 0 \\ 0 & 0.13 \times 10^{-6} \end{bmatrix}$$

$$P(2|2) = \begin{bmatrix} 400 & 400 & 0 & 0 & 0 & 0 \\ 400 & 1261.93 & 487.83 & 0 & 0 & 0 \\ 0 & 438.83 & 461.93 & 0 & 0 & 0 \\ 0 & 0 & 0 & 3.02 \times 10^{-6} & 3.02 \times 10^{-6} & 0 \\ 0 & 0 & 0 & 3.02 \times 10^{-6} & 7.386 \times 10^{-6} & 1.2787 \times 10^{-6} \\ 0 & 0 & 0 & 0 & 1.2787 \times 10^{-6} & 1.346 \times 10^{-6} \end{bmatrix}$$

2. Simplified Kalman Filter Evaluation

For the model assumed the following matrices were obtained:

$$\phi = \begin{bmatrix} 1 & 1 & 0 & 0 \\ 0 & 1 & 0 & 0 \\ 0 & 0 & 1 & 1 \\ 0 & 0 & 0 & 1 \end{bmatrix} \quad G = \begin{bmatrix} 0 & 0 \\ 1 & 0 \\ 0 & 0 \\ 0 & 1 \end{bmatrix}$$

$$H = \begin{bmatrix} 1 & 0 & 0 & 0 \\ 0 & 0 & 1 & 0 \end{bmatrix} \quad R = \begin{bmatrix} 400 & 0 \\ 0 & 3.02 \times 10^{-6} \end{bmatrix}$$

$$Q = \begin{bmatrix} 461.93 & 0 \\ 0 & 1.346 \times 10^{-6} \end{bmatrix}$$

$$P(2|2) = \begin{bmatrix} 400 & 400 & 0 & 0 \\ 400 & 1261.93 & 0 & 0 \\ 0 & 0 & 3.02 \times 10^{-6} & 3.02 \times 10^{-6} \\ 0 & 0 & 3.02 \times 10^{-6} & 7.386 \times 10^{-6} \end{bmatrix}$$

C. THE α - β FILTER EVALUATION

The α - β filter considered in this paper, and used for simulation, is one of many varieties possible in this class, is more easily implemented than either the Kalman or Simplified Kalman filters, and has been selected for evaluation since it is utilized extensively in tactical applications. Because it is designed to minimize the mean squared error in filtered position and velocity under the assumption of straight line target motion, it has little capability to track severely maneuvering vehicle. The α - β filter examined has no provision to adapt to different target types, as does the Kalman filter, since maneuver statistics are not taken into account. The Eqs. (2.1-2.3-2.37-2.38) for the α - β filter evaluated are:

$$x_s^N = x_p^N + \alpha(x_m^N - x_p^N)$$

$$v_s^N = v_s^{N-1} + \frac{\beta}{T}(x_m^N - x_p^N)$$

$$x_p^N = x_s^{N-1} + v_s^{N-1}T$$

where

$$\alpha = \frac{2(2N-1)}{N(N+1)}, \quad \beta = \frac{6}{N(N+1)} \quad \text{and} \quad T = 1 \text{ sec or } 10 \text{ sec}$$

in order to continually compute the least-squares line through the observations.

D. COMPARISON OF FILTER ACCURACIES

One hundred (100) Monte Carlo trials were made for each combination of tracking filter, tracking sensor and data entry procedure.

Experimental determined filtered and predicted accuracies in vehicle range coordinates (range, range rate, and range acceleration) and bearing coordinates (bearing, bearing rate, and bearing acceleration) with means and variances of estimation error histories, were then calculated and plotted and shown in Appendix A.

Table II shows a representative summary of the result, in which the prediction accuracies of each filter were compared on a percentage basis to that of the Kalman filter.

The entries in the table were determined by averaging the experimentally obtained percentage degradations in each of the above coordinates.

The Simplified Kalman filter, and the Kalman filter generally performed within twenty percent (20%) of each other.

The $\alpha-\beta$ filter performance, on the average, appears to be about equal to the above filters for the straight part of track, and about thirty to sixty percent (30-60%) worse,

Sensor Type	Air Search Radar	Surface and Air Search Radar
Filter Type		
$\alpha-\beta$ Filter	2	1
Simplified Kalman Filter	1	1
Kalman Filter	1	1

Key: 1 = within 10-20 percent of the Kalman filter

2 = within 30-50 percent of the Kalman filter

Table II. Synopsis of the Accuracy Comparison of the Three Tracking Filters

with the greatest degradation occurring for the maneuvering and accelerating part of track, because the gain vector quickly becomes too small to correct for the large estimation errors resulting from target maneuvers.

VI. SUMMARY AND CONCLUSIONS

While no extensive analysis is implemented, it is considered that a reasonable and unequivocal comparison of the filters can be made from the material presented.

The analysis of the filters and the radar system simulations presented in this paper is considered overall to be a simplified but realistic model of a sophisticated system which could be implemented with current "state of the art" hardware. Based on the ensemble averages the Kalman filter obviously provides a somewhat better tracking response for the target track tested.

The tracking ability of the α - β and Kalman filters appears to be about equal for "look alike" targets in close proximity, under the assumption of straight line motion. The α - β filter, however, provided unsatisfactory performance when the tracked vehicles executed maneuver. Based also on the simulation results, the Simplified Kalman filter becomes attractive for implementation, because it provided tracking accuracies within ten-twenty percent of the Kalman filter. The utility of this filter is greatest, when either the sensitivity of tracking performance to assumed maneuver correlation is small, or when the target maneuver approaches whiteness relative to the sensor data rate.

The filter implementation requirements increase in the following order: α - β filter, Simplified Kalman filter,

Kalman filter. Moreover, the "complexity factor" between the above filters is about two-to-one.

Finally, in most applications, the answer to the question, "which filter is most accurate?", does not alone determine filter selection. Indeed, the following questions must all be answered in the filter selection process to obtain the "best" filter for a particular system:

- a. What are the actual accuracies of each filter?
- b. What are the relative filter accuracies?
- c. What are the tracking accuracy requirements of the system?
- d. How sensitive is system performance to tracking accuracy?
- e. What are the computer requirements of the filter?
- f. What are the computer limitations of the system?

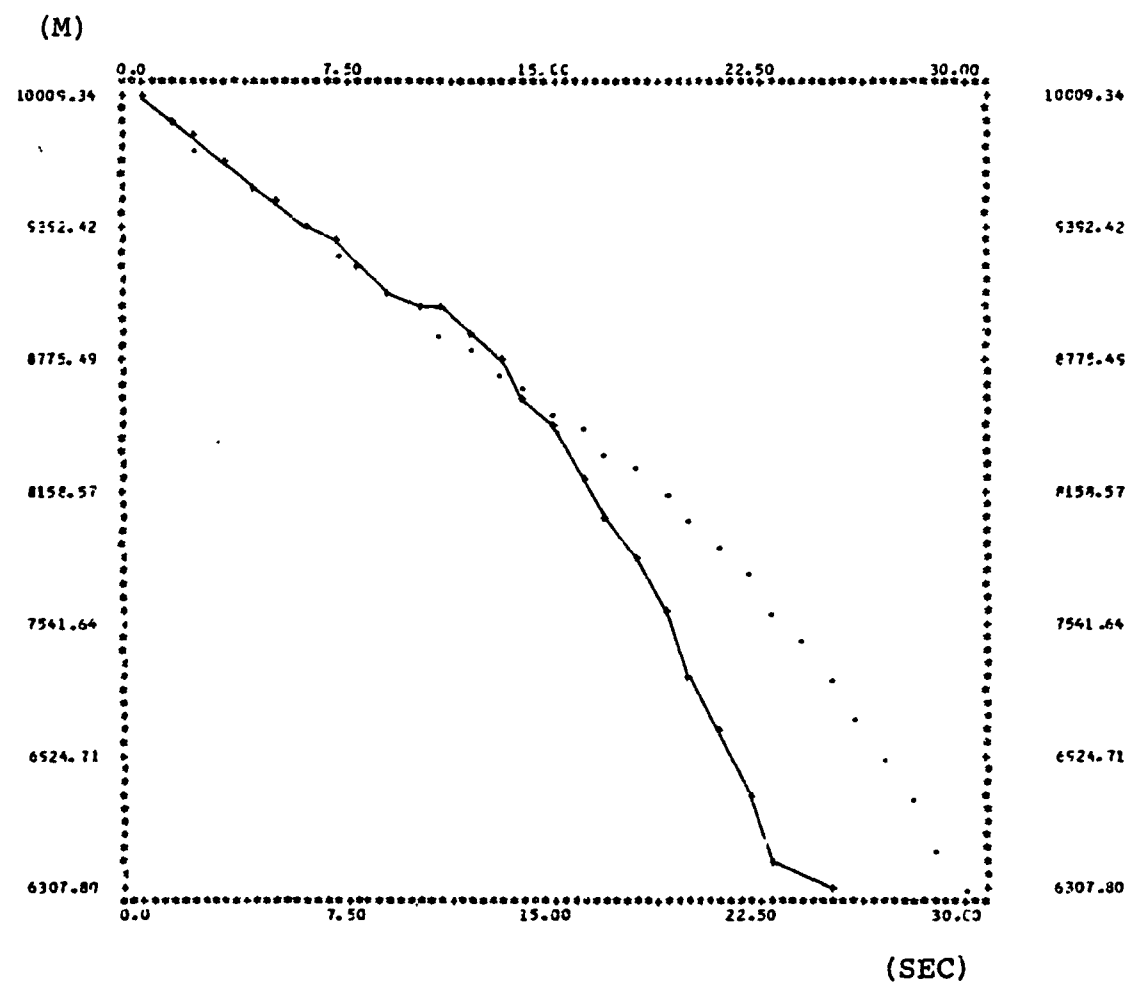
The list shows that filter selection involves careful balancing of filter accuracies, filter implementation requirements, and system performance goals and limitations.

APPENDIX A

Simulation results, of experimental filtered and predicted accuracies, in vehicle range and bearing coordinates, with means and variances of estimation error histories, provided for comparison of each of the three filters.

These results were generated using Monte Carlo simulation, with the following description of run:

	$\alpha-\beta$ Filter	Simplified Kalman Filter	Kalman Filter
order of system	2	4	6
no. of measured states	2	2	2
no. of time samples	31	31	31
no. of random forcing inputs	2	2	2
no. of members in ensemble	100	100	100



X-Scale: 0.375 units (____+) Actual
 Y-Scale: 61.7 units (.....) Filtered

FIG. 46. RANGE VS TIME FOR α - β FILTER

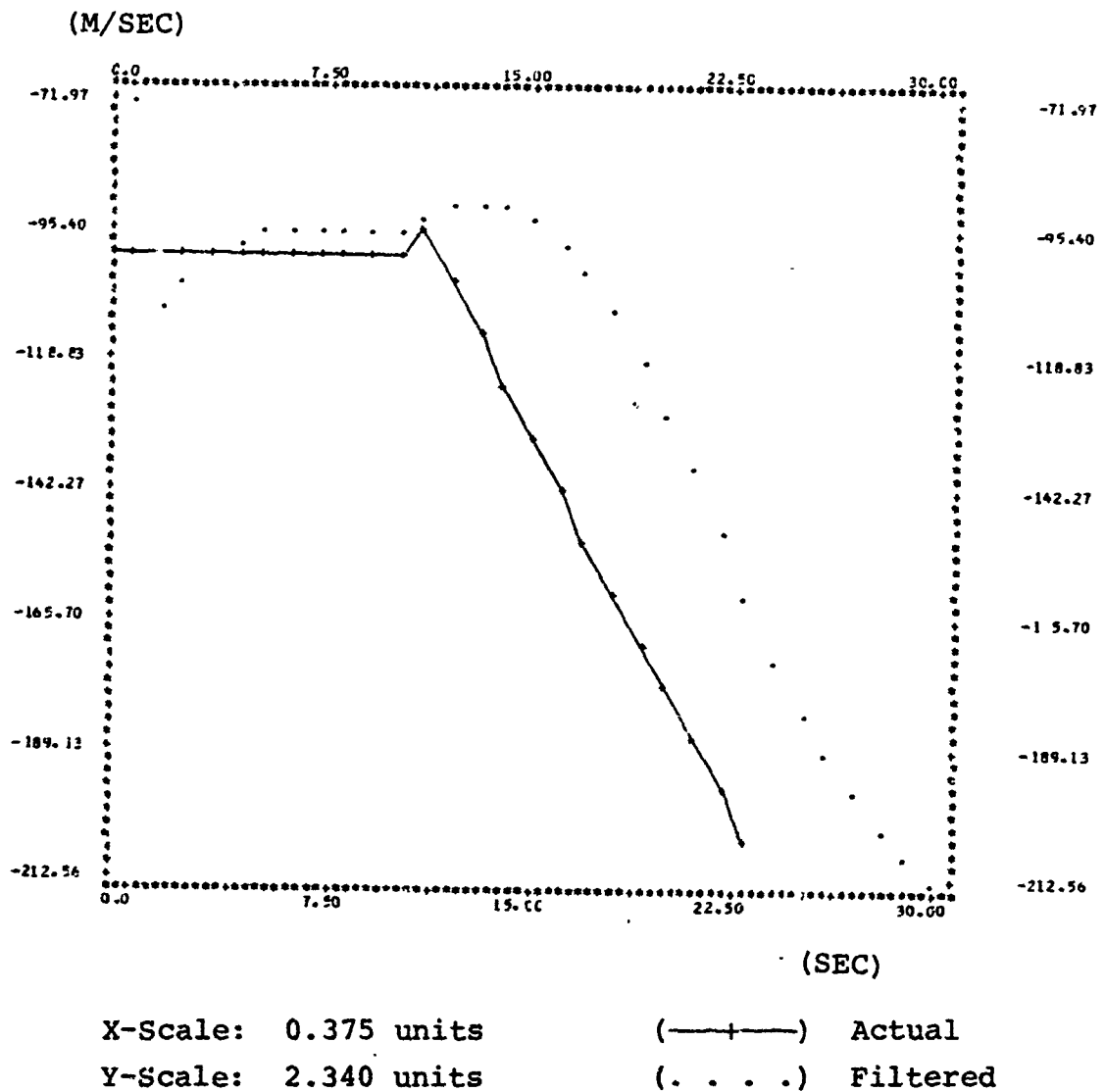


FIG. 47. VELOCITY VS TIME FOR α - β FILTER

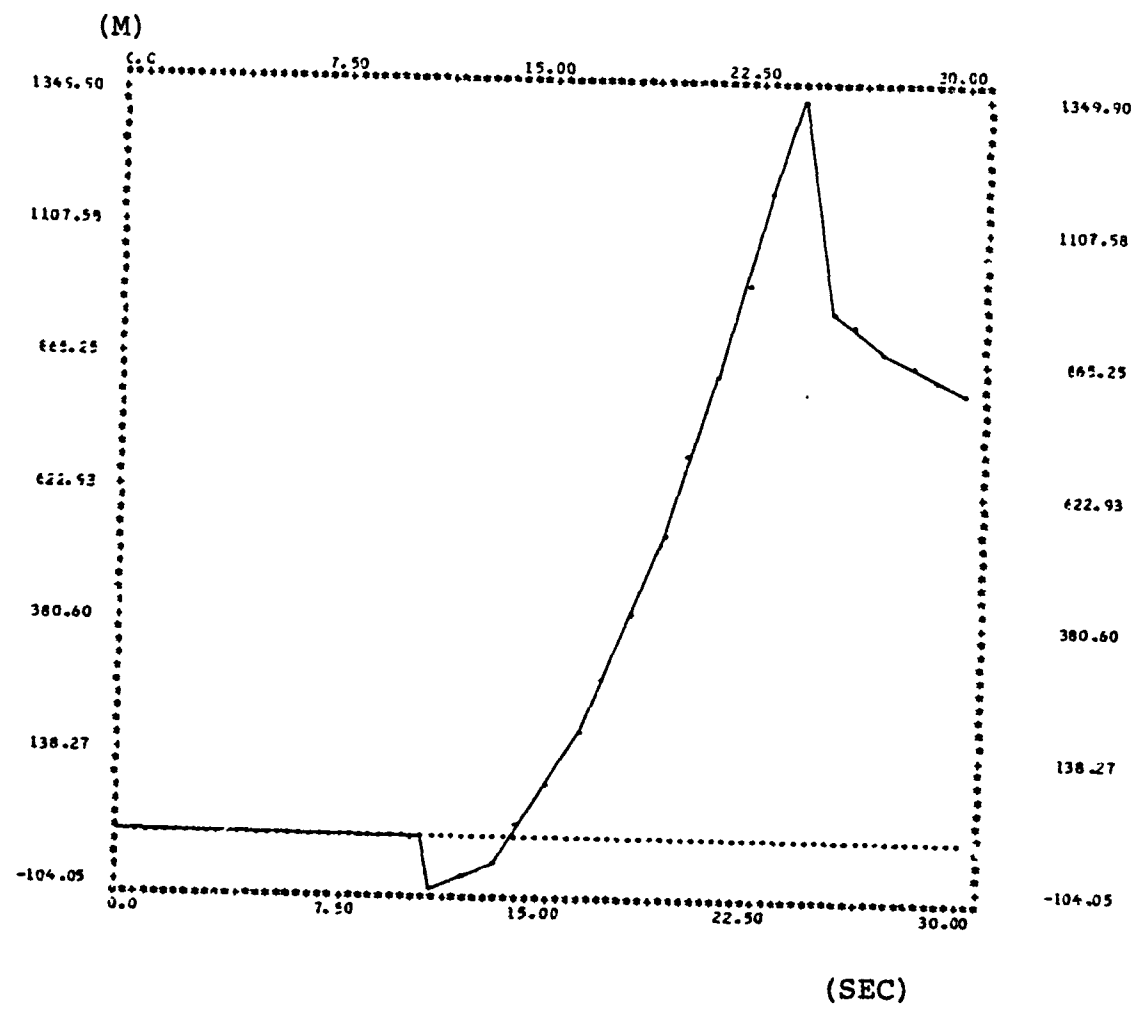
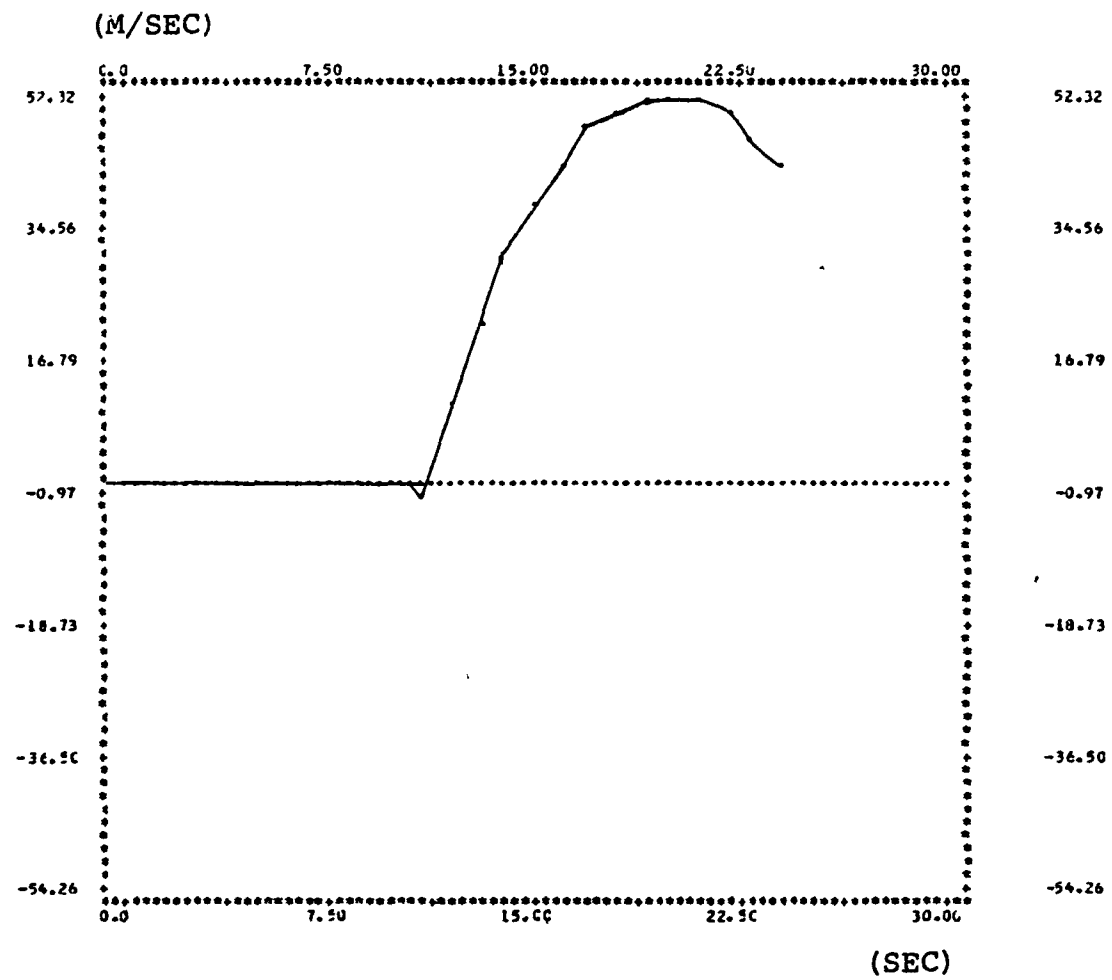
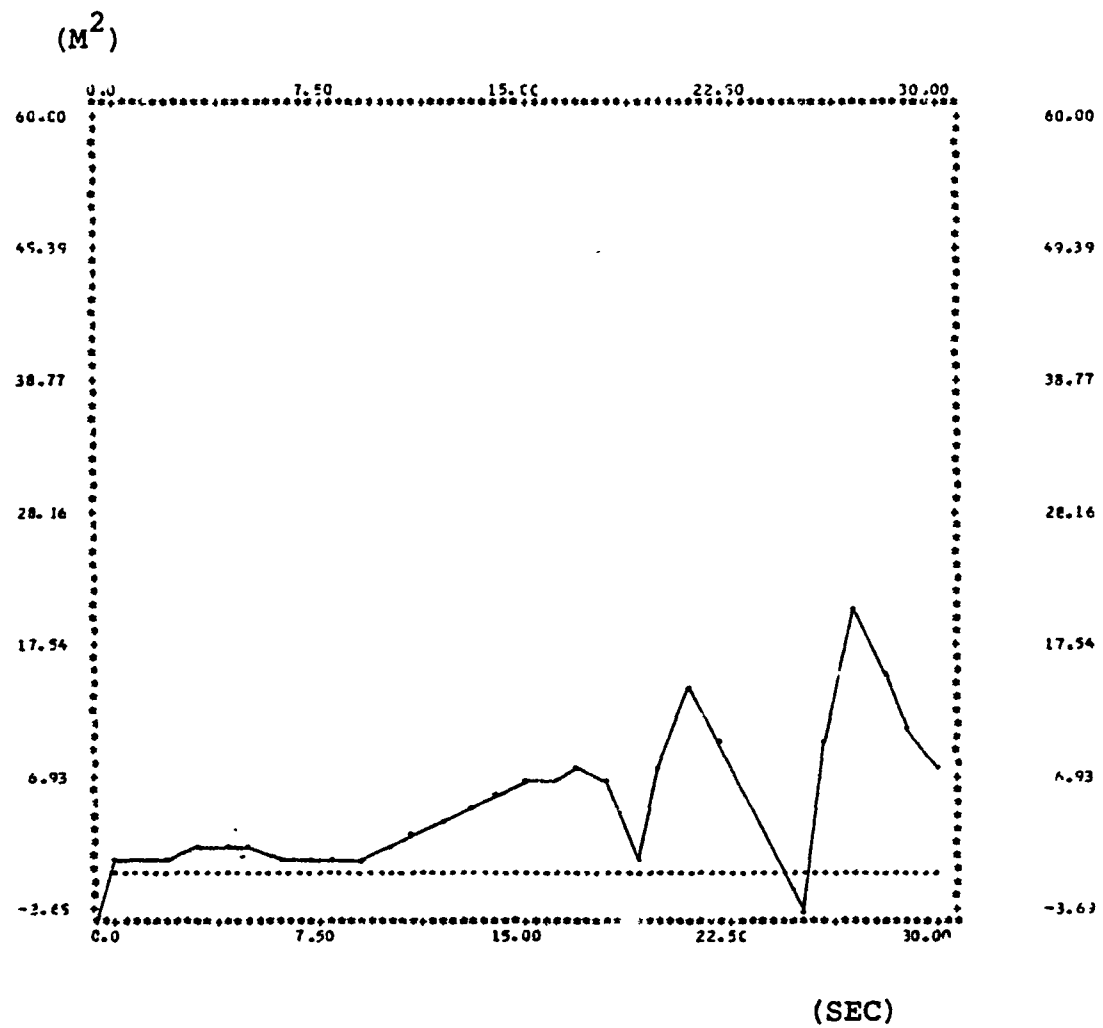


FIG. 48. MEAN RANGE ERROR VS TIME FOR α - β FILTER



X-Scale: 0.375 units
Y-Scale: 1.780 units

FIG. 49. MEAN VELOCITY ERROR VS TIME FOR α - β FILTER



X-Scale: 0.375 units

Y-Scale: 1.060 units

FIG. 50. VARIANCE OF RANGE ERROR VS TIME FOR α - β FILTER

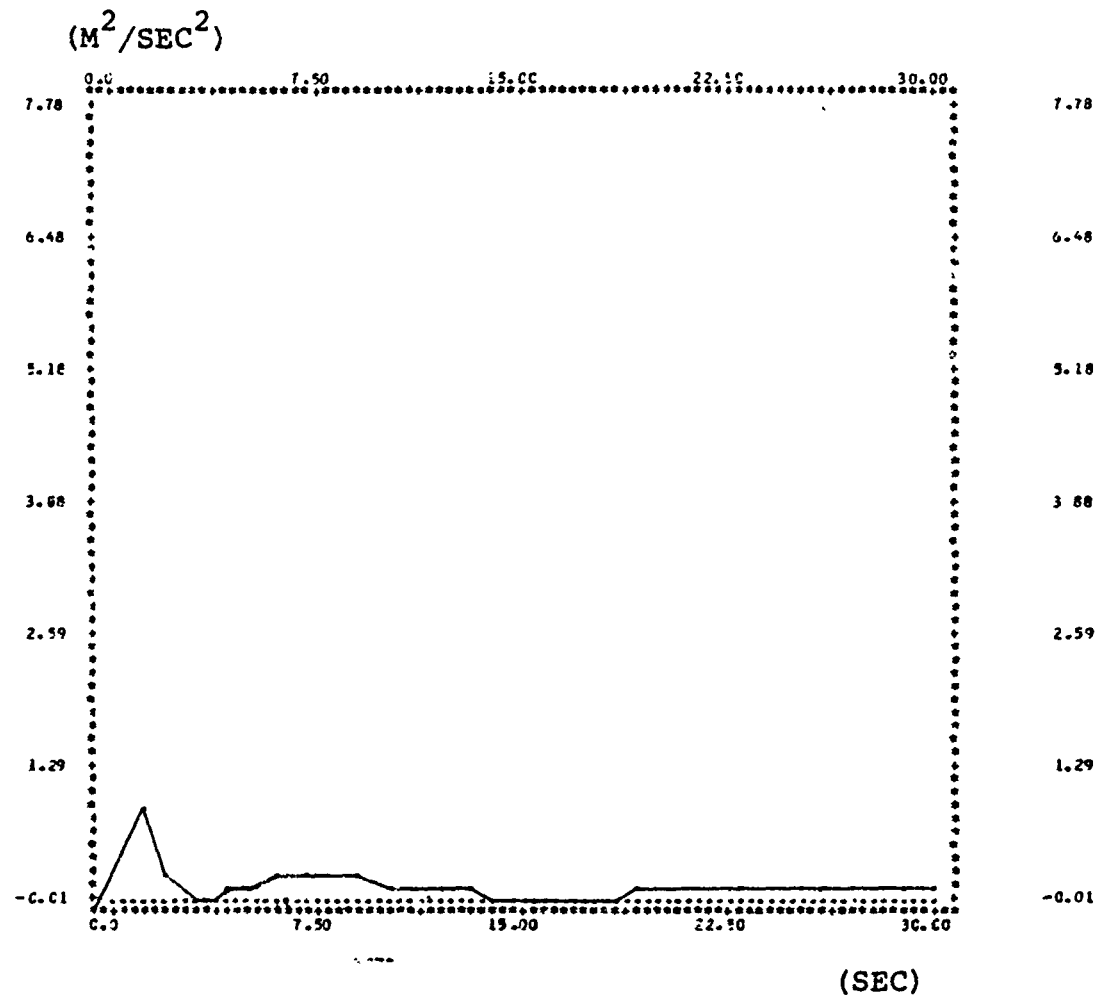


FIG. 51. VARIANCE OF VELOCITY ERROR VS TIME FOR $\alpha-\beta$ FILTER

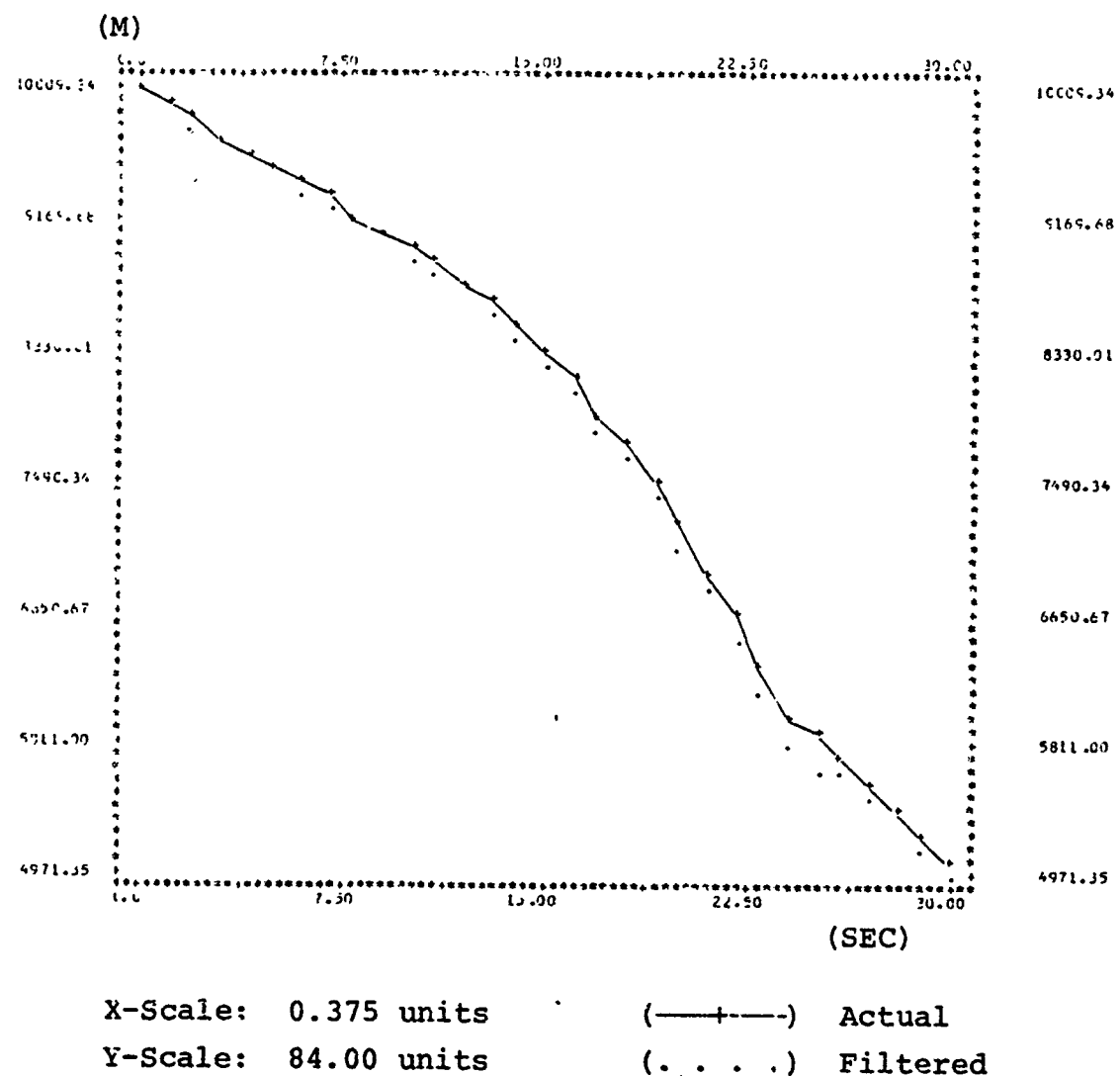


FIG. 52. RANGE VS TIME FOR SIMPLIFIED KALMAN FILTER

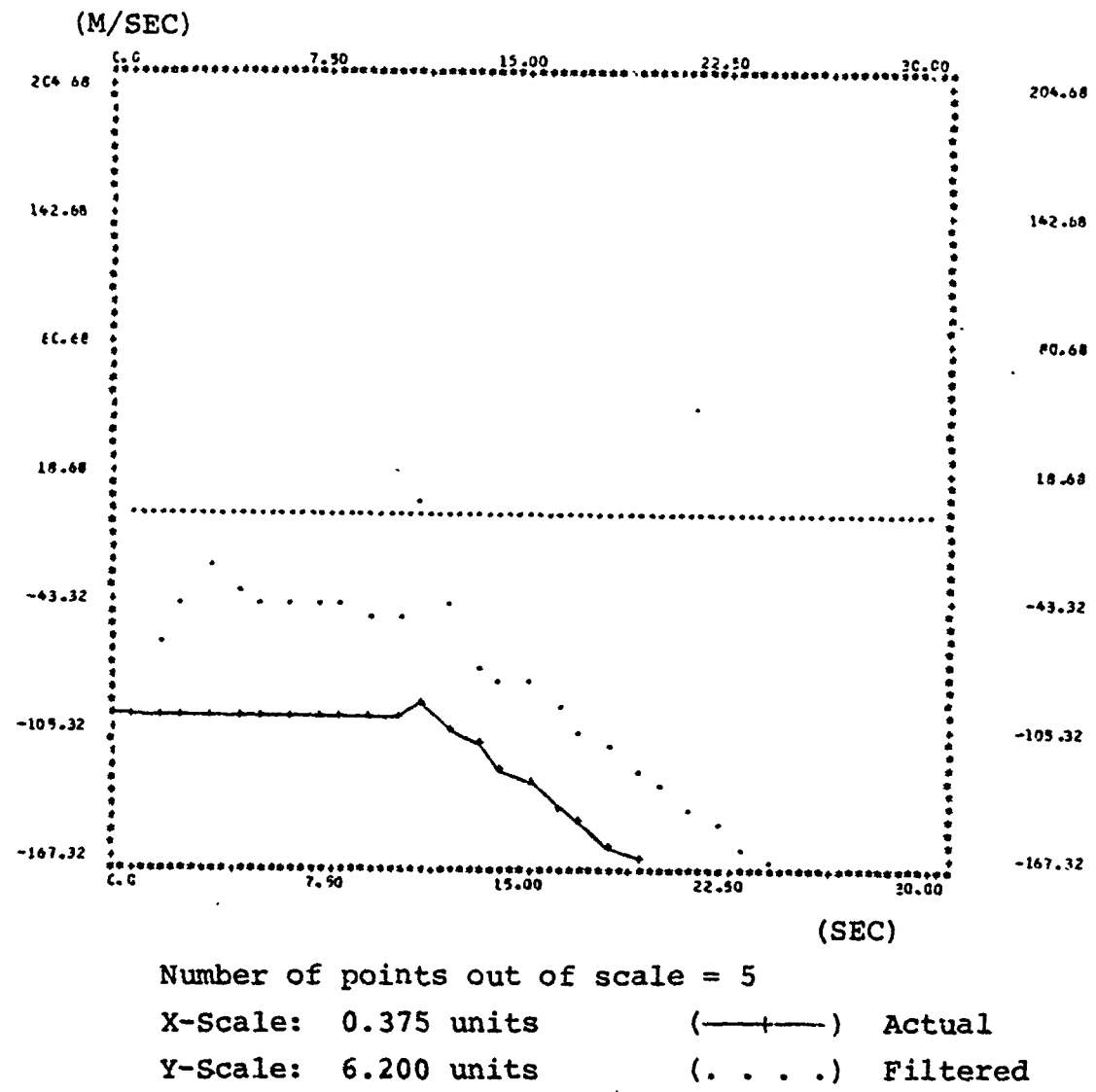


FIG. 53. VELOCITY VS TIME FOR SIMPLIFIED KALMAN FILTER

(RADIANs)

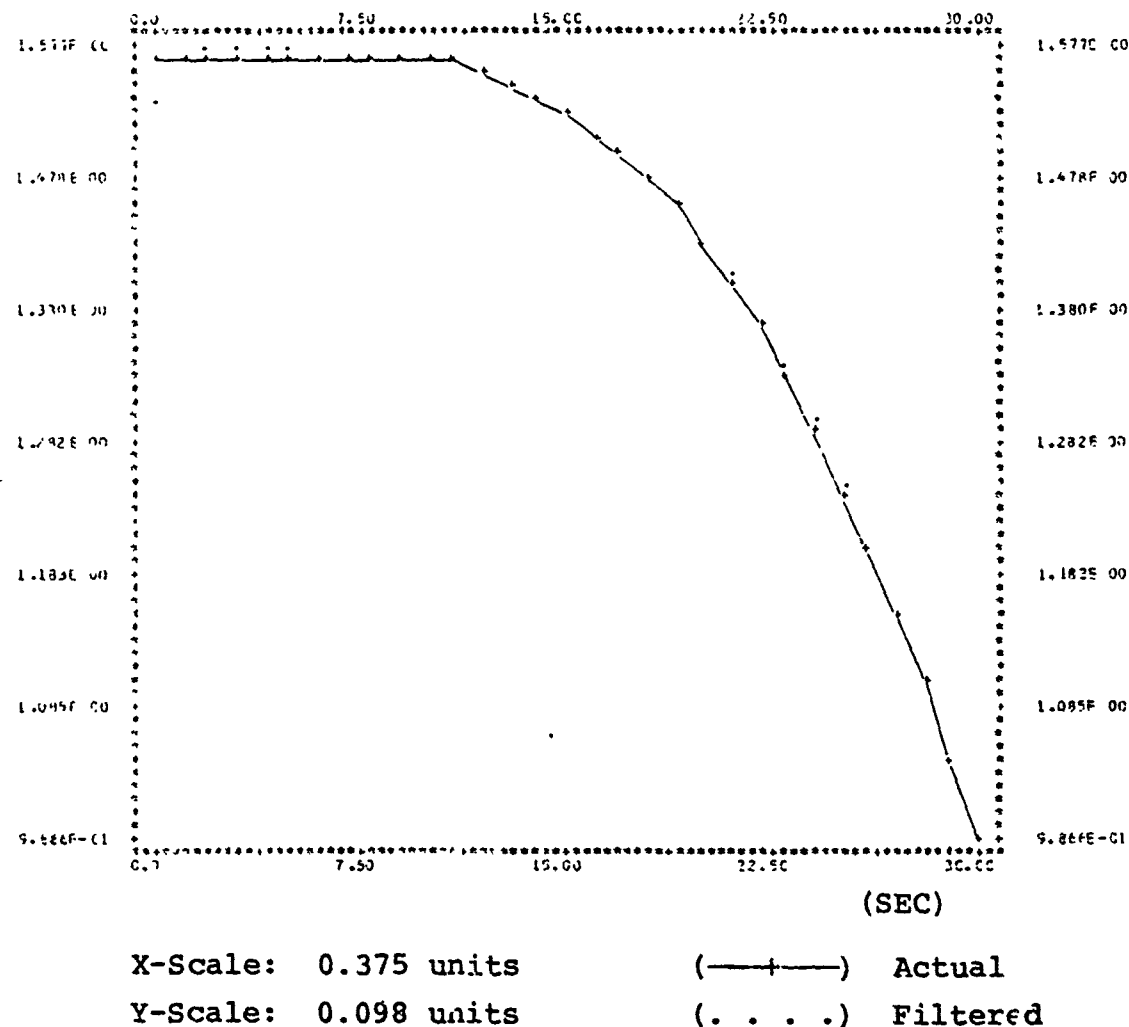


FIG. 54. BEARING VS TIME FOR SIMPLIFIED KALMAN FILTER

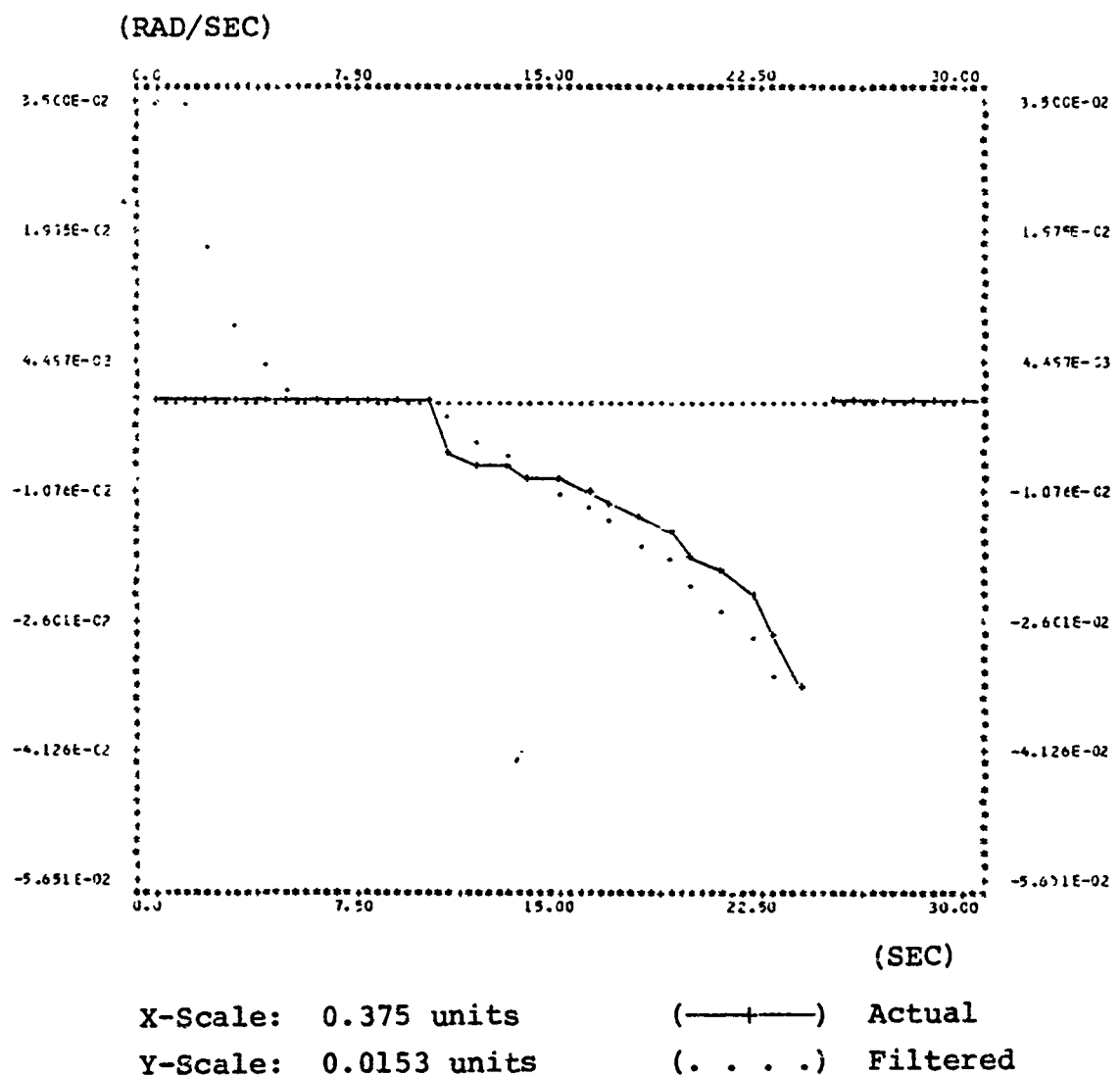
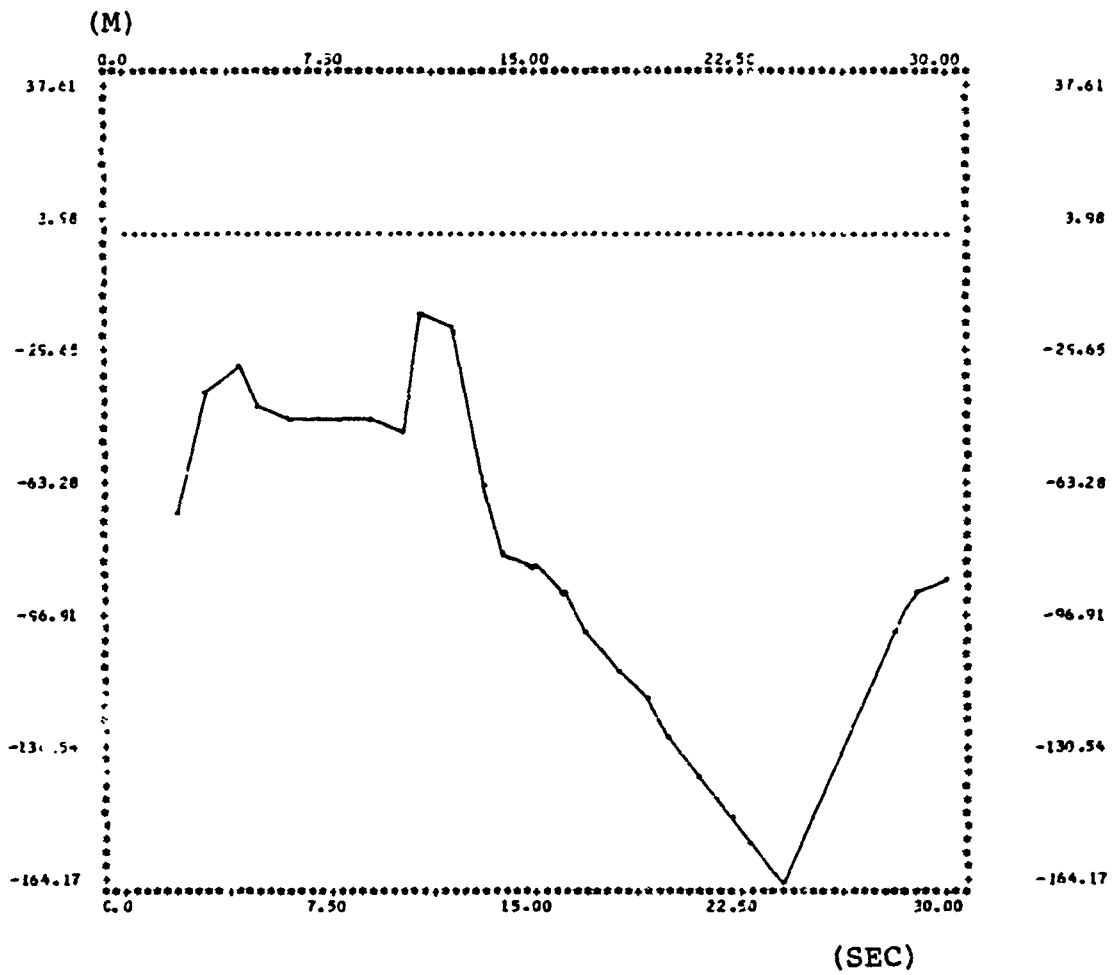


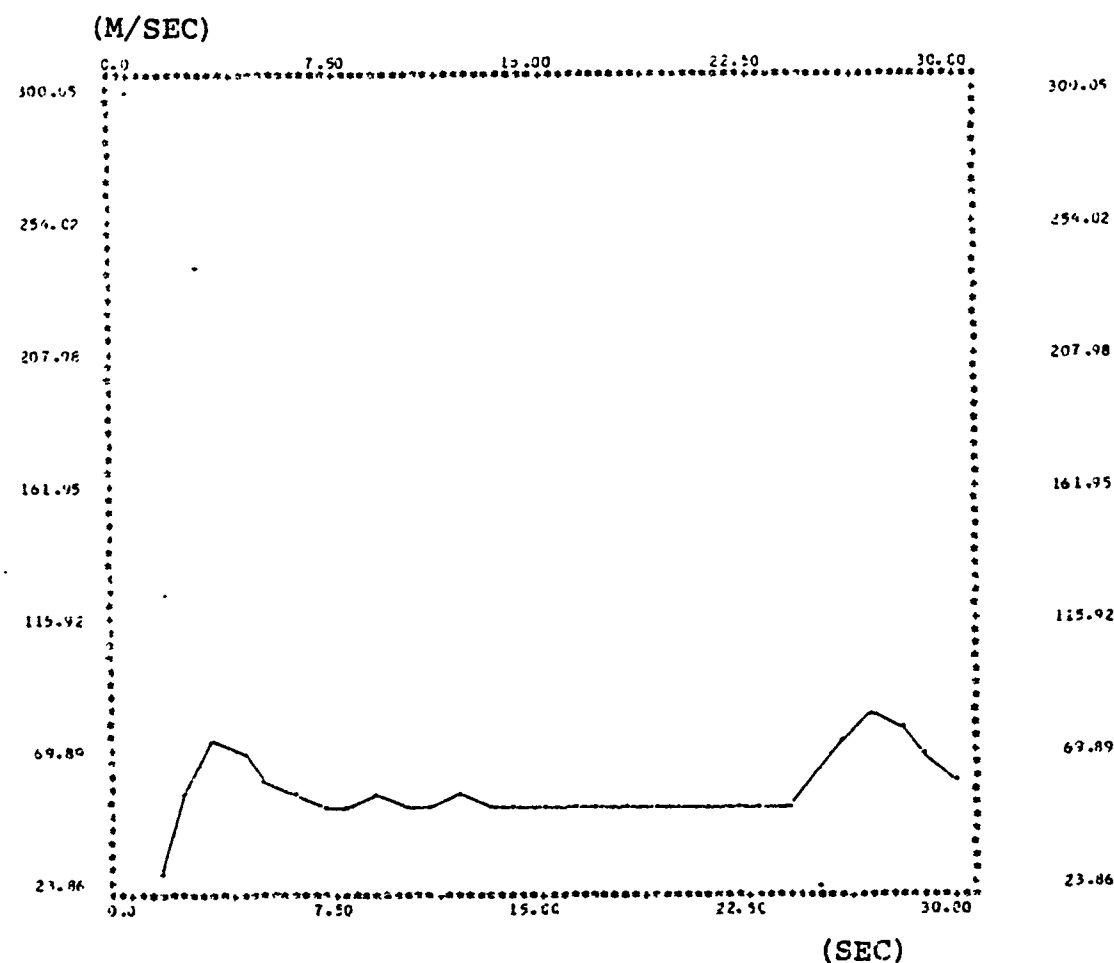
FIG. 55. BEARING VS TIME FOR SIMPLIFIED KALMAN FILTER



X-Scale: 0.375 units

Y-Scale: 3.360 units

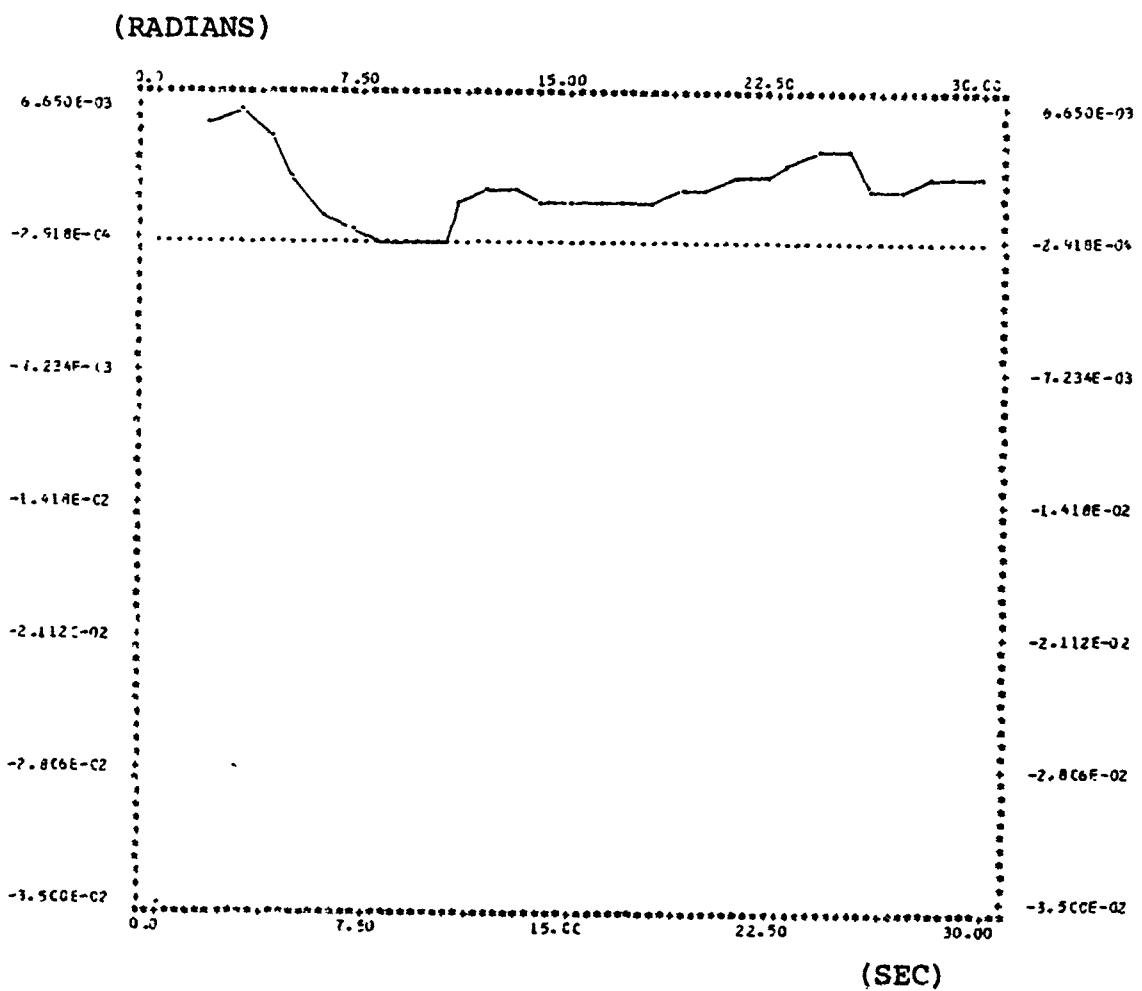
FIG. 56. MEAN RANGE ERROR VS TIME FOR SIMPLIFIED KALMAN FILTER



X-Scale: 0.375 units

Y-Scale: 4.600 units

FIG. 57. MEAN VELOCITY ERROR FOR SIMPLIFIED KALMAN FILTER



X-Scale: 0.375 units

Y-Scale: 0.0069 units

FIG. 58. MEAN BEARING ERROR VS TIME FOR SIMPLIFIED KALMAN FILTER

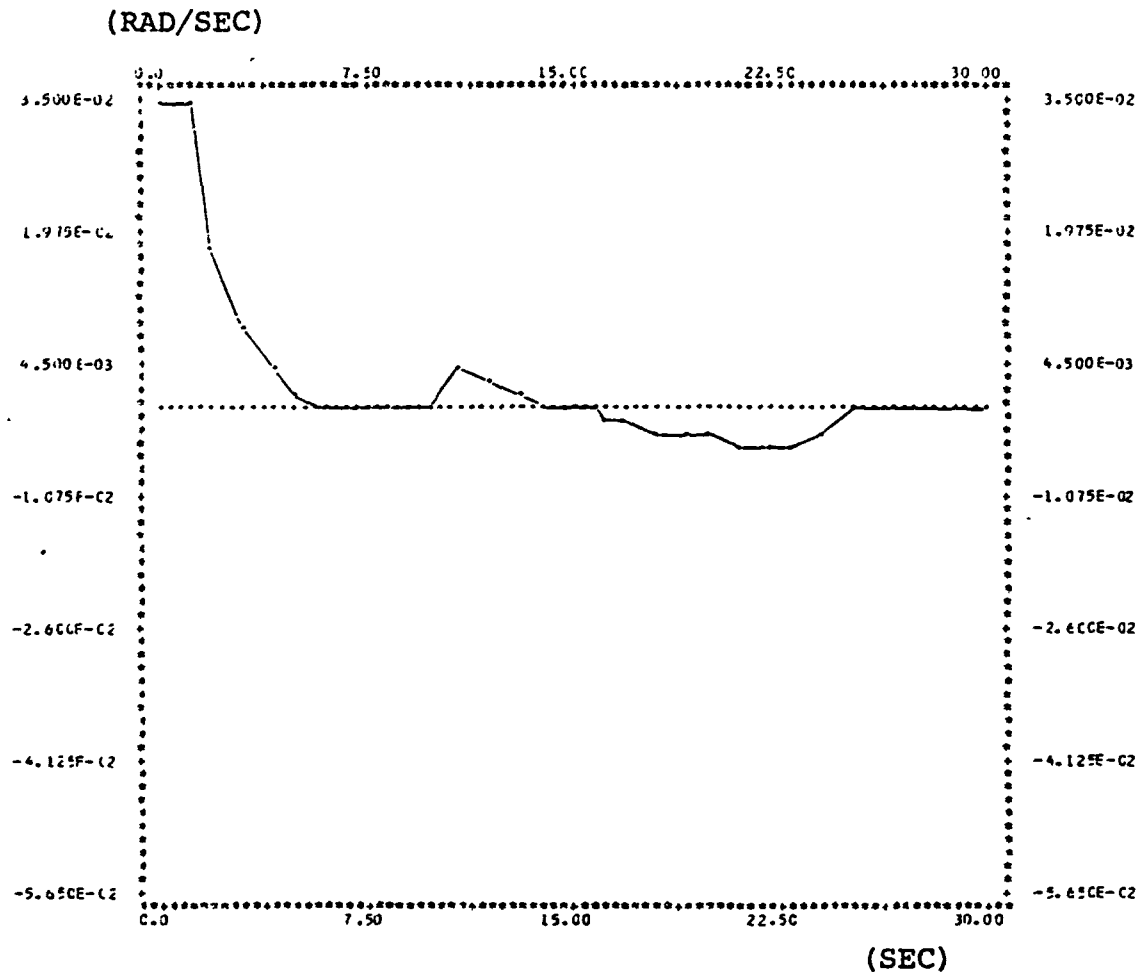


FIG. 59. MEAN BEARING RATE ERROR VS TIME FOR SIMPLIFIED KALMAN FILTER

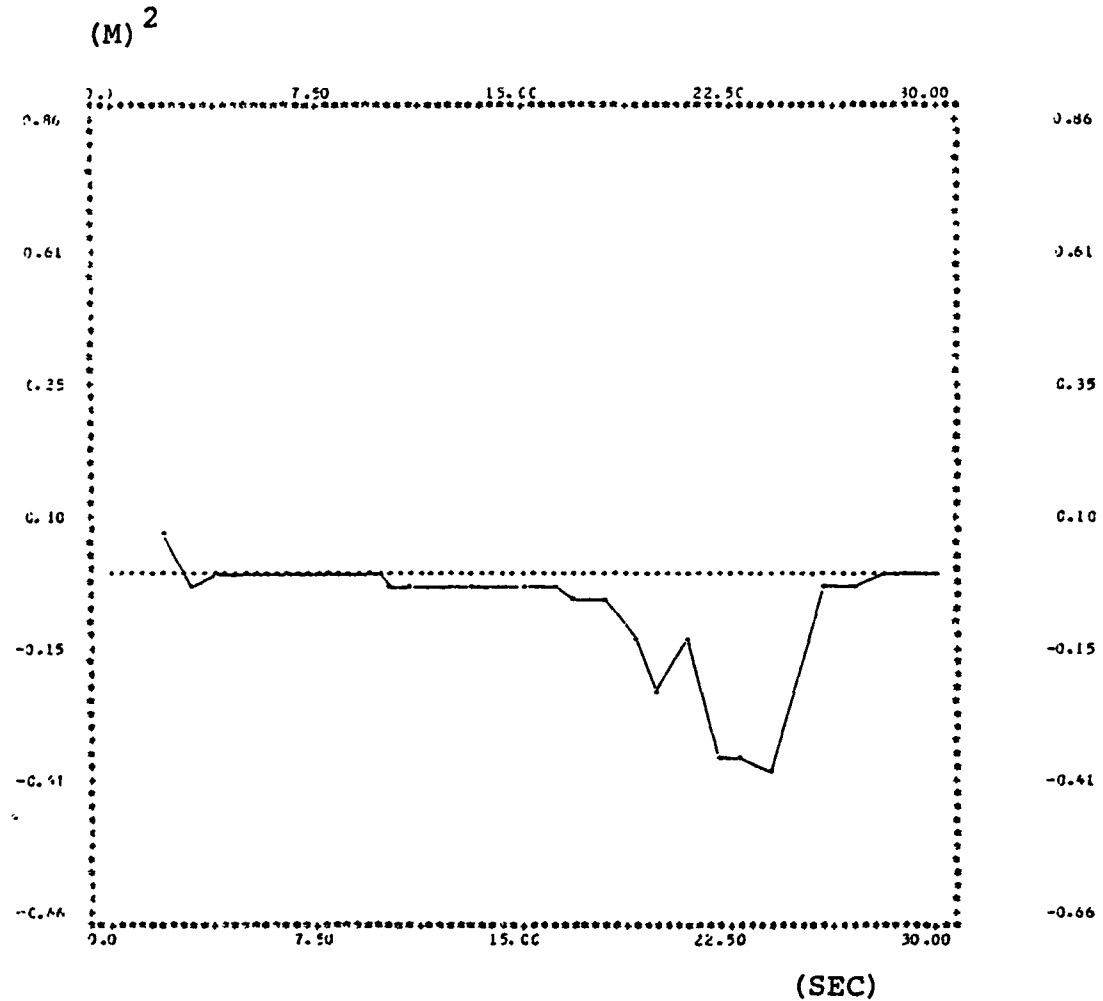


FIG. 60. VARIANCE OF RANGE ERROR VS TIME FOR SIMPLIFIED KALMAN FILTER

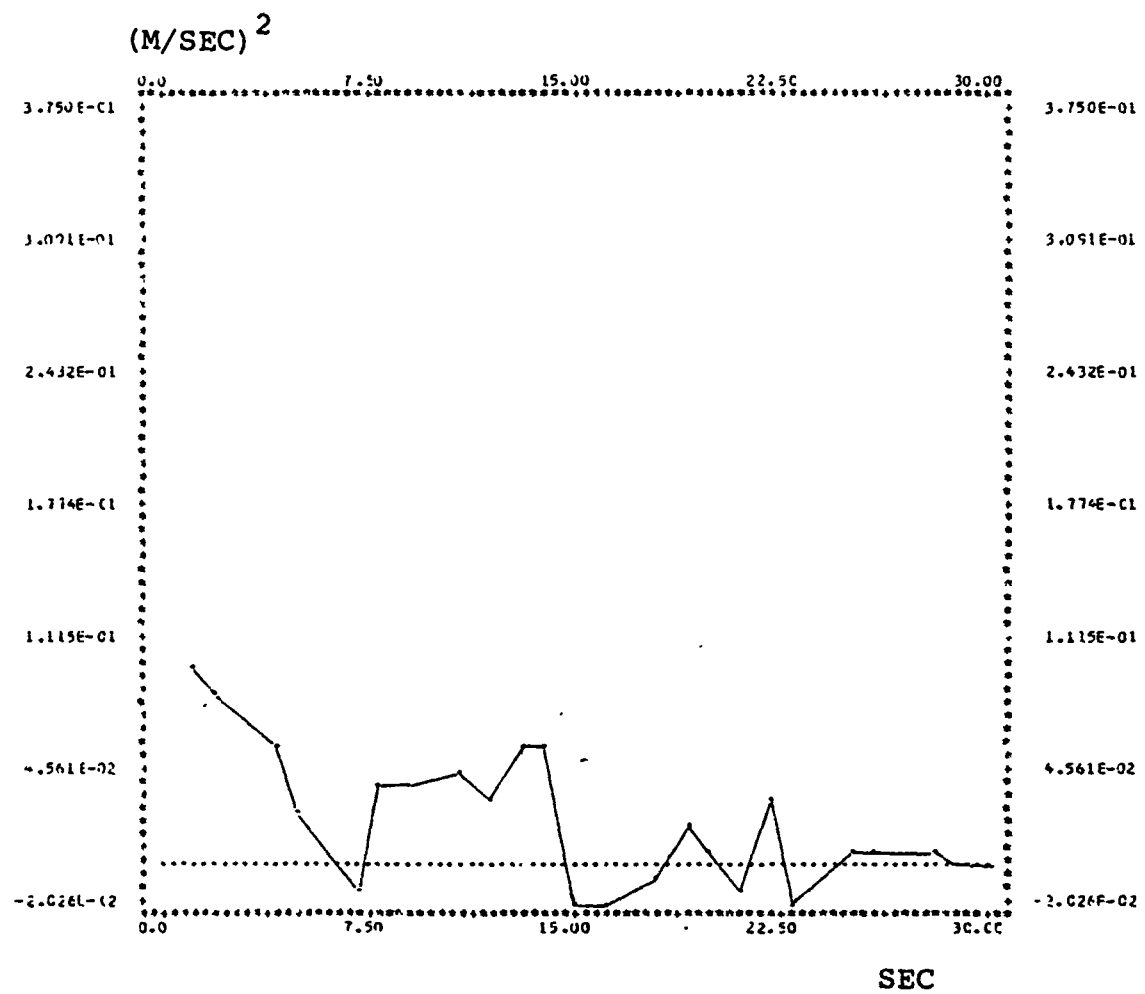


FIG. 61. VARIANCE OF VELOCITY ERROR VS TIME FOR SIMPLIFIED KALMAN FILTER

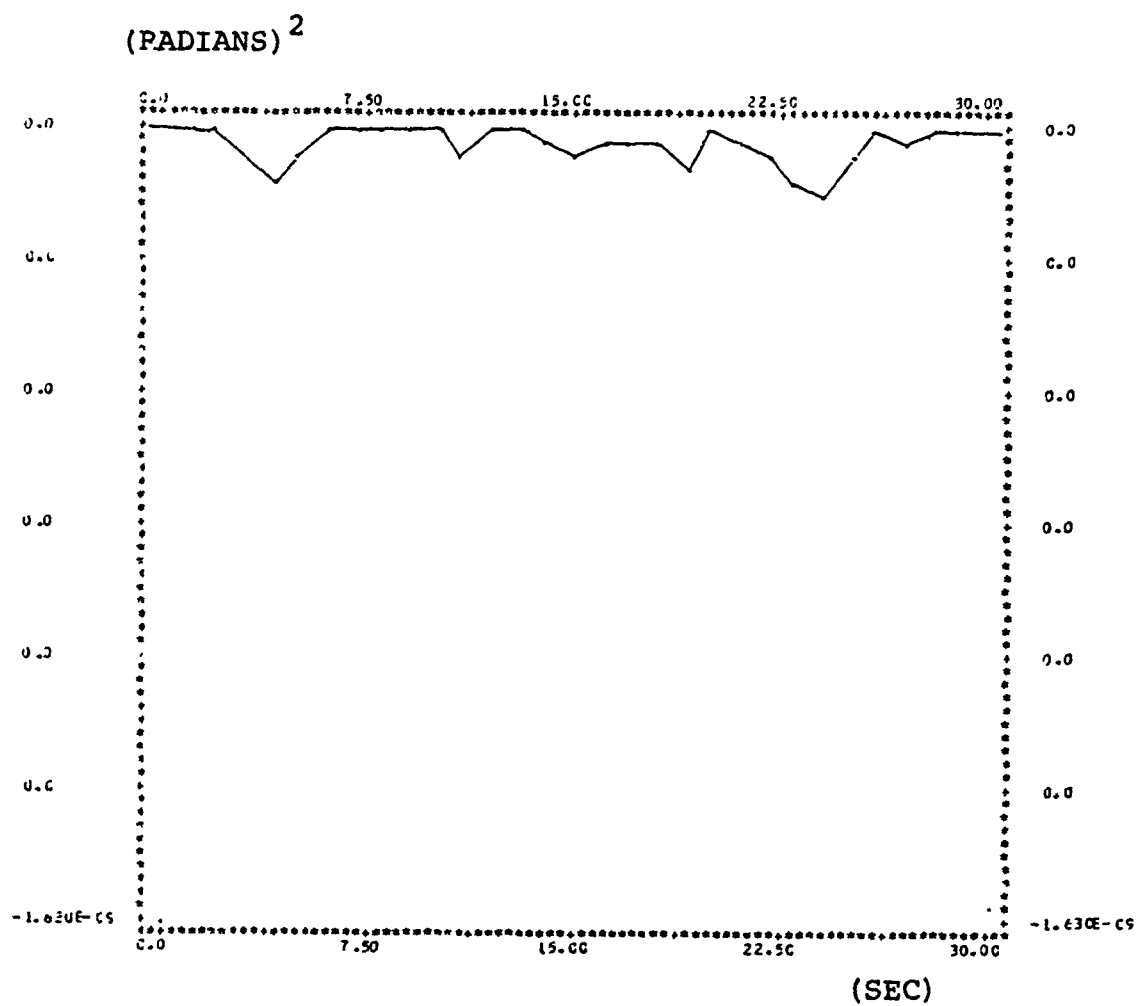
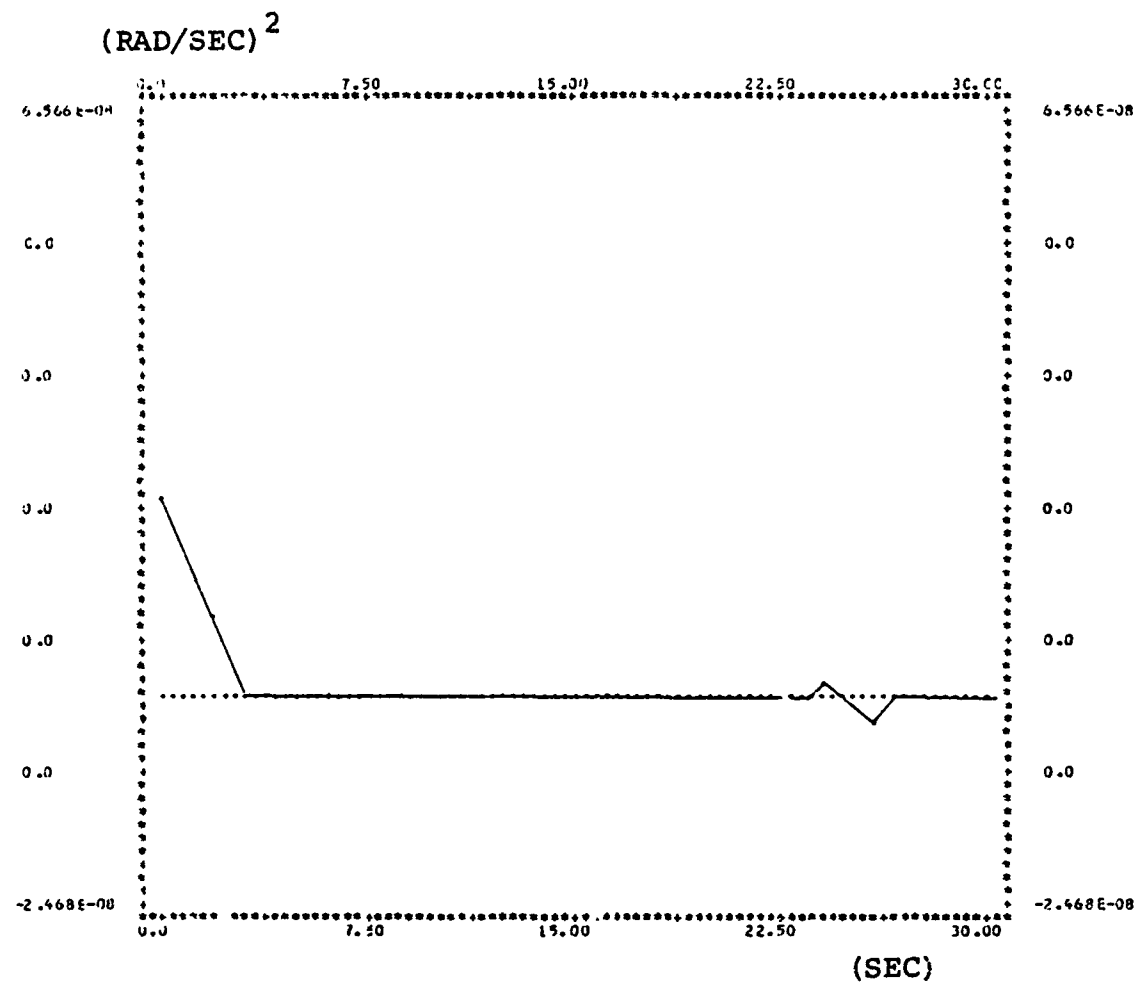


FIG. 62. VARIANCE OF BEARING ERROR VS TIME FOR SIMPLIFIED KALMAN FILTER



X-Scale: 0.375 units
Y-Scale: 0.151E - 08 units

FIG. 63. VARIANCE OF BEARING RATE ERROR VS TIME FOR SIMPLIFIED KALMAN FILTER

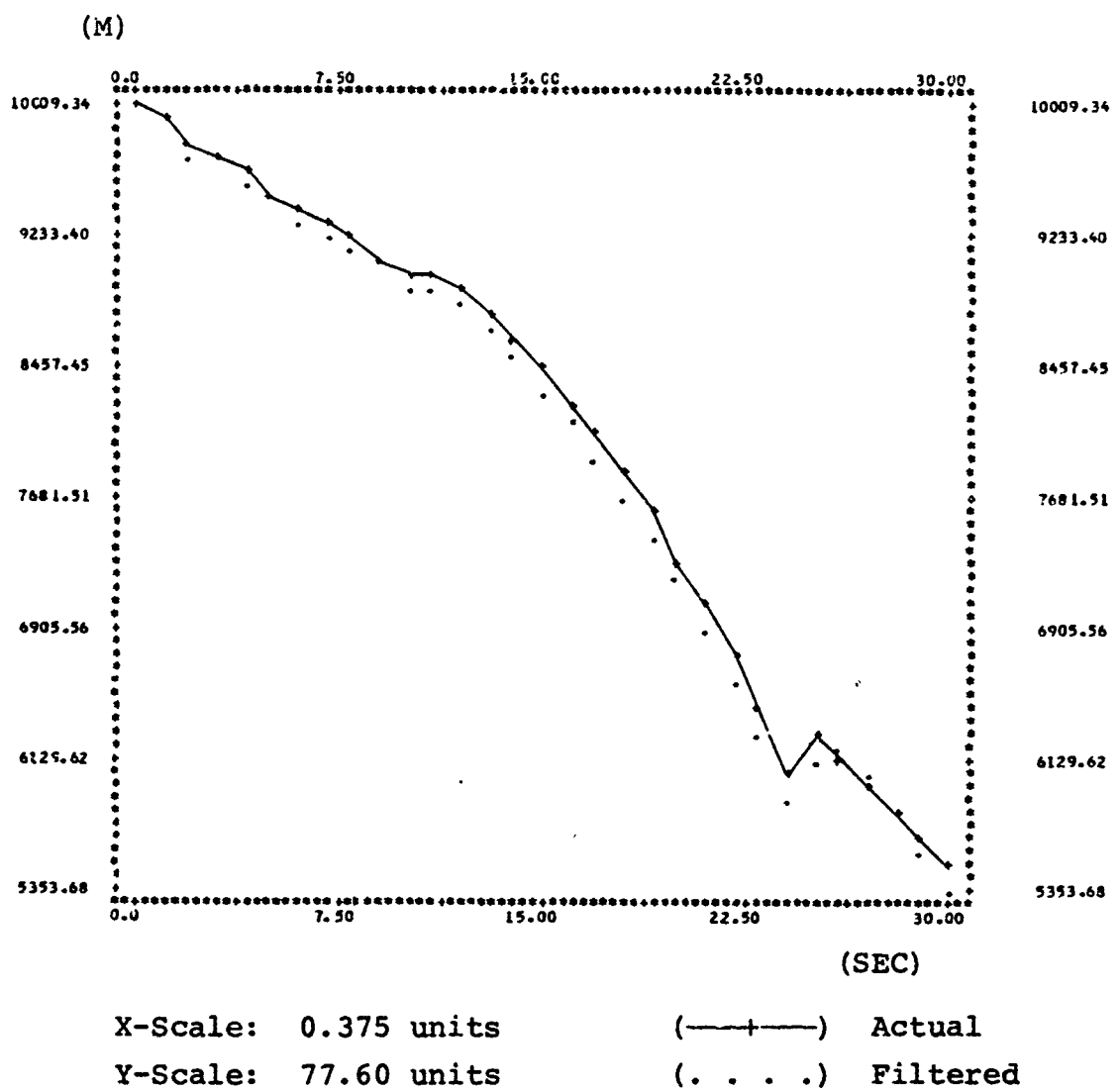


FIG. 64. RANGE VS TIME FOR KALMAN FILTER

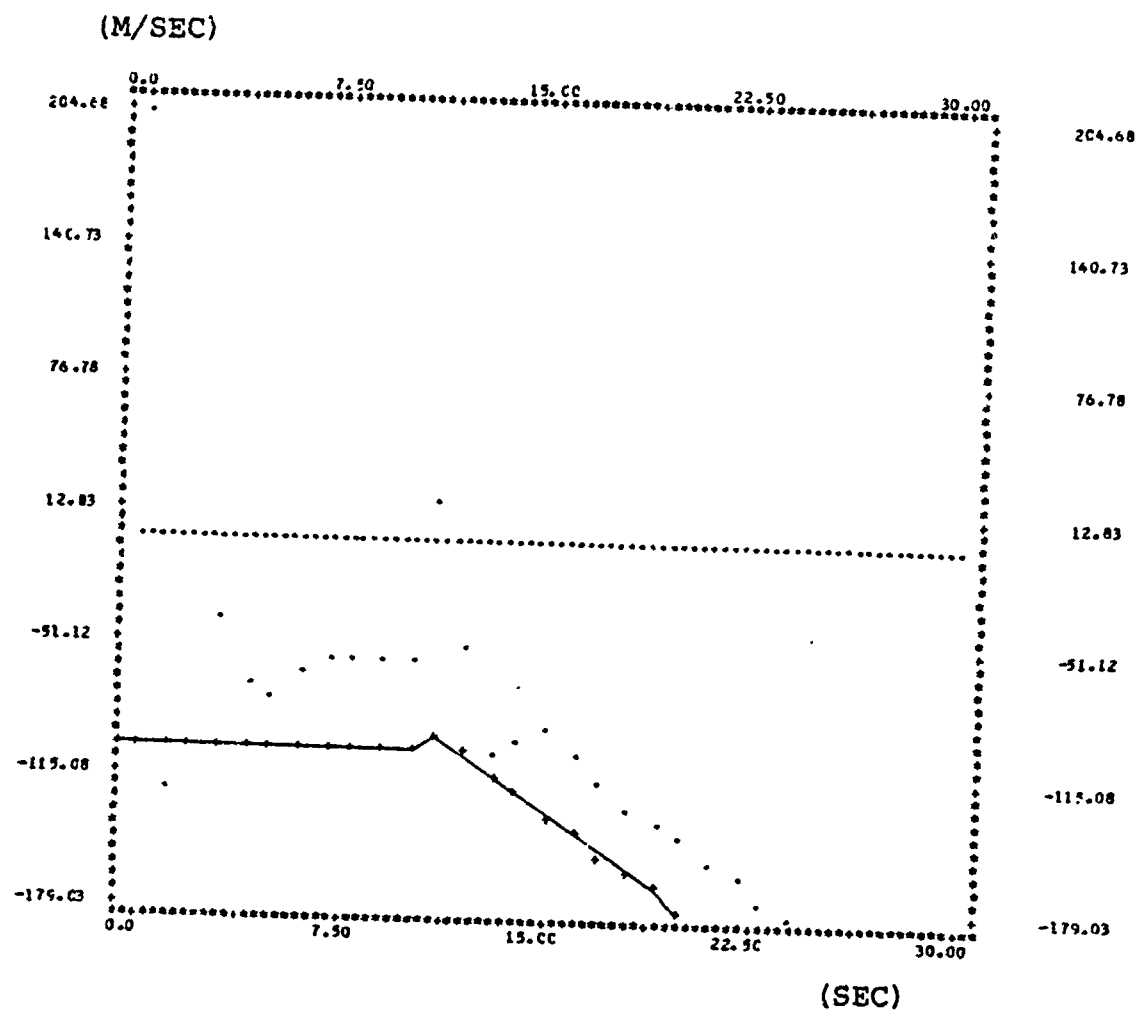


FIG. 65. VELOCITY VS TIME FOR KALMAN FILTER

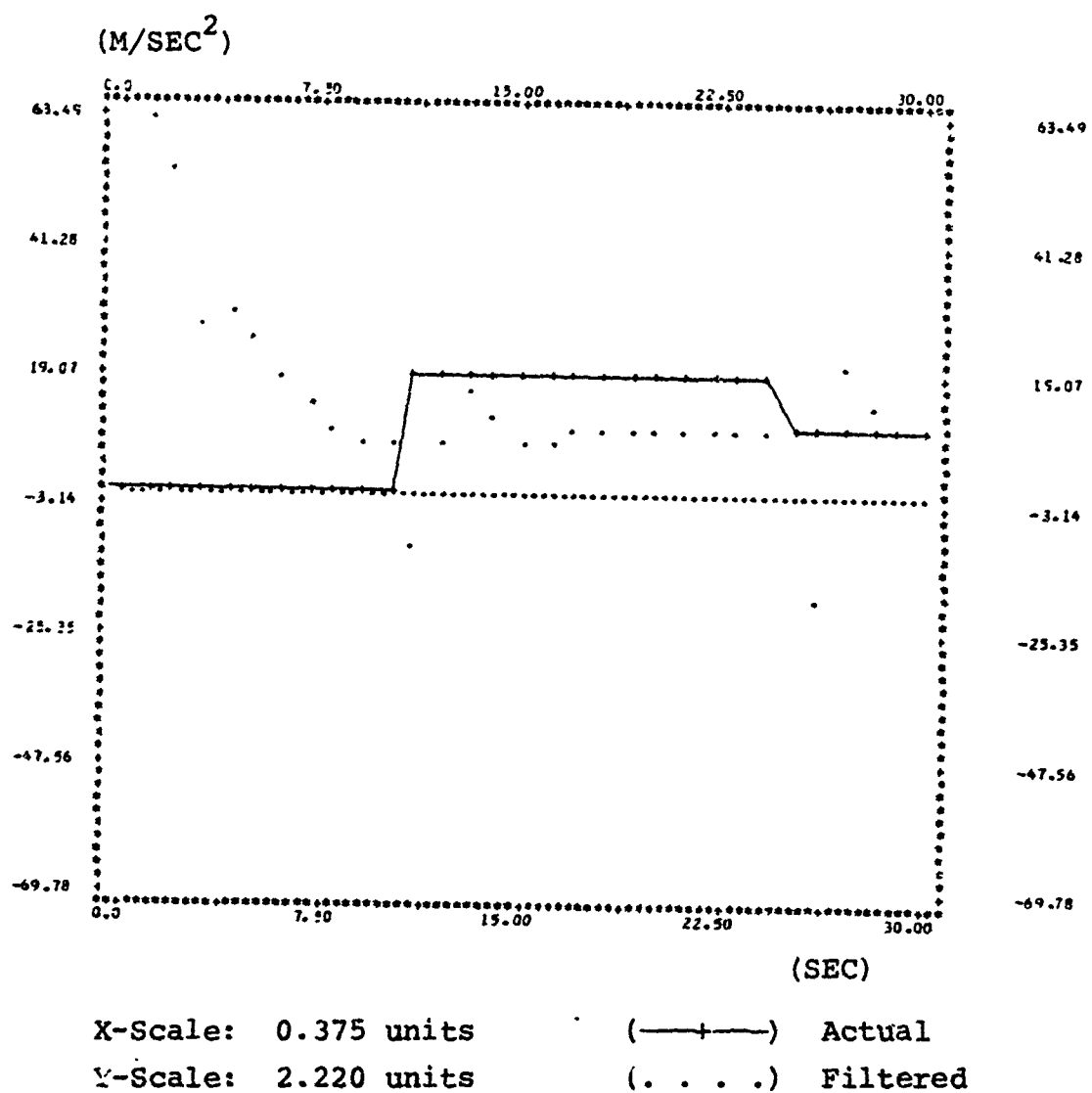
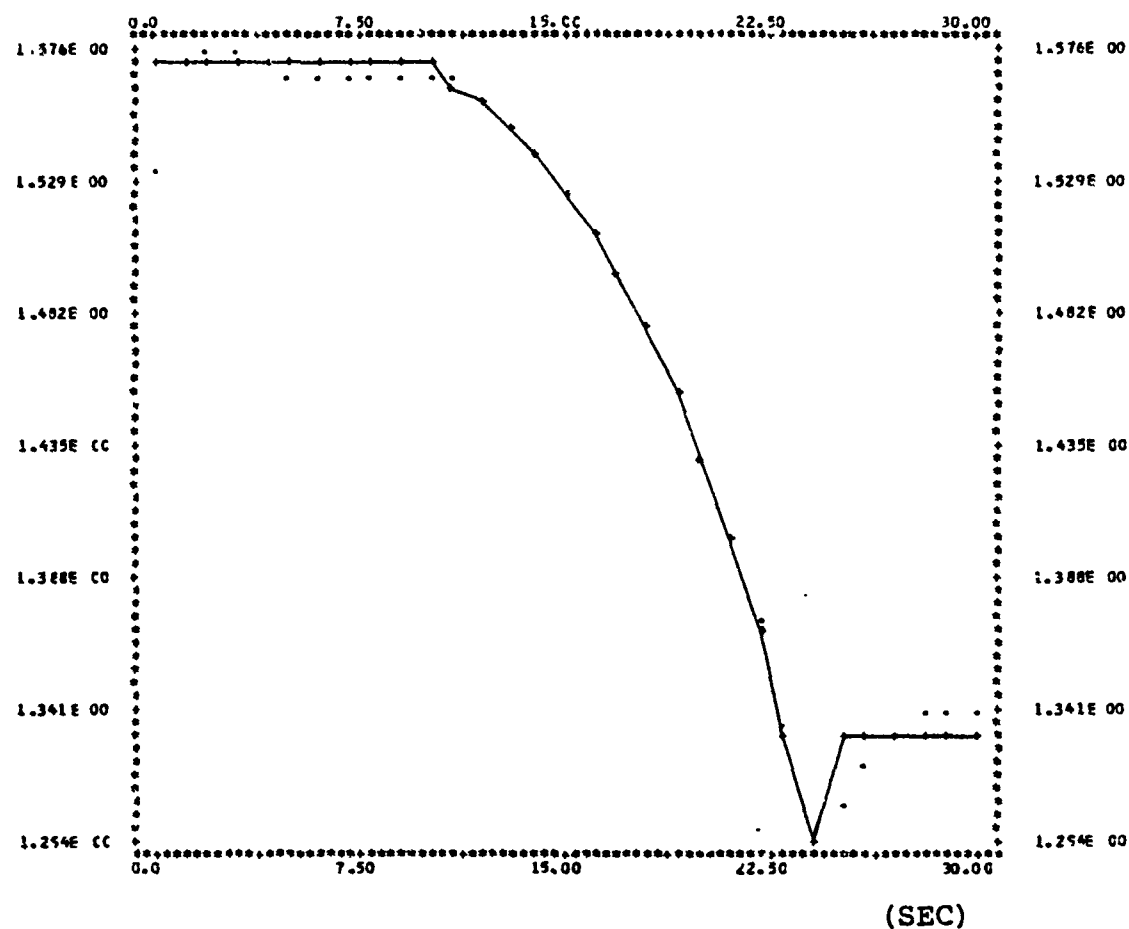


FIG. 66. ACCELERATION VS TIME FOR KALMAN FILTER

(RADIAN)



X-Scale: 0.375 units
Y-Scale: 0.0047 units

(—+—) Actual
(....) Filtered

FIG. 67. BEARING VS TIME FOR KALMAN FILTER

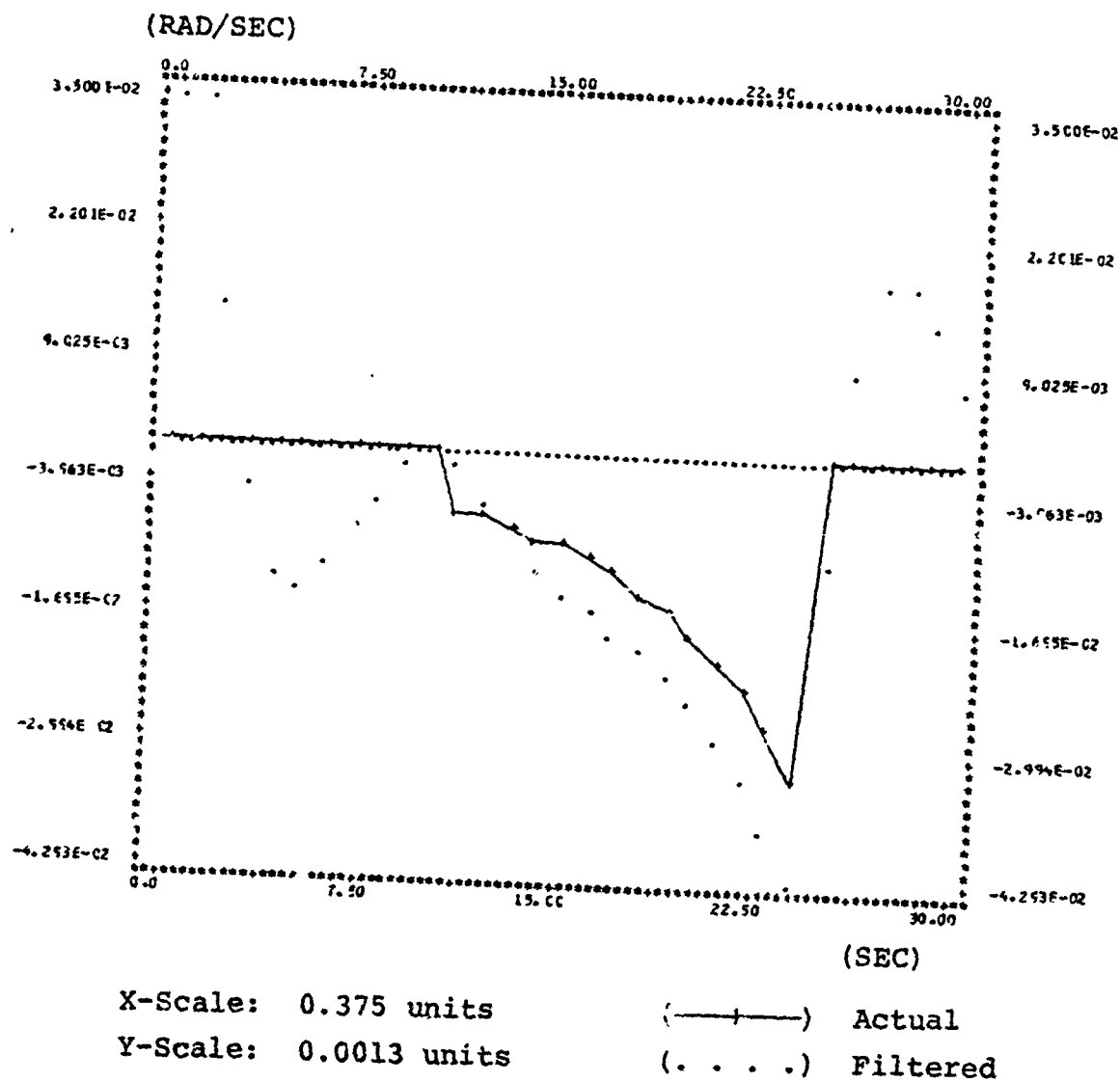
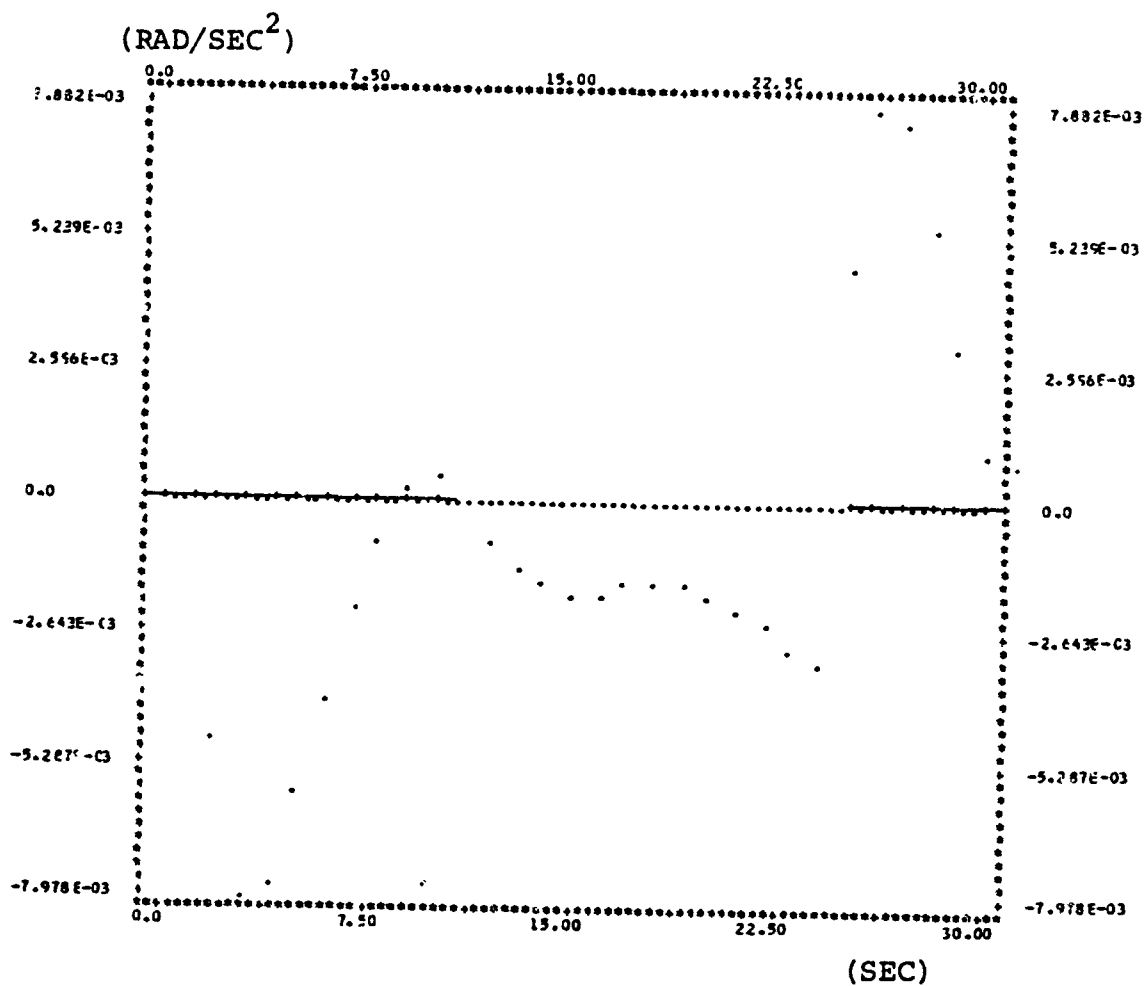


FIG. 68. BEARING RATE VS TIME FOR KALMAN FILTER



Number of points out of scale: 14

X-Scale: 0.375 units (—+—) Actual

Y-Scale: 0.00026 units (....) Filtered

FIG. 69. BEARING ACCELERATION VS TIME FOR KALMAN FILTER

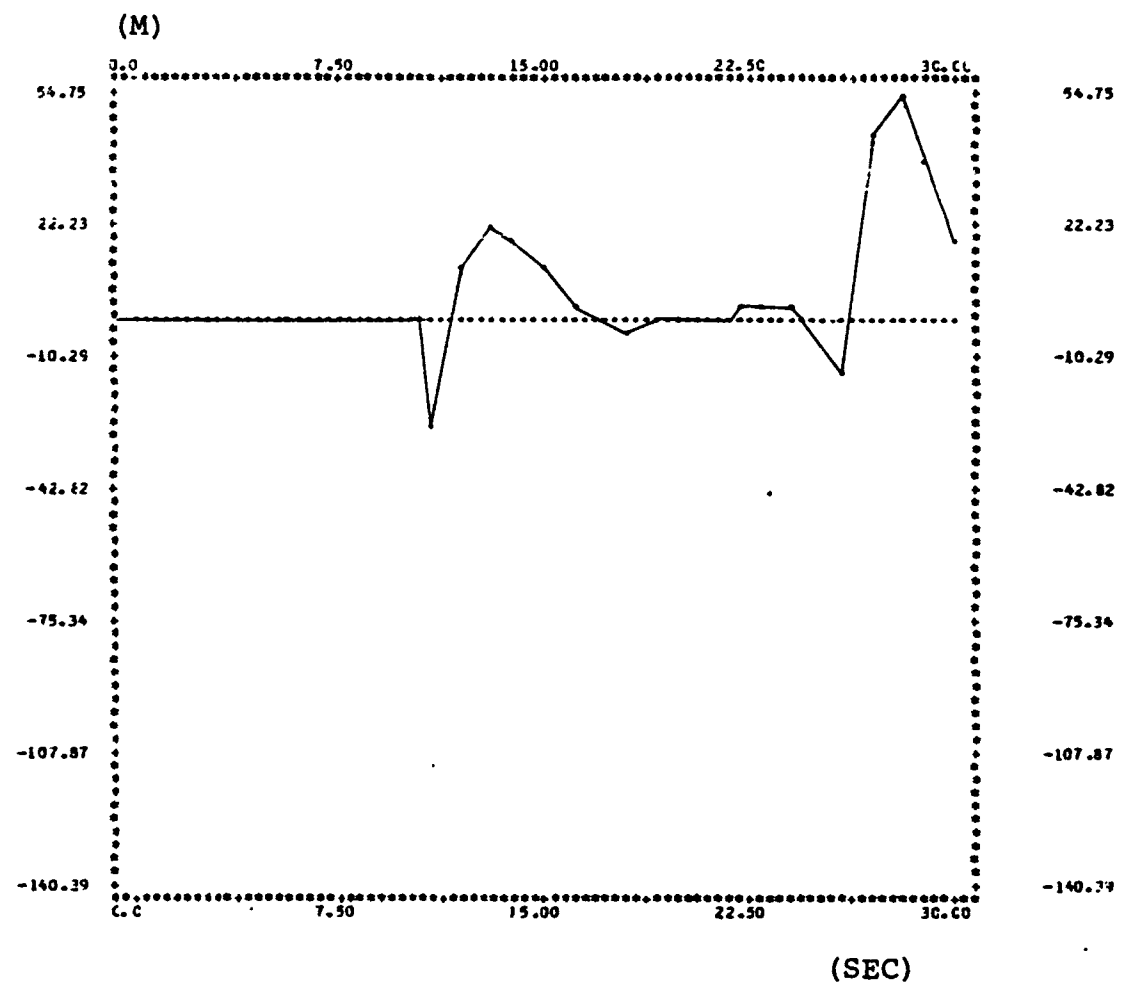


FIG. 70. MEAN RANGE ERROR VS TIME FOR KALMAN FILTER

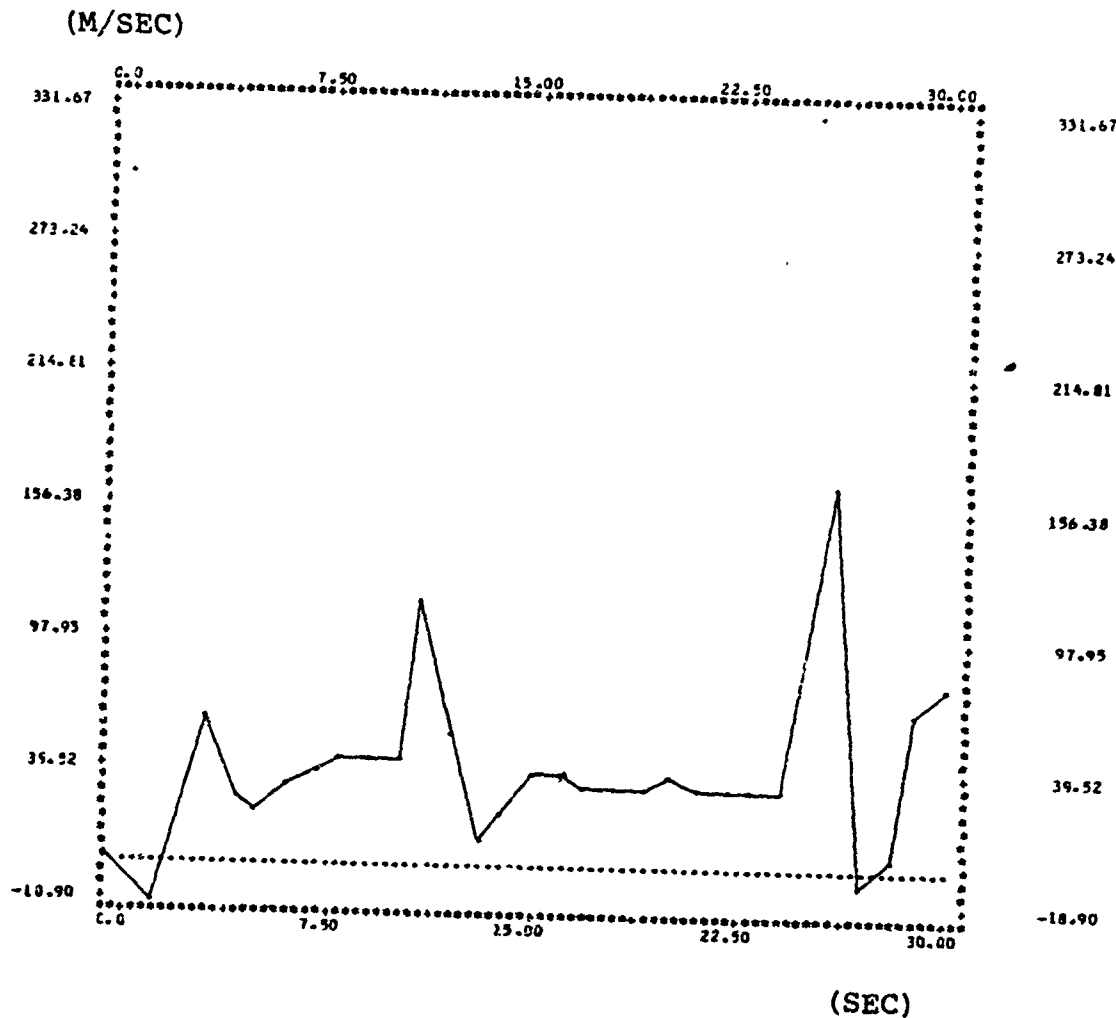


FIG. 71. MEAN VELOCITY ERROR VS TIME FOR KALMAN FILTER

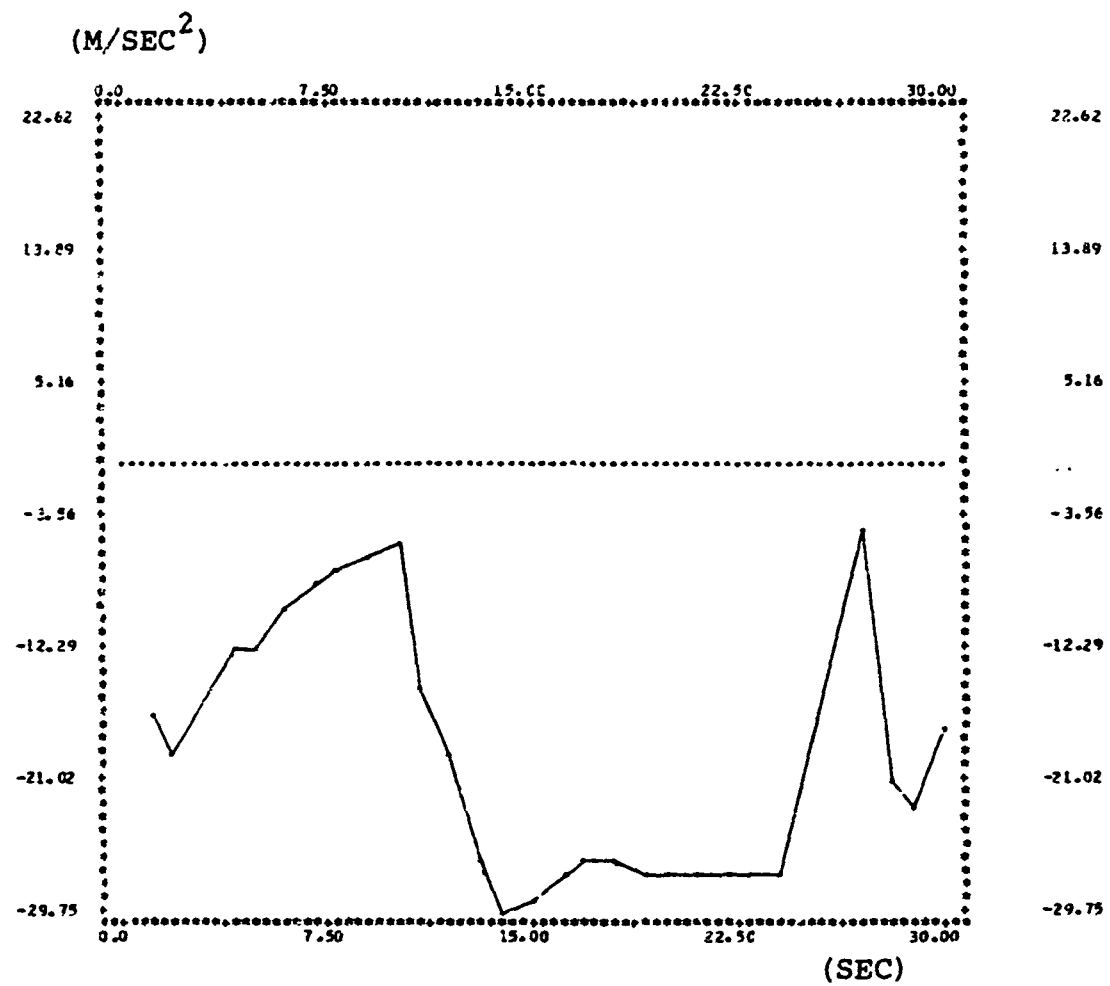


FIG. 72. MEAN ACCELERATION ERROR VS TIME FOR KALMAN FILTER

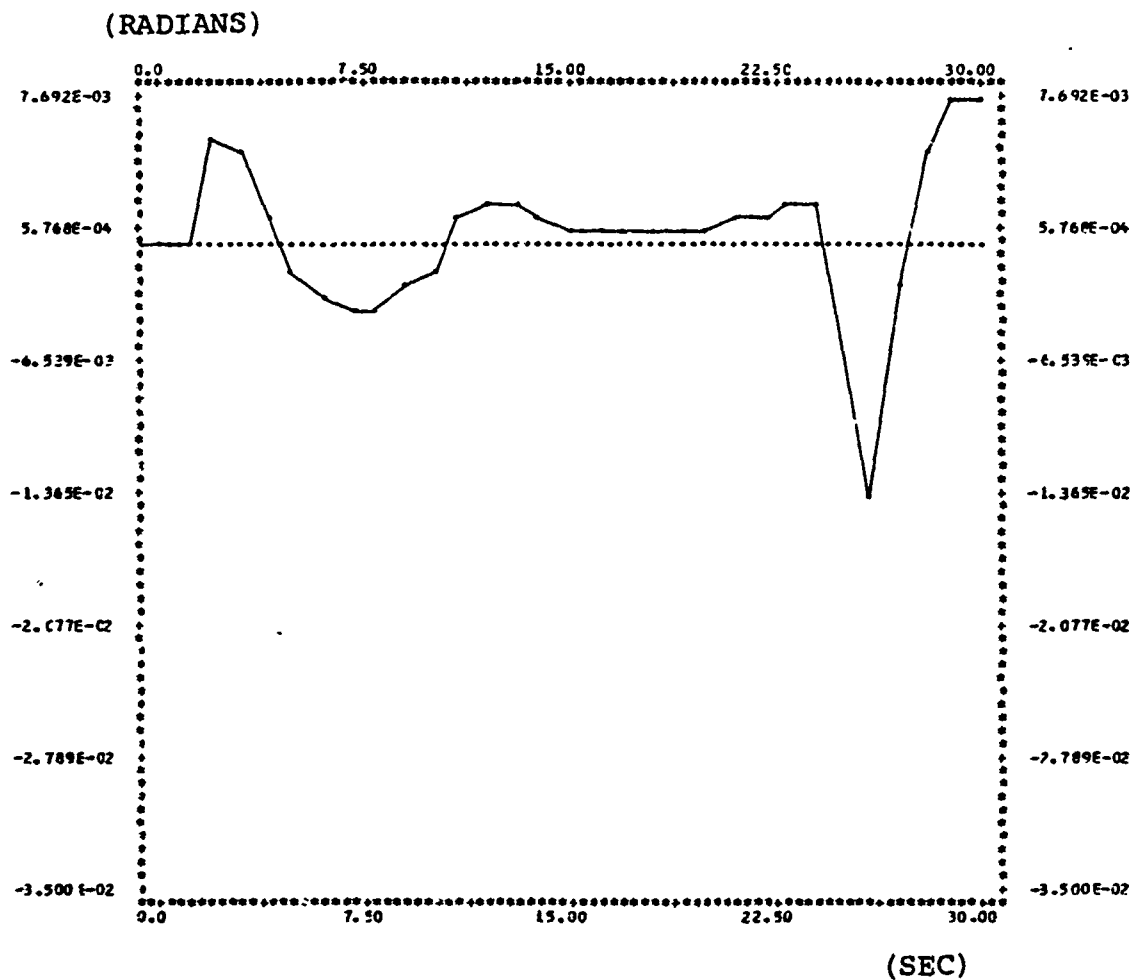


FIG. 73. MEAN BEARING ERROR VS TIME FOR KALMAN FILTER

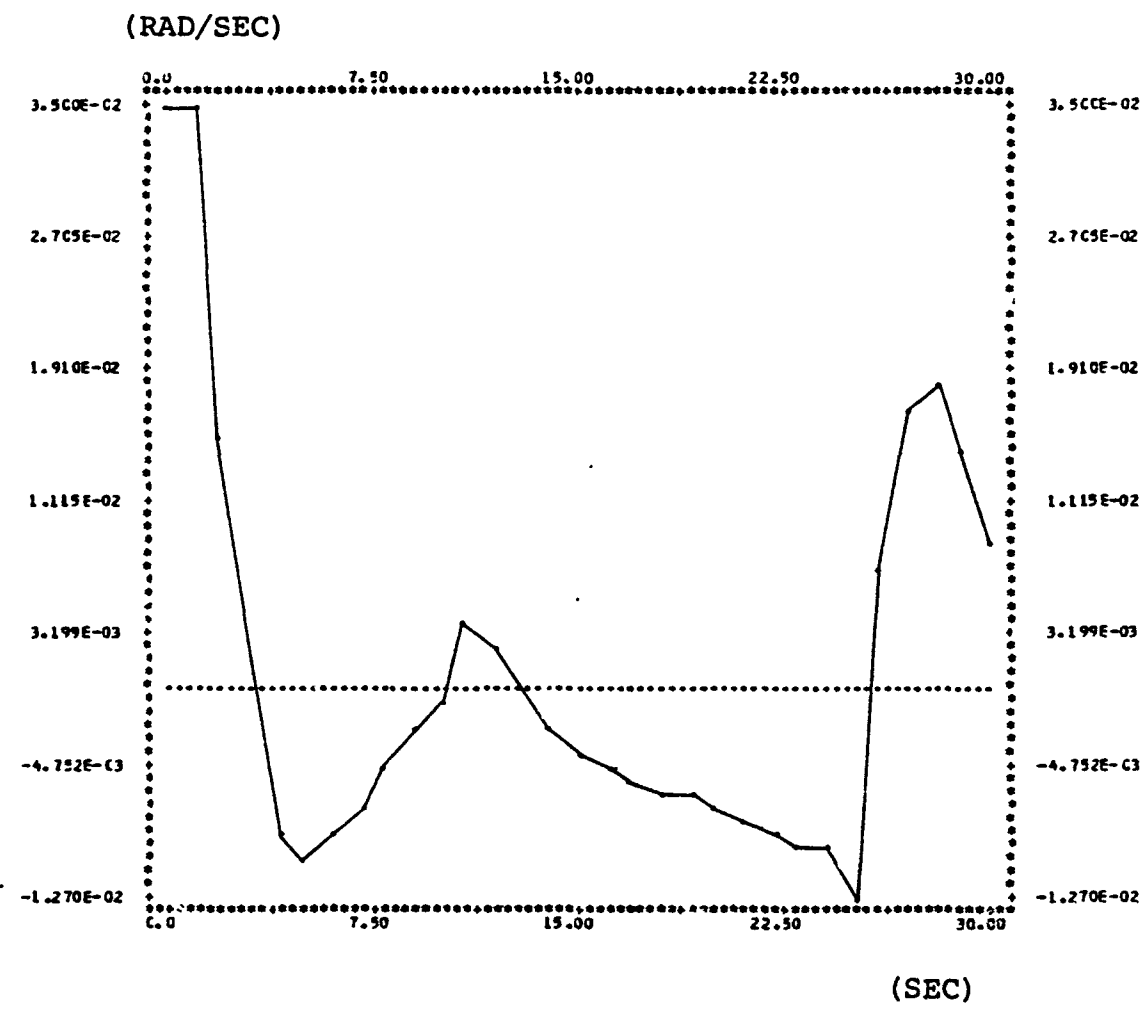
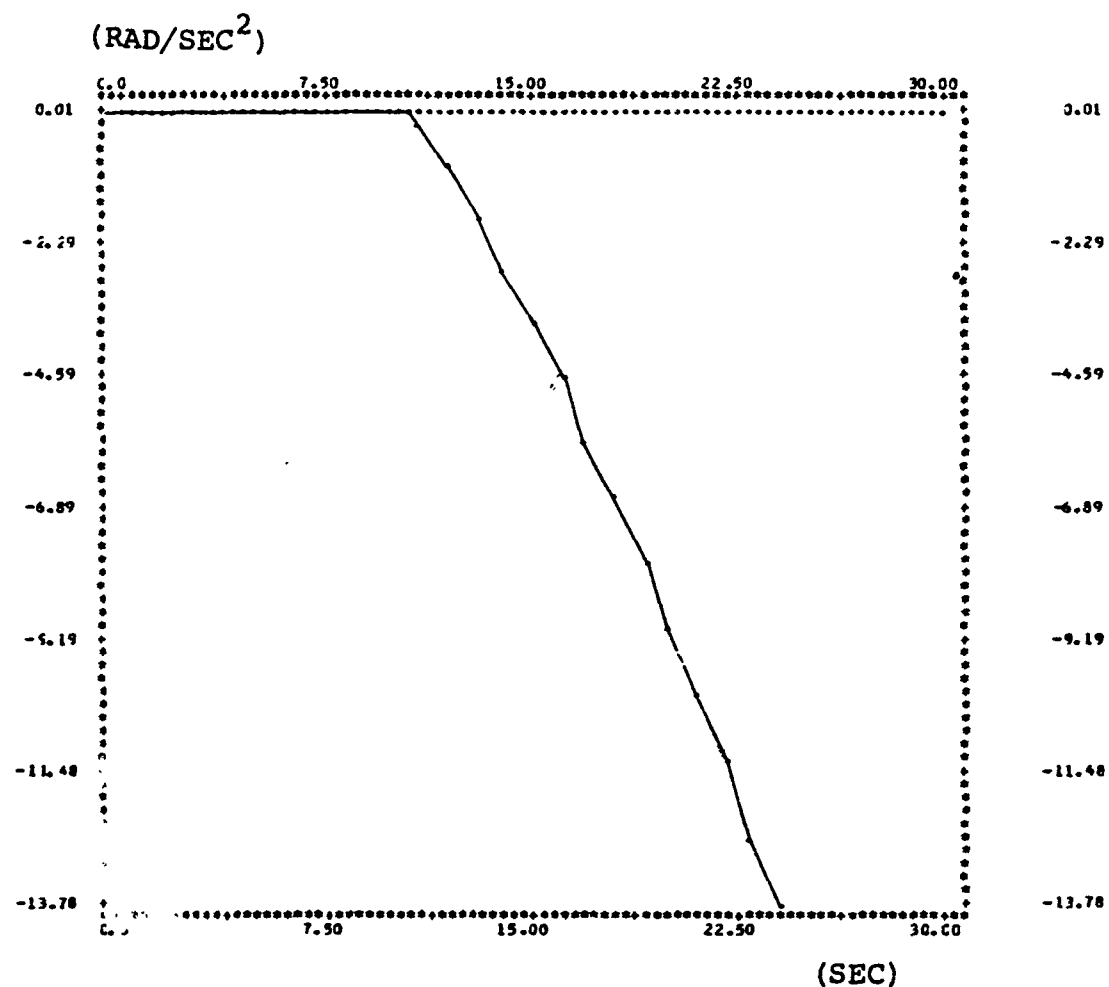


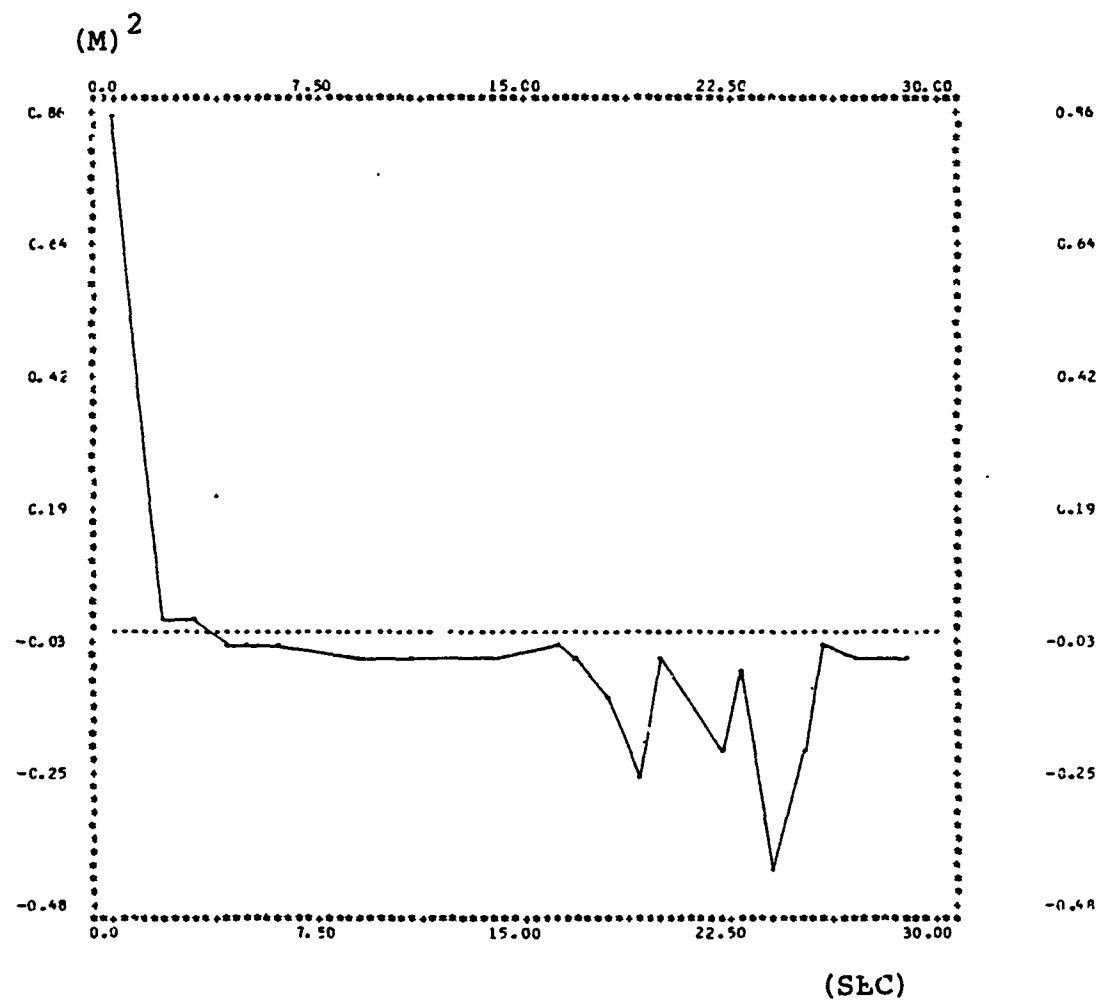
FIG. 74. MEAN BEARING RATE ERROR VS TIME FOR KALMAN FILTER



X-Scale: 0.375 units

Y-Scale: 0.230 units

FIG. 75. MEAN BEARING ACCELERATION ERROR VS TIME
FOR KALMAN FILTER



X-Scale: 0.375 units
Y-scale: 0.0223 units

FIG. 76. VARIANCE OF RANGE ERROR VS TIME FOR KALMAN FILTER

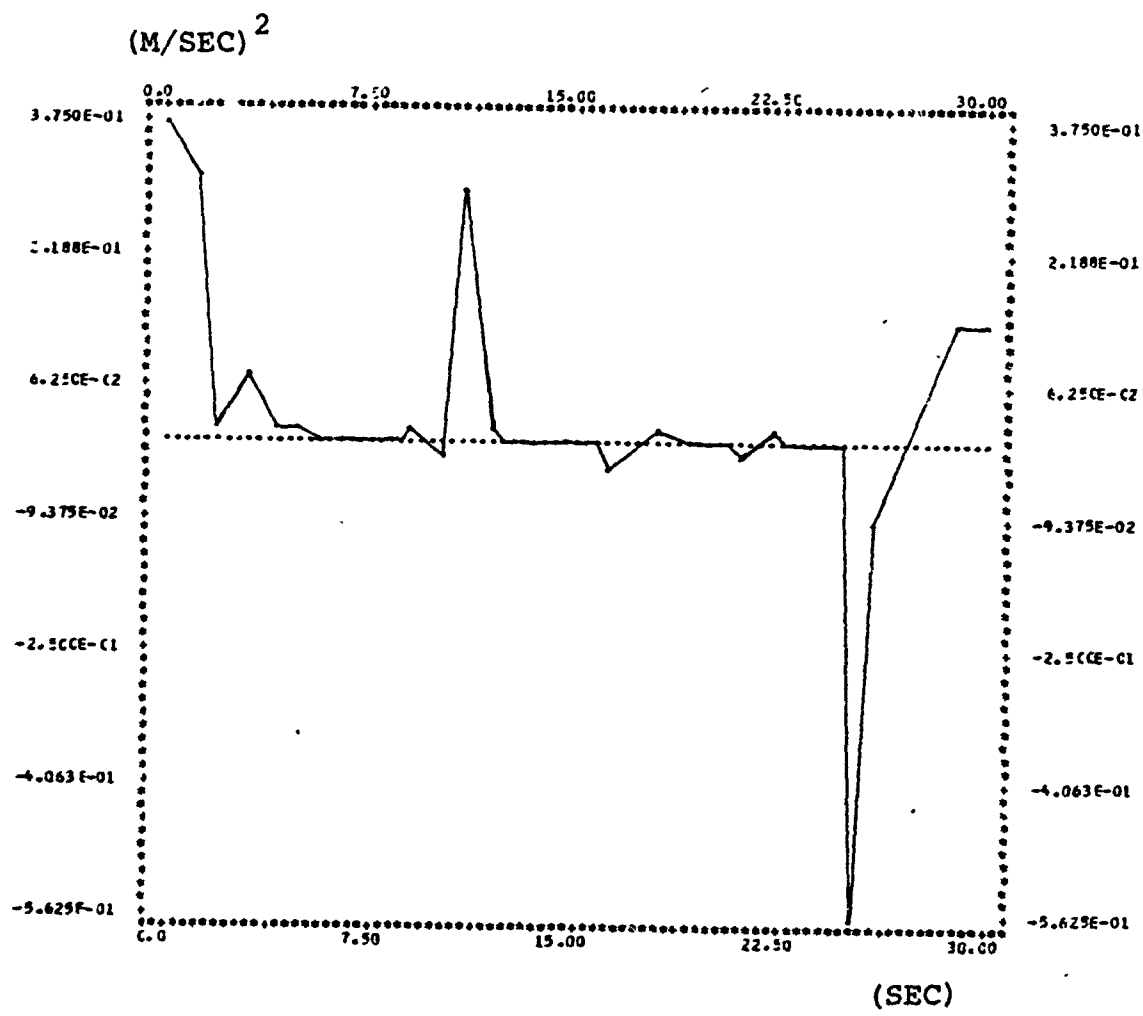


FIG. 77. VARIANCE OF VELOCITY ERROR VS TIME FOR KALMAN FILTER

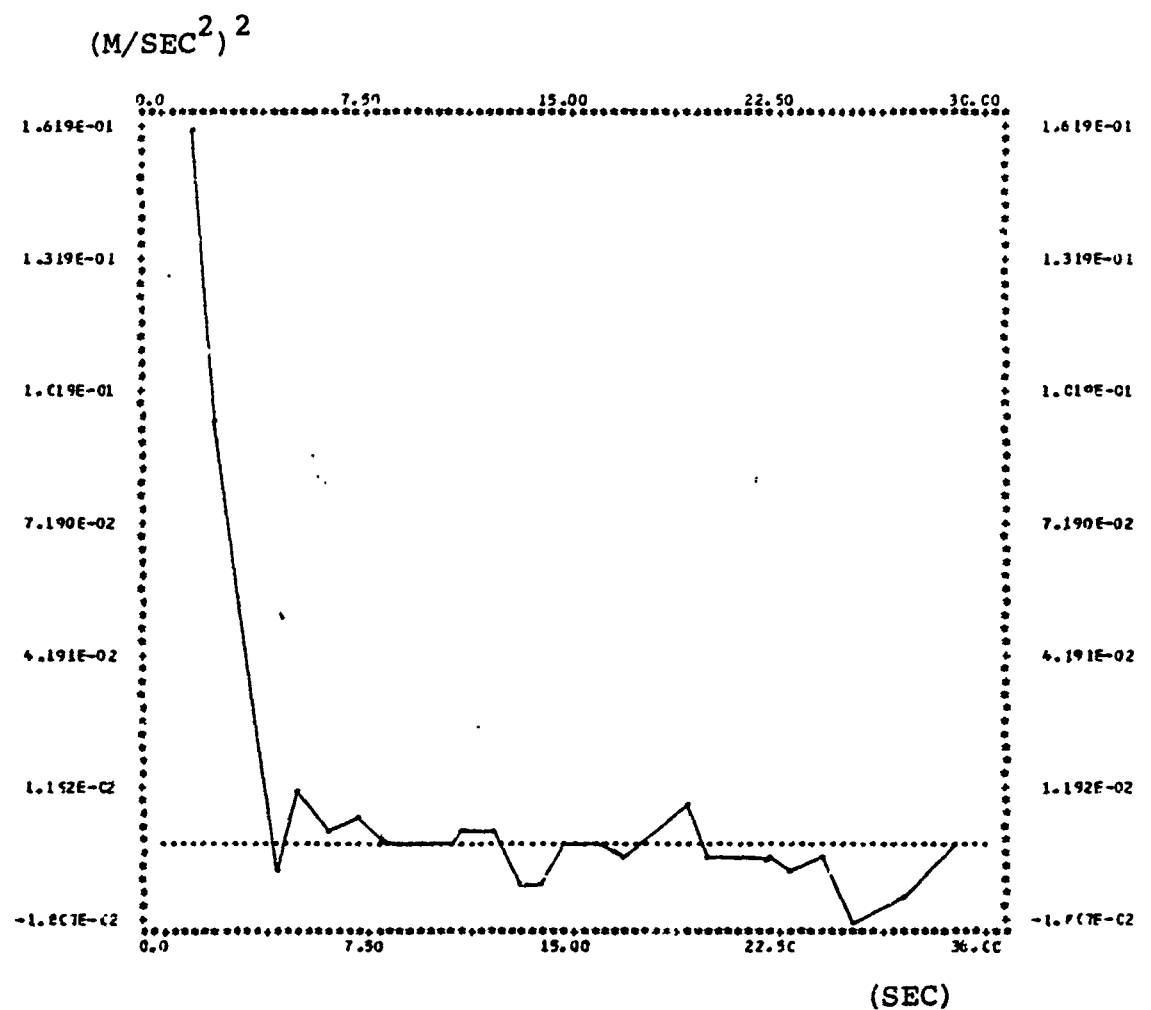


FIG. 78. VARIANCE OF ACCELERATION ERROR VS TIME FOR KALMAN FILTER

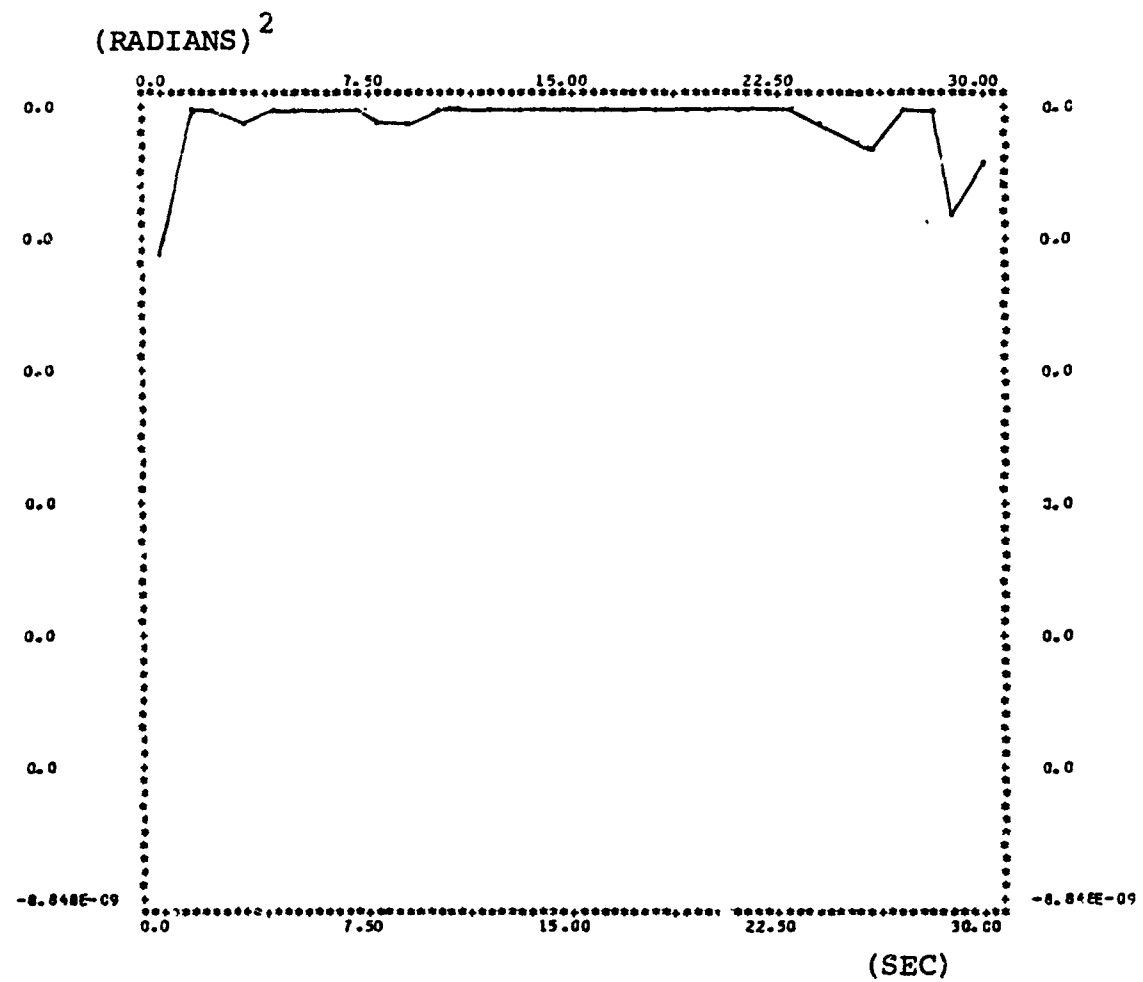
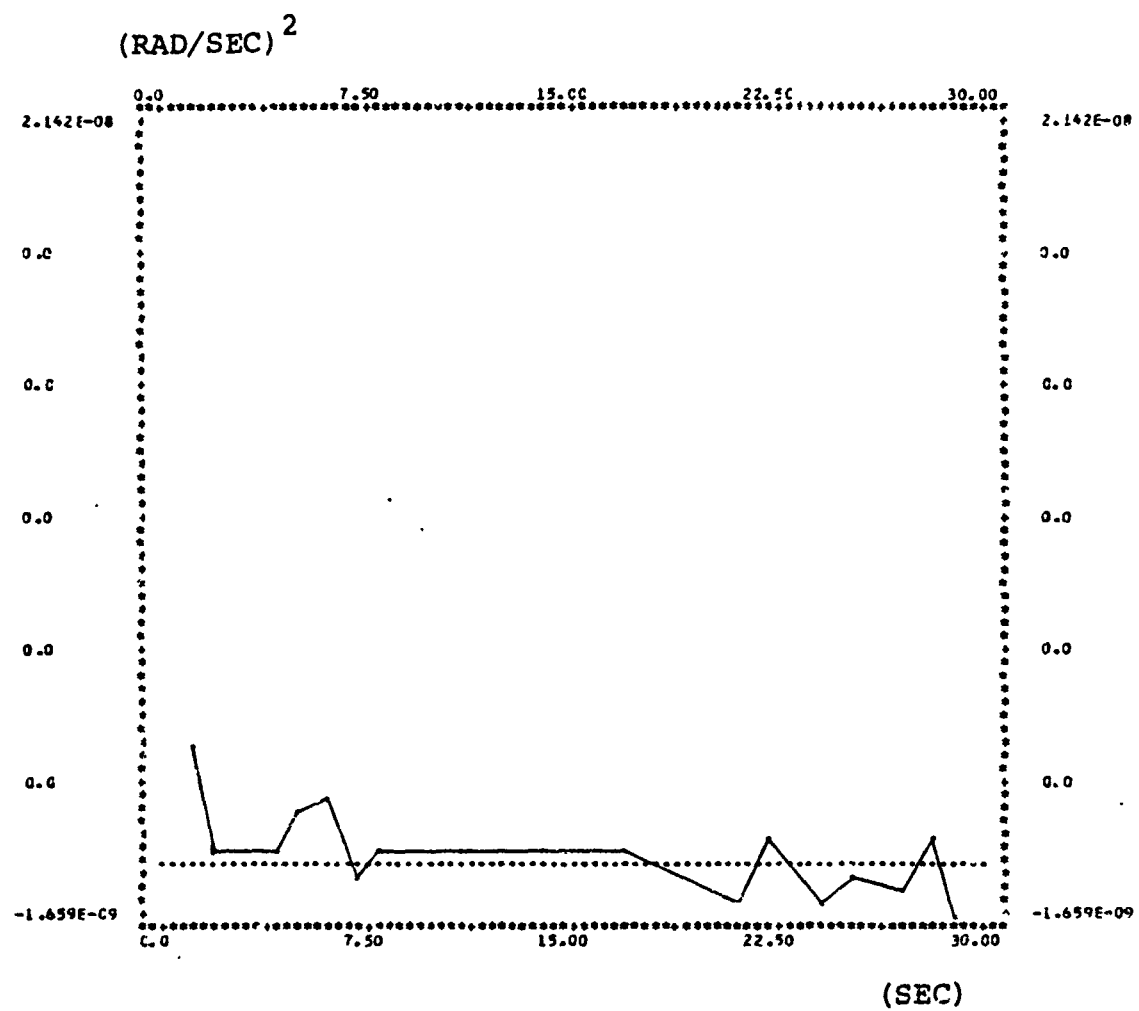
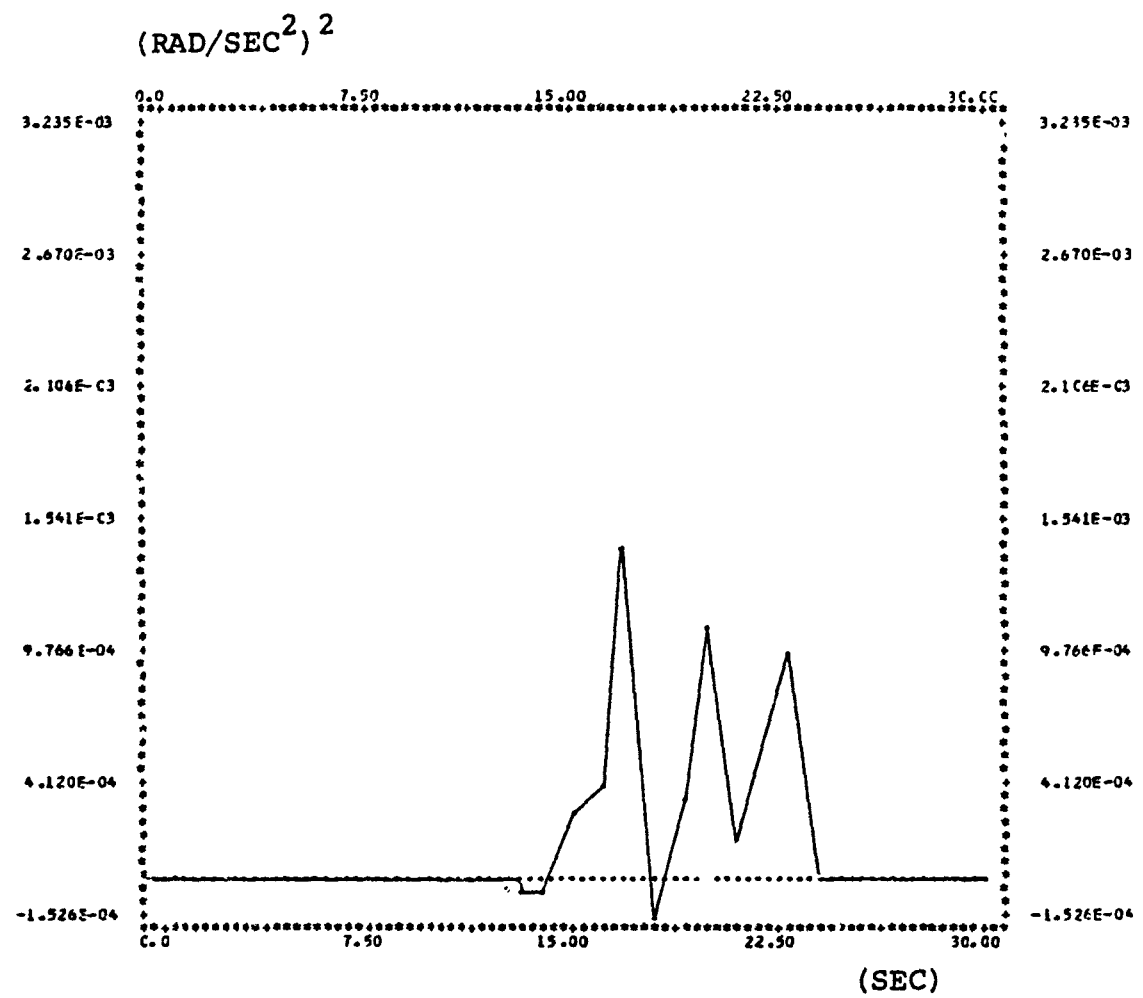


FIG. 79. VARIANCE OF BEARING ERROR VS TIME FOR KALMAN FILTER



X-Scale: 0.375 units
Y-Scale: 0.385×10^{-9} units

FIG. 80. VARIANCE OF BEARING RATE ERROR VS TIME
FOR KALMAN FILTER



X-Scale: 0.375 units
Y-Scale: 0.565E - 04 units

FIG. 81. VARIANCE OF BEARING ACCELERATION ERROR VS TIME FOR KALMAN FILTER

LIST OF REFERENCES

1. T.R. Benedict and G.W. Bordner, "Synthesis of an optimum of radar track-while-scan smoothing equations," IRE Trans. Automatic Control, Vol. AC-7, pp. 27-32, July 1962.
2. A.J. Kanyuck, "Transient response of tracking filters with densely interrupted data," IEEE Trans. Aerospace and Elec. Systems, Vol. AES-6, no. 3, pp. 313-322, May 1970
3. R.E. Kalman, "A new approach to linear filtering and prediction problems," Journal of Basic Engineering, Vol. 82, pp. 34-45, March 1960.
4. R.A. Singer, "Estimating optimal tracking filter performance for manned maneuvering targets," IEEE Trans. Aerospace and Electronic Systems, Vol. 6, pp. 473-483, July 1970.
5. R.A. Singer and J.J. Stein, "An optimal tracking filter for processing sensor data of imprecisely determined origin in surveillance systems," Proceedings of the IEEE Conference on Decision and Control, Miami Beach, pp. 171-175, December 1971.
6. B.H. Cantrell, "Description of an α - β filter in cartesian coordinates," NRL Report 7548, March 1973.
7. S.R. Neal, "Design criterion for three digital filter predictors," U.S. Naval ordnance test station, China Lake, Technical Note No. 304-135, December 1966.
8. H.R. Simpson, "A method of processing radar plot data to obtain position, velocity and turn information," RPE Memo 1924, July 1962.
9. B.L. Marks, "Adjustment rules for automatic tracking," RAE Technical Note Math 79, November 1961.
10. M.I. Skolnik, Radar Handbook, New York, McGraw-Hill, 1970.
11. N. Wiener, "Extrapolation, Interpolation, and Smoothing of stationary Time series," New York, Wiley, 1949.
12. D.E. Kirk, "Optimal Estimation: An Introduction to the theory and applications," Naval Postgraduate School 1975 (unpublished).

13. D.E. Kirk, "Evaluation of state estimators and predictors for five control systems," Naval Postgraduate School, October 1974.
14. H.P. Semmelhack-S.G. Hope, "Modern techniques for automatic TWS," 2nd Hawaii Intern. Conference, January 1969.

INITIAL DISTRIBUTION LIST

	No. Copies
1. Defense Documentation Center Cameron Station Alexandria, Virginia 22314	2
2. Library, Code 0142 Naval Postgraduate School Monterey, California 93940	2
3. Department Chairman, Code 62 Department of Electrical Engineering Naval Postgraduate School Monterey, California 93940	1
4. Prof. D.E. Kird, Code 62Ki Department of Electrical Engineering Naval Postgraduate School Monterey, California 93940	2
5. Professor J. Bouldry, Code 62Bo Department of Electrical Engineering Naval Postgraduate School Monterey, California 93940	2
6. Professor S. Parker, Code 62Px Department of Electrical Engineering Naval Postgraduate School Monterey, California 93940	5
7. General Hellenic Naval Staff Department of Education c/o Embassy of Greece (Naval Attache) 2228 Massachusetts Ave. N.W. Washington, D.C. 20008	3
8. Hellenic Navy Fast Patrol Boat, Flotilla (STAS) 2 c/o Embassy of Greece (Naval Attache) 2228 Massachusetts Ave. N.W. Washington, D.C. 20008	2
9. Captain, G.F. Leloudas, H.N. Salamis Naval Base c/o Embassy of Greece (Naval Attache) 2228 Massachusetts Ave. N.W. Washington, D.C. 20008	1

- | | | |
|-----|---|---|
| 10. | Commander J.P. Theofilopoulos, H.N.
Hellenic Naval Academy
c/o Embassy of Greece (Naval Attaché)
2228 Massachusetts Ave.
N.W. Washington, D.C. 20008 | 1 |
| 10. | Commander, G.S. Ginis, H.N.
Aid-de-Camp of Secretary of Defense
c/o Embassy of Greece (Naval Attaché)
2228 Massachusetts Ave.
N.W. Washington, D.C. 20008 | 1 |
| 12. | Major A.I. Liaskos
SMC 2358
Naval Postgraduate School
Monterey, California 93940 | 2 |
| 13. | LCDR D.E. Maiyatis, H.N.
11-13 Lomvardou Street
Athens 701, GREECE | 3 |